2011

SYNTHESIS AND CHARACTERIZATION OF POLYMERIC ANTIOXIDANT DELIVERY SYSTEMS

Paritosh P. Wattamwar
University of Kentucky, paritoshwattamwar@gmail.com

STUDENT AGREEMENT:

I represent that my thesis or dissertation and abstract are my original work. Proper attribution has been given to all outside sources. I understand that I am solely responsible for obtaining any needed copyright permissions. I have obtained and attached hereto needed written permission statements(s) from the owner(s) of each third-party copyrighted matter to be included in my work, allowing electronic distribution (if such use is not permitted by the fair use doctrine).

I hereby grant to The University of Kentucky and its agents the non-exclusive license to archive and make accessible my work in whole or in part in all forms of media, now or hereafter known. I agree that the document mentioned above may be made available immediately for worldwide access unless a preapproved embargo applies.

I retain all other ownership rights to the copyright of my work. I also retain the right to use in future works (such as articles or books) all or part of my work. I understand that I am free to register the copyright to my work.

REVIEW, APPROVAL AND ACCEPTANCE

The document mentioned above has been reviewed and accepted by the student's advisor, on behalf of the advisory committee, and by the Director of Graduate Studies (DGS), on behalf of the program; we verify that this is the final, approved version of the student's dissertation including all changes required by the advisory committee. The undersigned agree to abide by the statements above.

Paritosh P. Wattamwar, Student

Dr. Thomas D. Dziubla, Major Professor

Dr. Stephen E. Rankin, Director of Graduate Studies

SYNTHESIS AND CHARACTERIZATION OF POLYMERIC ANTIOXIDANT DELIVERY SYSTEMS

DISSERTATION

A dissertation submitted in partial fulfillment of the
requirements for the degree of Doctor of Philosophy in the
College of Engineering
at the University of Kentucky

By
Paritosh P. Wattamwar

Lexington, Kentucky

Director: Dr. Thomas D. Dziubla, Assistant Professor of Chemical Engineering

Lexington, Kentucky

2011

ABSTRACT OF DISSERTATION

SYNTHESIS AND CHARACTERIZATION OF POLYMERIC ANTIOXIDANT DELIVERY SYSTEMS

Even though the role of oxidative stress in a variety of disease states is known, strategies to alleviate this oxidative stress by antioxidants have not been able to achieve clinical success. Particularly, treatment of oxidative stress by small molecule antioxidants has not received due attention because of the challenges associated with its delivery. Antioxidant polymers, where small molecule antioxidants are incorporated into the polymer backbone, are an emerging class of materials that can address some of these challenges.

In this work, biodegradable polymers incorporating phenolic antioxidants in the polymer backbone were synthesized. Antioxidant polymers were then characterized for their *in vitro* degradation, antioxidant release and their effect on oxidative stress levels (redox state) in the cells. Trolox, a water-soluble analogue of vitamin E, was polymerized to synthesize poly(trolox ester) with 100% antioxidant content which undergoes biodegradation to release trolox. Nanoparticles of poly(trolox ester) were able to suppress oxidative stress injury induced by metal nanoparticles in an *in vitro* cell injury model.

In another study, we polymerized polyphenolic antioxidants (e.g. curcumin, quercetin) using a modified non-free-radical polymerization poly(β-amino ester) chemistry. This synthesis scheme can be extended to all polyphenolic antioxidants and allows tuning of polymer degradation rate by choosing appropriate co-monomers from a large library of monomers available for β-amino ester chemistry. Poly(antioxidant β-amino esters) (PABAE) were synthesized and characterized for their degradation, cytotoxicity and antioxidant activity. PABAE degradation products suppressed oxidative stress levels in the cells confirming antioxidant activity of degradation products.

KEYWORDS: Antioxidant polymers, oxidative stress, biocompatibility, polyphenols, controlled release of antioxidants

Paritosh P. Wattamwar

11/18/2011

SYNTHESIS AND CHARACTERIZATION OF POLYMERIC ANTIOXIDANT DELIVERY SYSTEMS

By

Paritosh P. Wattamwar

Dr. Thomas D. Dziubla
Director of Dissertation

Dr. Stephen E. Rankin
Director of Graduate Studies

November 18th, 2011
Date

DEDICATION

I dedicate my PhD to my

Aajji

Aai, Pappa

Dada and Vahini.

Thank you for all the sacrifices that you have made to help me achieve my goals. I could not have been where I am today without your love, support and encouragement.

ACKNOWLEDGEMENTS

First and foremost, I want to take this opportunity to sincerely thank my PhD advisor, Dr. Tom Dziubla, for his mentoring throughout the course of my PhD. He has been very helpful, supportive, encouraging and patient during this entire time. I highly appreciate the guidance he has provided me in designing experiments, analyzing results, and writing and publishing articles. I absolutely adore that he also provided me opportunities to develop collaborations and to work with undergraduate trainees, which helped me develop my networking and mentoring skills. I do not have enough words to thank him for providing me an absolutely wonderful and complete doctoral training which has metamorphosed me into a scientific investigator to excel in my future career goals. He has been a true "*GURU*" for me.

I am grateful to Dr. J. Zach Hilt and Dr. Kim Anderson for their resourceful insights and discussions for project development. I would like to thank Dr. Dipti Biswal and Dr. John Medley for their help with developing new protocols and techniques. I thank my collaborators Dr. Qunwei Zhang at University of Louisville, Dr. D. Allan Butterfield and Sarita Hardas for their help in characterization of my materials. I also thank my committee members Drs. Stephen Rankin, Tonglei Li and Younsoo Bae for their time and insights on my work. I acknowledge Sundar Prasanth Authimoolam, Kevin Baldridge, Justin Byarski, David Cochran, Prachi Gupta, Andrew Vasilakes and Rob Wydra, fellow students in the department for maintaining a conducive work environment and making work fun.

I would like to acknowledge my friends, Archisman Ghosh, Nitin Satarkar, Nikhil Hebbar, Nikhil Patil, Vinod Patil and Suraj Nagpure for their unconditional support,

affection, discussions and most importantly for making me feel at home. Finally, I would like to specially thank Ranjana Singh who has been a *friend cum mentor* and helped me get through the good and bad phases during my PhD. Her support was invaluable.

TABLE OF CONTENTS

LIST OF TABLES

LIST OF FIGURES

Chapter 1. Introduction

Oxidative stress is a pathological condition that has been implicated in variety of diseases including non-healing wounds, incompatibility of biomaterials and vascular diseases. During oxidative stress, reactive oxygen species (ROS) and reactive nitrogen species (RNS) are produced in excess in relationship to the antioxidant defense mechanism leading to an imbalanced redox state. Methods proposed to alleviate oxidative stress include delivery of antioxidants, either small molecule antioxidants (e.g. vitamin E, vitamin C, glutathione, etc.) or antioxidant enzymes (e.g. SOD, catalase, etc.), that can eliminate oxidative species and restore normal redox state. Small molecule antioxidants are generally non-specific and scavenge a variety of ROS and RNS. Also, they are well tolerated, stable for long term storage, resistant to complex and/or aggressive formulation processing methods and relatively inexpensive. However, these small molecule scavengers typically reduce free radicals and other oxidizing species in stoichiometric ratios, being consumed in the process. Hence, large sustained doses are expected to be required in order to observe a significant clinical effect. Also, small molecule antioxidants can have a concentration dependant anti- or pro-oxidant effect, where delivery of small molecule antioxidants in excess (e.g. burst release from micro/nanocarriers) can induce an undesired pro-oxidant effect in host tissue. One of the major challenges in translating small molecule antioxidant therapy into clinical success is its delivery at the injury site at concentrations that can have a therapeutic effect. Carriers for small molecule antioxidants should be designed for delivery of significant amounts, but at a gradual and controlled rate. Antioxidant polymers, where small molecule antioxidants are incorporated in a biodegradable polymer backbone using covalent bonds,

allow to achieve both these goals by, 1.) enhancing the total mass of antioxidant in the carrier polymer and 2.) allowing chemical cleavage to control the release rate. Many small molecule antioxidants have reactive groups like phenols, which can be easily functionalized and incorporated into polymers using polyester, polyanhydride or poly(β-amino ester) chemistry. This approach provides that added benefit of protecting the labile center from premature oxidation.

In this work, biodegradable polymers incorporating phenolic antioxidants in the polymer backbone were synthesized. Antioxidant polymers were then characterized for their *in vitro* degradation, antioxidant release and their effect on oxidative stress levels (redox state) in the cells. Trolox, a water-soluble analogue of vitamin E, was polymerized to synthesize poly(trolox ester) with 100% antioxidant content which undergoes biodegradation to release trolox. Nanoparticles of poly(trolox ester) were able to suppress oxidative stress injury induced by metal nanoparticles in an *in vitro* cell injury model. In another study, we polymerized polyphenolic antioxidants (e.g. curcumin, quercetin) using β-amino ester chemistry. Poly(β-amino esters) are known to be pH sensitive and hydrolytically degradable. Also, a large library of monomers available for β-amino ester chemistry allows for careful tuning of the degradation rates. Poly(antioxidant β-amino esters) (PABAEs) were synthesized and characterized for their degradation and antioxidant activity. The effect of the degradation of PABAE on cytotoxicity and oxidative stress levels in the cells was also studied. Based on the encouraging results from these studies, we plan to study application of antioxidant polymers in, i.) targeted delivery of antioxidant polymer nanoparticles to injured vascular endothelium (e.g. ischemia/reperfusion injury) ii.) coating biomedical implants to suppress implant induced

inflammatory response which is marked by elevated oxidative stress in surrounding tissue, iii.) wound healing materials (e.g. dermal patches) for sustained delivery of antioxidants at wound site.

Chapter 2. Background

Based on the book chapter and a review article published in :

> P.P. Wattamwar and T.D. Dziubla, "Modulation of Wound Healing Response Through Oxidation Active Materials", To appear in : "Engineering Biomaterials For Regenerative Medicine: Novel Technologies for Clinical Applications", S. Bhatia (Editor), Springer (*Submitted*)
>
> E. Hood, E. Simone, P.P. Wattamwar, T.D. Dziubla and V.R. Muzykantov, "Nanocarriers for vascular delivery of antioxidants", Review article, Nanomedicine, 2011, 6(7), 1257-1272
>
> *My contribution to this article is the review section titled "Polymer nanocarriers for delivery of antioxidants".*

2.1 Introduction

Oxidative stress is the pathophysiological condition which is characterized by the imbalance between an excess production of oxidants, called reactive oxygen species (ROS) and reactive nitrogen species (RNS), in relationship to the antioxidant defense mechanism's ability to scavenge these oxidants. When produced in excess, ROS/RNS interact with and damage cellular and subcellular membranes, DNA, proteins, etc. and thereby impair normal functioning of cells. This process represents a primary and/or a secondary mechanism in inflammation and various disease states including neurodegenerative diseases, cardiovascular diseases and host tissue inflammatory response to biomaterial implants **(Table 2-1)**. Methods that have been proposed to alleviate oxidative stress attempt to restore antioxidant defenses by the delivery of antioxidants that could eliminate oxidative species. As with many pharmacological approaches, a significant hurdle in the translation of antioxidant therapies into viable clinical treatment strategies lies in the inefficient and inadequate delivery of these agents to their intended site of action (e.g., the vascular endothelium, biomaterial implant site)

[1]. Indeed, mixed results from several decades of antioxidant research, including large scale clinical trials [2-4], have demonstrated that for antioxidant therapy to work, it must 1.) scavenge the correct oxidant radicals, 2.) be targeted directly to the cells undergoing injury and 3.) remain functional for the duration of pathology [5-7]. While designing an antioxidant therapy for treatment, it is also necessary to understand the dynamic role of oxidative stress in disease processes and how different antioxidants interact with oxidative stress cycle in different settings. For example, treatment of an acute oxidative stress injury (e.g. ischemia-reperfusion) would require antioxidants to be delivered over a time frame of few hours to days. Whereas treatment of non-healing wound or suppression of a chronic biomaterial-induced oxidative stress, antioxidants need to be delivered over a time frame of a few weeks to months. Antioxidant polymers, where small molecule antioxidants are incorporated in polymer backbone using biodegradable covalent bonds, provide a promising platform for developing tunable antioxidant therapies for a variety of settings. Particularly, antioxidant polymers could make a significant impact in the areas of i.) wound healing, ii.) biocompatibility of materials and iii.) management of vascular oxidative stress. In the following sections, mechanism and role of oxidative stress in each of these disorders is discussed along with the challenges in delivery of antioxidants for treatment and how antioxidant polymers can overcome these limitations.

2.2 Oxidative Stress

While not fully elucidated, ROS/RNS play an important role in cell signaling directly via oxidation of cysteine residues on proteins [8] or indirectly by stimulating inflammatory signals (e.g. up-regulation of cytokines and cell adhesion molecules) [1] and mediate cellular responses like differentiation, proliferation, apoptosis and migration

Table 2-1. Role of Oxidative Stress in Various Disease States.

SMC: Smooth muscle cell, CBP: Cardiopulmonary bypass.

Disease or Syndrome	ROS Sources	References
Atherosclerosis	ROS-generating enzymes in vascular cells (EC, SMC). Activated leukocytes and macrophages. Oxidized LDL.	[9-13]
Myocardial infarction	Cardiomyocytes. Activated leukocytes and platelets.	[10, 11]
Hypertension	ROS-generating enzymes in vascular cells (EC, SMC).	[13-15]
Diabetes and Pancreatitis	ROS-generating enzymes in vascular cells (EC, SMC). Activated leukocyte	[13, 16]
Acute lung injury, ARDS, sepsis, inflammation	Activated leukocytes and macrophages. ROS-generating enzymes in vascular cells (EC, SMC).	[17-20]
Ischemia-reperfusion, transplantation, cardio-pulmonary bypass (CBP), Hypoxia	ROS-generating enzymes in endothelial cells. Activated leukocytes	[10, 21-24]
Hyperoxia	High level of environmental oxygen and ROS. ROS-generating enzymes in endothelial cells. Activated macrophages and leukocytes	[24, 25]
Aging and other neurodegenerative diseases	ROS-generating enzymes in endothelial cells. Activated macrophages and leukocytes	[10, 26-28]
Smoke inhalation, asbestoses	Activated macrophages and leukocytes	[29, 30]

[31-35]. When ROS/RNS production exceeds the cells antioxidant capacity, a degenerative pathological state known as oxidative stress occurs. For designing a successful antioxidant therapy to intervene the progression of oxidative stress, it is necessary to understand the source and location of ROS/RNS in the cell and their interactions with different antioxidants. The following sections review the mechanisms of ROS/RNS generation and the antioxidant defense mechanisms against oxidative stress.

2.2.1 Mechanism and Chemistry

Generation of various ROS/RNS by different reactions is highlighted in **Figure 2-1**. Oxidative stress is often initiated by the generation of the superoxide anion ($O_2^{\cdot-}$) during mitochondrial respiration or by enzymes like NADPH-oxidase (NADPHox), xanthine oxidase (XO), cyclooxygenases (COX) and P450 reductase. Upon activation, NADPHox converts molecular O_2 to $O_2^{\cdot-}$, which can then react with nitric oxide ($NO^{\cdot}$) to form peroxynitrite anion ($ONOO^-$). $NO^{\cdot}$ is a diffusible gaseous signaling molecule produced by the enzyme nitric oxide synthase (NOS) and affects vasorelaxation and platelet inhibition [36]. Preventing undesired oxidation by superoxide, superoxide dismutase (SOD) enzymatically converts $O_2^{\cdot-}$ to H_2O_2 (hydrogen peroxide). In the presence of the chloride anion (Cl^-), myeloperoxidase (MPO) converts H_2O_2 into a very potent oxidant, hypochlorous acid (HOCl). H_2O_2 can also react with reduced transition metals like Fe^{2+} and Cu^+ to form hydroxyl radicals ($OH^{\cdot}$) [37], which can react with polyunsaturated fatty acid (LH) to cause lipid peroxidation and form a carbon-centered lipid radical ($L^{\cdot}$). This lipid radical can then react with molecular oxygen to give a lipid peroxyl radical ($LOO^{\cdot}$). Lipid hydroperoxides (LOOH) are formed by reaction of $LOO^{\cdot}$ with other lipids (LH). Lipid peroxidation continues when LOOH undergoes a fast

reaction with Fe^{2+} to form lipid alkoxyl radical ($LO^{\cdot}$) or a slow reaction with Fe^{3+} to form $LOO^{\cdot}$ [38]. These radicals, in turn, oxidize more lipids and propagate the cycle.

Compared to other molecules, ROS/RNS are relatively unstable, having very short half-lives on account of their ability to react with and oxidatively damage cellular proteins, DNA and lipids affecting normal functioning of cells/tissue. Even though ROS/RNS have a random destructive effect, in many pathological conditions that are subject to redox-sensitive pathways, production of ROS/RNS is tightly regulated with a specific downstream target [8, 20, 39]. Depending on pathological condition and the enzymes involved, ROS/RNS are generated within the cell, in cell lipid membrane or extracellularly. Extracellular milieu and outer leaflet of plasma membrane are the first target of extracellular ROS/RNS attack, where as intracellular ROS/RNS damage cytosolic proteins and the inner leaflet of the plasma membrane [40]. Location of the ROS/RNS generation should therefore be considered while designing an antioxidant therapy, and **Figure 2-2** highlights generation of ROS/RNS at different subcellular locations.

2.2.2 Antioxidants

Antioxidants are the primary way cells and tissue are able to maintain a balance in the redox state (**Figure 2-1**) and can be classified into two major categories, small molecule oxidant scavengers (e.g. tocopherol, glutathione, quercetin, etc.) and antioxidant enzymes (e.g. SOD, catalase, etc.). Depending on their octanol/water partitioning coefficient, small molecule antioxidants can either localize in cellular cytoplasm or cellular and intracellular lipid membranes. For example, Vitamin E (T-OH), which can partition itself in lipid bilayer, scavenges $LOO^{\cdot}$ to reduce it to lipid

hydroperoxide (LOOH) and in the process forms a Vitamin E radical (T-O$^{\cdot}$). There are some regenerative pathways (e.g., tocopherol/ascorbic acid redox cycling) [41] that exist within the cell that can help extend the useful life of a radical scavenger. However, these recycling loops depend strongly upon the cell's own glutathione reducing pathway (e.g. Vitamin C/Ascorbic acid (AscH) or glutathione (GSH) react with T-O$^{\cdot}$ to regenerate T-OH). Water soluble antioxidants like vitamin C and GSH can also react with cytoplasmic ROS/RNS. Small molecule antioxidants are generally non-specific, scavenge a variety of ROS and RNS and are consumed in the process.

Antioxidant enzymes, on the other hand, are not consumed in reaction, allowing a single enzyme to react with millions of copies of radicals before becoming inactivated. For instance, catalase, which reduces H_2O_2 to water and oxygen, has a turnover number of 40 million hydrogen peroxide molecules degraded per second, allowing for even small delivered amounts to have profound cellular effects [42]. The enzyme glutathione peroxidase (GPx) can reduce lipid hydroperoxides and free H_2O_2 to corresponding alcohols and water respectively. The redox cycle of GPx requires an electron obtained from NADPH via GSH and glutathione reductase to catalyze the reduction of peroxides [43, 44]. Peroxiredoxins is another class of enzymes that use either thioredoxin or GSH or both as an electron donor to catalyze the reduction of H_2O_2, other hydroperoxides (e.g. LOOH) and $ONOO^-$ [45, 46]. While antioxidant enzymes have higher activity, they are typically limited to the scope of ROS which they can treat (e.g. SOD only decomposes $O2^{\cdot-}$).

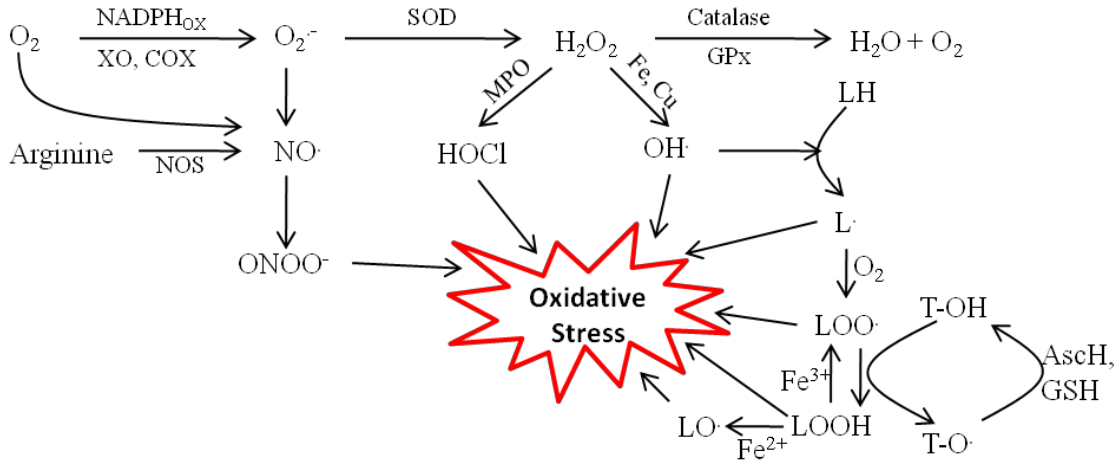

Figure 2-1. Oxidants, Antioxidants and Antioxidant Enzymes

Molecular oxygen is reduced to superoxide anion ($O_2^{\cdot -}$) by NADPH-oxidase ($NADPH_{OX}$), xanthine oxidase (XO) and cyclooxygenases (COX). $O_2^{\cdot -}$ is dismutated by superoxide dismutase (SOD) to form hydrogen peroxide (H_2O_2) which then reacts with myeloperoxidase (MPO) and transient metals like Fe and Cu to form hypochlorous acid (HOCl) and hydroxyl radical ($OH^{\cdot}$) respectively. Antioxidant enzymes like catalase and glutathione peroxidase (GPx) reduces H_2O_2 into water and oxygen. $OH^{\cdot}$ reacts with polyunsaturated fatty acid (LH) to cause lipid peroxidation and form carbon-centered lipid radical ($L^{\cdot}$) which further reacts with molecular oxygen to give lipid peroxyl radical ($LOO^{\cdot}$). Lipid peroxidation continues until antioxidants like Vitamin E (T-OH) scavenge lipid oxidants. Vitamin E (T-OH), which can partition itself in lipid bilayer, scavenges $LOO^{\cdot}$ to reduce it to lipid hydroperoxide (LOOH) and in the process forms a Vitamin E radical ($T\text{-}O^{\cdot}$). Vitamin C/Ascorbic acid (AscH) or glutathione (GSH) react with $T\text{-}O^{\cdot}$ to regenerate T-OH. Lipid peroxidation continues further where LOOH undergoes a fast reaction with Fe^{2+} to form lipid alkoxyl radical ($LO^{\cdot}$). LOOH can also react slowly with Fe^{3+} to form $LOO^{\cdot}$.

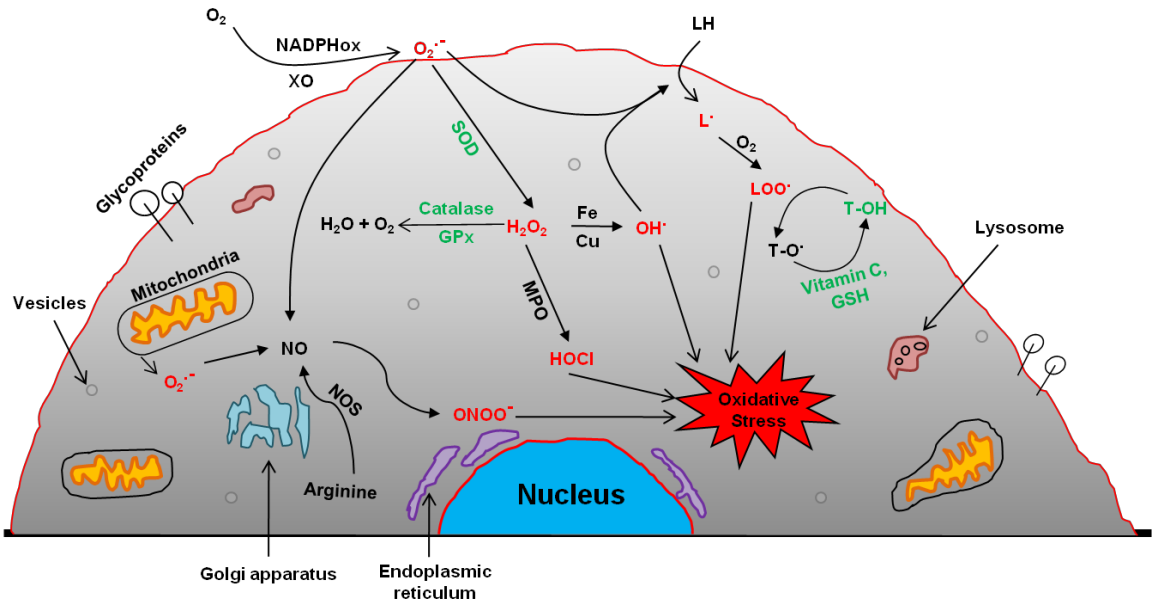

Figure 2-2. A Simplified View of the Cellular Generation of ROS/RNS.

Upon activation, membrane bound NADPHox and XO reduce molecular oxygen (O_2) to generate superoxide anion ($O_2^{\cdot-}$) at plasma membrane which can result in lipid peroxidation. $O_2^{\cdot-}$ is also generated in the mitochondria of cells as a result of electron leak from the respiratory chain [47]. In endothelial cells, endothelial NOS (eNOS) is primarily localized in caveolae (a cholesterol enriched microdomain in plasma membrane) and in Golgi apparatus [48]. Subcellular localization of tyrosine-nitrated proteins, product of protein oxidation by RNS, is determined by proximity to NOS and ROS generating enzymes [49]. In endothelial cells, tyrosine-nitrated proteins were observed in mitochondria, endoplasmic reticulum, cytosol and nucleus, indicating the presence of RNS in these cellular compartments. Fat-soluble antioxidants like Vitamin E (T-OH) which partition themselves in plasma membrane and membranes of subcellular compartments provide protection against lipid peroxidation. Water-soluble antioxidants like Vitamin C and GSH scavenge radicals in the cytosolic compartment. Different isoforms of antioxidant enzyme SOD (SOD1, SOD2, SOD3) are located in cytosol, mitochondria and extracellular matrix respectively [50].

2.3 Biocompatibility of Implanted Materials

Surgical injury to vascular tissue during the implantation of a biomaterial (e.g. prostheses, drug delivery devices) brings the biomaterial in contact with blood and triggers wound healing process, which is classically broken down into four distinct yet overlapping phases - i.) blood protein adsorption on biomaterial surface, ii.) recruitment of inflammatory cells (neutrophils and monocytes) at the implant site, iii.) new tissue formation and iv.) foreign body reaction and fibrous capsule formation [51]. If any step becomes compromised (e.g. excessive inflammation), a chronic inflammatory response can be established, negatively impacting the biomaterial implantation. As a result, much attention has been given to biomaterial surface chemistry and topography that would dictate protein adsorption onto surface, effects of cytokines, signaling molecules, and growth factors on the wound response and using these to control biocompatibility of materials. However, a parallel process of oxidative stress which also plays an important role in wound healing has been generating growing consideration as a means of tuning the wound healing process. It is the inflammation phase of the wound healing response, where excess generation of free radicals and other reactive species, which can result in loss of redox balance at the implant site resulting in a prolonged inflammation phase. This section reviews the role of oxidative stress in the inflammatory phase of wound healing and in the new tissue formation process. It also provides a summary of approaches that have been and can be used to intervene in the redox cycles as a way of additional control over wound healing, providing an additional tool by which to design antioxidant polymers as novel biomaterials.

2.3.1 Role of Oxidative Stress in Biocompatibility of Implanted Materials

Wound healing response around an implant is very similar to the classical wound healing process that can be broken down into four main phases, a.) formation of blood clot and platelet plug, b.) inflammation, c.) new tissue formation and d.) tissue remodeling (**Figure 2-3**). The immediate first step response to a wound is to stop blood flow by initiating thrombosis. This fibrin clot serves as a temporary seal to the wound and provides a scaffold where other cells can migrate and proliferate. The hemostasis process is followed by inflammatory phase where the fibrin clot acts as a pool for variety of cytokines (e.g. interleukins, interferons, tumor necrosis factors) and growth factors (e.g. platelet-derived growth factor, transforming growth factor, etc.) that are released from degranulating activated platelets and the immune cells. Chemoattractants, which include growth factors released from the platelets and other cues like by-products of fibrin proteolysis or peptides cleaved from bacteria, result in the accumulation of inflammatory cells (neutrophils and monocytes) from the circulation. Also, cytokines and ROS upregulate expression of cell adhesion molecules (CAMs) (e.g. CD54) which recruit neutrophils and monocytes from circulation [40, 52].

One of the major roles of neutrophils is to combat wound infection by eliminating the invading microorganisms (e.g. bacteria) through burst release of oxidative species [53]. Monocytes at the inflamed wound site differentiate into macrophages which phagocytose apoptotic neutrophils and other cellular/bacterial debris. Macrophages are responsible for the long term wound repair process not only by amplifying the inflammatory response but also by initiating the growth of new tissue. Macrophages and

other inflammatory cells also release cytokines and other growth factors that can activate fibroblasts and keratinocytes [54].

One to two days after wounding, new tissue formation begins and is marked by migration and proliferation of various cells like endothelial cells, fibroblasts, keratinocytes and inflammatory cells. Keratinocytes (in case of dermal wounds) migrate over the injured dermis with concomitant angiogenesis to restore blood flow at the wound site. Fibroblasts along with macrophages replace the fibrin matrix with granulation tissue (called so due to appearance of several small capillaries) which also serves as a substrate for keratinocyte migration and proliferation. Macrophages activate fibroblasts to differentiate into myofibroblasts, which contract the wound gradually bringing edges of the wound closer together. Fibroblasts and myofibroblasts together also produce collagen rich extracellular matrix which forms bulk of the scar. The wound healing process is completed by a long phase of tissue remodeling that can last up to a year or more and is characterized by attenuation of all the activated processes [55]. Many of the recruited cells (endothelial, fibroblasts, macrophages) either undergo apoptosis or exit the wound leaving behind an acellular tissue mostly composed of collagen and some extracellular-matrix proteins. Matrix metalloproteinases (e.g. MMP-1 and MMP-9) that are secreted by the cells replace type III collagen in the granulation tissue with type I collagen [56].

ROS and RNS are involved in redox-sensitive cell signaling pathways that induce various responses like chemotaxis, proliferation, differentiation, etc. and therefore oxidative stress (ROS and RNS) play a critical role in orchestration of each of these wound healing phases [57]. A better understanding of role and effect (both positive and

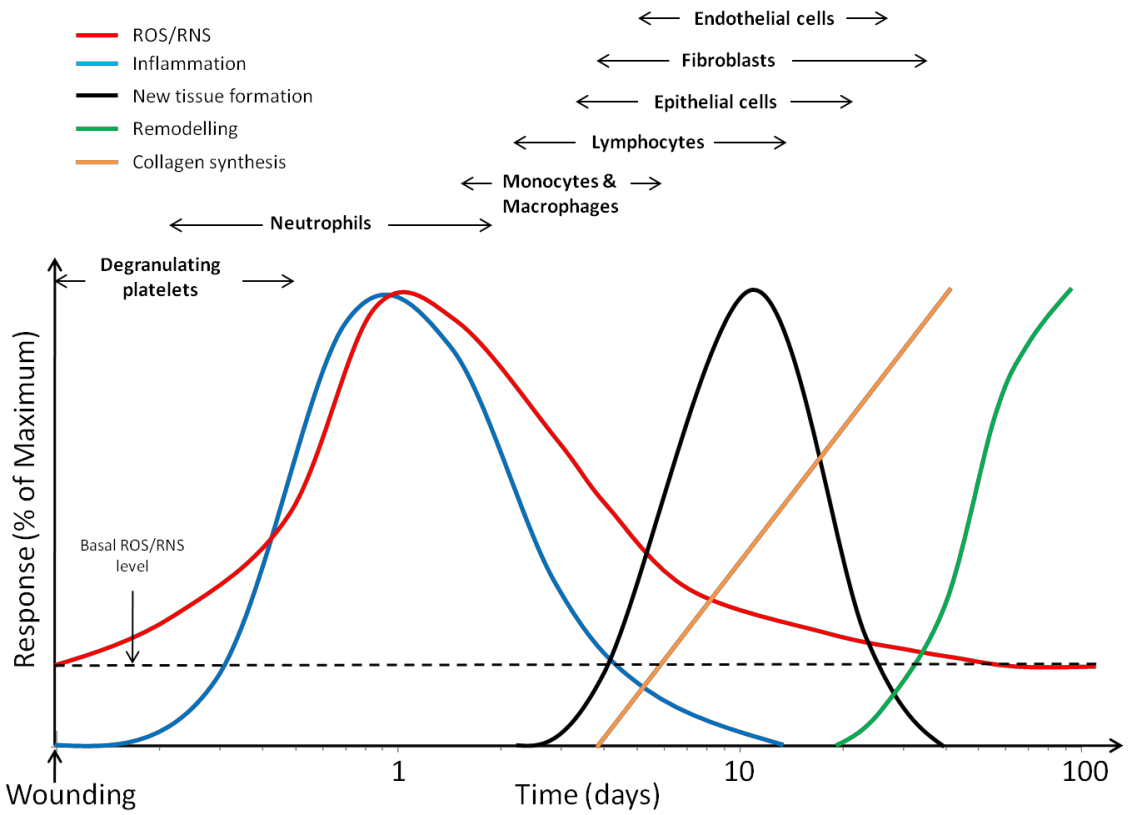

Figure 2-3. The Temporal Compositional Changes Expected in a "healthy" Wound Healing Response.

Different cells are recruited at the wound site during the four phases of wound healing. ROS/RNS levels are elevated around day 1 and then gradually decrease to their basal level.

negative) of oxidative stress in each of the wound healing phases is necessary for optimal design of the therapeutic intervention strategy by using antioxidants.

The following sections include detailed discussion of the role of ROS/RNS in the inflammatory phase and new-tissue formation phase of wound healing. Redox state plays an important role in the hemostasis process and is reviewed in detail by Gorlach and Sen et. al. [57, 58].

2.3.1.1 Inflammation

ROS at the wound site play an important role in the recruitment/chemotaxis and the function of neutrophils and other immune cells. Chemotaxis is the migration of cells based on the concentration gradient cues. In a recent study with a zebrafish wound model, it has been shown that during the initial phase of wound detection, H_2O_2 gradient at low concentration (~ 0.5-50 μM) induces chemotaxis in leukocytes [59, 60]. Experiments have also shown that inhibition of NADPHox within the neutrophils affected their chemotactic migration, possibly by affecting ROS-based intracellular signaling [61]. Elevated levels of thioredoxin, an important redox protein, in circulation inhibit lipopolysaccharide-stimulated (LPS) chemotaxis as well as the recruitment of leukocytes induced by murine chemokine KC/GROα, RANTES (regulated upon activation, normal T-cell expressed and secreted) and monocyte chemoattractant protein-1 (MCP-1) [62]. Immune response to a kill a pathogen is comprised of a respiratory burst by the immune cells. Neutrophils, phagocytes as well as other immune cells undergo respiratory burst, a rapid and non-mitochondrial conversion of O_2 to battery of ROS and RNS by activation of membrane-bound NADPHox via chemoattractants or other inflammatory stimuli, to eliminate bacteria or other microorganisms that could cause an infection [63-65]. Any

defect in the NADPHox system, which is critical for the respiratory burst, results in the loss of resistance to infections [66, 67].

Leukocytes are recruited to the wound site by a variety of chemoattractants, including fragmented extracellular matrix protein, tumor necrosis factor (TNF), transforming growth factor β (TGFβ), MCP-1, granulocyte colony-stimulating factor (G-CSF), granulocyte/macrophage CSF (GM-CSF) and macrophage- inflammatory protein (MIP). Through ROS like H_2O_2 and $O2^{-}$, oxidative stress increases production of MIP-1α, MIP-2, MCP-1, CSF-1 and other chemoattractants and is very critical in recruitment of immune cells at the wound site [68-73]. Oxidative stress also up-regulates the production of cytokines by cells. Expression of inflammatory cytokines expected at the wound site (e.g. TNFα, IL-8, IL-1β and IL-6) is stimulated by oxidative stress [74-76]. Effect of oxidative stress on expression and release of various inflammatory cytokines is summarized in **Table 2-2**.

ROS and RNS are important in the functioning of immune cells. Exogenous H_2O_2 induces calcium release from the intracellular compartments of neutrophils increasing their phagocytic activity [77]. H_2O_2 also modulates the respiratory burst of monocytes and neutrophils, where low concentrations of H_2O_2 stimulate $O2^{-}$ production where as higher concentrations inhibit $O2^{-}$ production [78-80]. Monocytes and macrophages protect themselves from the respiratory burst by H_2O_2 triggered increase in the uptake of GSH [81]. High mobility group box-1 (HMGB1), an endogenous pro-inflammatory cytokine, is passively released by necrotic cells or actively secreted by monocytes/macrophages to exogenous and endogenous stimuli such as TNF-α, IL-1, endotoxins and interferon-γ (IFN-γ) [82]. HMGB1 also mediates innate and adaptive

immune responses by promoting dendritic cell maturation [83]. Oxidative stress induces HMGB1 release, both actively and passively, from monocytes and macrophages in a mitogen-activated protein kinase (MAPK) and chromosome region maintenance (CRM1)-dependent mechanism. At non-toxic concentrations of H_2O_2 (< 0.125 mM), it stimulated interaction of HMGB1 with the nuclear export factor CRM1 where as at higher concentrations of 0.25 mM, H_2O_2 exhibited cell toxicity triggering active and passive release of HMGB1 [84]. Hypoxia induced HMGB1 release by hepatocytes during ischemia/repurfusion injury, is also regulated via toll-like receptor 4 (TLR4)-dependent ROS production and downstream calcium-mediated signaling [85].

Neutrophils and monocytes are recruited from the circulation due to their receptivity to certain molecular signals that are expressed on the endothelial cells as a response to the wound. Expression of surface molecular signals on the endothelium alters as the wound healing progresses allowing for sequential recruitment of different classes of leukocytes at the wound site. Initially, selectin family of cell adhesion molecules expressed on the endothelium mediate tethering of leukocytes to the vessel wall, allowing for their rolling in the direction of the blood flow. The light adhesion to selectins is followed by tighter adhesions and arrest mediated by β2 subfamily of integrins. Attached leukocytes then follow directional cues from chemoattractants using integrins for traction and then crawl across the endothelium into extravascular space [52, 86]. Once the leukocytes leave the circulation and enter the extracellular matrix, they interact with matricellular proteins through the β1 subfamily of integrins. Both β1 and β2 integrins induce different signaling pathways in monocytes which are important for their

Table 2-2. ROS/RNS Play an Important Role in Inflammatory Phase by Affecting Expression and Release of Various Cytokines and Chemoattractants

Cytokines and Chemoattractants	Source	Effect of ROS/RNS	[Ref]
MIP-1α	Rat alveolar macrophages	• H_2O_2 treatment induced MIP-1α mRNA expression	[69]
MIP-2	Rat alveolar macrophages, Rat lung epithelial cells	• H_2O_2 increased MIP-2 mRNA expression • Quartz, TiO2, and crocidolite asbestos particles induced oxidative stress, resulting in increased MIP-2 expression	[68, 72]
MCP-1	Human aortic smooth muscle cells, monocytes	• PDGF stimulated $O2^{-}$ release resulting in increased MCP-1 mRNA expression • X/XO stimulated monocyte to produce MCP-1	[70]
CSF-1	Endothelial cells	• TGF-β1 stimulated macrophage CSF via H2O2 based signalling	[73]
TNF-α	Human dendritic cells, Rat alveolar epithelial cells	• H_2O_2 stimulated production of TNF-α • LPS induced glutathione depletion resulted in release of cytokines	[74, 76]
IL-8	Human dendritic cells, Rat alveolar epithelial cells, Monocytes	• H_2O_2 stimulated production of IL-8 • LPS induced glutathione depletion resulted in release of cytokines • X/XO stimulated monocyte to produce IL-8	[74-76]
IL-1β	Rat alveolar epithelial cells	• LPS induced glutathione depletion resulted in release of cytokines	[76]
IL-6	Rat alveolar epithelial cells	• LPS induced glutathione depletion resulted in release of cytokines	[76]

functioning (migration and phagocytocis) and differentiation into the repairing macrophages [87].

H_2O_2 promotes β2-integrin leukocyte function-associated antigen-1 (LFA-1)-dependent attachment of neutrophils to cardiac myocytes and in presence of exogenous chemoattractants (e.g. c5a), there is a transition from LFA-1 to macrophage 1 antigen (Mac-1) dependent adhesion, resulting in prolonged attachment of neutrophils to myocytes [88, 89]. Also, neutrophils at early stages utilize the interaction of LFA-1 with inter-cellular adhesion molecule 1 (ICAM-1) to trigger H_2O_2 production without requiring chemotactic stimulation whereas the cytokine-induced respiratory burst of neutrophils is augmented by Mac-1-dependent adhesion of neutrophils [90-92]. This mechanism could result in additional recruitment of neutrophils by neutrophils whose ROS production is based on Mac-1-dependent adherence to myocytes. Cellular redox state affects expression of LFA-1 in myeloid lineage, where exogenous use of antioxidants like N-acetyl-L-cysteine and pyrrolidine dithiocarbamate suppressed expression of protein CD11a/LFA-1α [93]. Exposure of leukocytes to H_2O_2 and superoxide upregulated the expression of leukocyte adhesion molecules and promoted leukocyte-endothelial adhesion [94].

Mediators of inflammation (e.g. TNFα, IL-1 and IFN-γ), including ROS, modulate expression of endothelial surface adhesion molecules. Both endogenously and exogenously (as a result of attached leukocytes) released ROS from the endothelium upregulates expression of intercellular adhesion molecule-1 (ICAM-1, CD54), vascular cellular adhesion molecule-1 (VCAM-1) and P-selectin on surface of endothelial cells recruiting more leukocytes from the circulation [95-98]. Antioxidants N-acetyl-L-

cysteine and pyrrolidine dithiocarbamate inhibited H_2O_2-induced and cytokine-induced expression of ICAM-1 respectively [99, 100].

Redox state of the cell also plays an important role in regulating chemokines and their receptors. Antioxidants pyrrolidine dithiocarbamate (PDTC), N-acetyl-L-cysteine (NAC) and 2-mercaptoethanol inhibited mRNA expression of chemokine receptors CCR2 (CC chemokine receptor-2), CCR5 and CXCR4 (CXC chemokine receptor-4) in human monocytes. Oxidative stress induced either by xanthine/xanthine oxidase, H_2O_2 or buthionine sulfoximine (a glutathione-depleting drug) counteracted the inhibitory effects of antioxidants and increased the expression of chemokine receptors [101, 102]. TNFα and bacterial lipopolysaccharide-mediated inhibition of CCR5 and CXCR4 mRNA expressions was opposed by generation of ROS (xanthine/xanthine oxidase), which increased both CCR5 and CXCR4 mRNA expressions and cell migration (3-fold) in response to MIP-1β [101]. Homocysteine-induced stimulation of CCR2 mRNA level is also mediated through superoxide formation [103]. Oxidative stress up-regulates the production of cytokines by cells. ROS stimulated synthesis of IL-8 and TNFα by dendritic cells [74]. A flow diagram of the relationship between oxidative stress and inflammation is provided in **Figure 2-4**. As shown, a failure to resolve oxidative stress can lead to chronic inflammation and, thereby, aberrant healing.

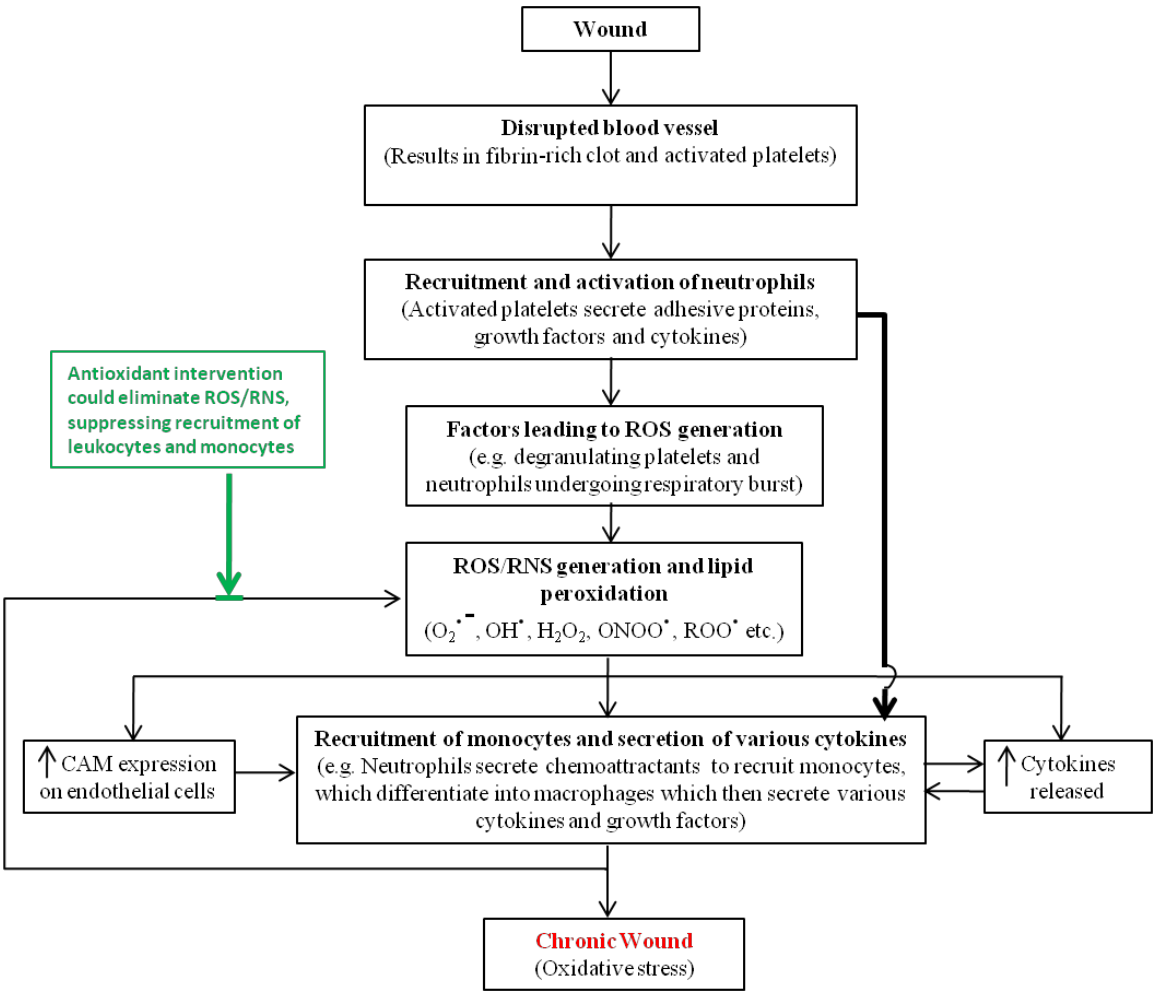

Figure 2-4. Initiation and Propagation of Oxidative Stress after Wounding.

Failure to suppress excessive generation of ROS/RNS could result in prolonged inflammatory phase, finally resulting in a chronic non-healing wound. *CAM: Cell adhesion molecules*

2.3.1.2 New-tissue Formation

2-10 days after the injury, wound closure and new-tissue formation starts which is characterized by migration of epithelial cells and, in the case of dermal wounds, keratinocytes. Any defect in the migration mechanism of the keratinocytes can result in a chronic non-healing wound [104]. Insulin-like growth factor-1 (IGF-1) facilitates cell spreading, stimulates membrane protrusion and migration of keratinocytes [105]. IGF-1-induced signaling events are subject to redox control and ROS-induced oxidative stress can upregulate IGF-1 action by increasing expression of IGF-1 and IGF-1 receptor (IGF-1R) [106-108].

Oxidative stress can induce proliferation and migration of smooth muscle cells and epithelial cells [109, 110]. Extracellular oxidative stress activates redox-sensitive pathways that increase Nox1-based NADPHox expression and vascular smooth muscle cell (VSMC) proliferation [111]. Matrix metalloproteinases (MMPs) are a class of enzymes that can degrade various components of cell-cell junction, cell-matrix contacts and extracellular matrix allowing different cells to migrate across the wound to promote re-epithelialization. Exogenous oxidative stress can activate MMP-2 and MMP-9 secreted from VSMCs [112]. Cells produce MMP-1 via Nox4 mediated and ROS-dependent pathway [113] and sustained exposure to ROS induced activation of pro-MMP-2 and increased cell motility [114]. Epidermal growth factor (EGF), transforming growth factor α (TGFα) and keratinocyte growth factor (KGF) are required for the proliferation of epidermal cells behind the migrating front [115]. ROS are capable of triggering EGF and KGF-dependent signaling and can also induce TGFα in fibroblasts [57]. Fibroblast

proliferation results in a collagen-rich scar tissue (granulation tissue) along with the formation of new blood vessels for nutrients and oxygen supply.

The importance of ROS in angiogenesis and tissue vascularization can be inferred from the study by Roy et. al. where decomposition of H_2O_2 by adenoviral gene transfer of catalase resulted in impaired wound tissue vascularization [116]. Also, Nox1 induced molecular markers of angiogenesis [e.g. vascular endothelial growth factor (VEGF)] were eliminated after co-expression of Nox1 and catalase, indicating that H_2O_2 plays an important role in the angiogenic switch [117]. Oxidants not only induce VEGF expression but play a central role in VEGF signaling and is discussed in detail by Sen and Roy [57]. Several small molecule antioxidants like GSH, vitamin C, vitamin E and polyphenols (quercetin, curcumin, resveratrol, etc.) have anti-angiogenic properties, which suggest a positive role for oxidants in tissue vascularization [57, 118].

As discussed in the above sections, cells use ROS for intracellular as well as intercellular cell-cell signaling and there by switch ON/OFF different responses in a timely manner to orchestrate wound healing. Two sources of ROS production at the wound site are i.) respiratory burst by immune cells and ii.) ROS producing Nox/Duox family of enzymes (e.g. NADPHox, NOS, SOD) that are also expressed in other cells like endothelial cells, fibroblasts, keratinocytes. ROS levels at the wound site are attenuated by small molecule antioxidant scavengers and antioxidant enzymes and the following section explains their role in wound healing mechanisms.

2.3.2 Role of Antioxidants in Wound Healing

2.3.2.1 Role of Small Molecule Antioxidants in Wound Healing

The importance of small molecule antioxidant scavengers in the wound healing process is evident from the findings that the levels of antioxidants decrease post-injury and their sustained deficiency results in an impaired or chronic wound. Small molecule antioxidants like glutathione, vitamin C, vitamin E (tocopherol) and polyphenols (e.g. catechins, flavanoids, etc.) regulate the redox state at wound sites by eliminating free radicals. **Table 2-3** provides a summary of effect of small molecule antioxidants on wound healing outcomes and their mechanism of action. Kamencic et. al. showed that oxidative stress caused after spinal cord injury resulted in reduced GSH levels. Post-injury administration of L-2-oxothiazolidine-4-carboxylate (OTC), a compound used to increase intracellular cysteine level required for GSH synthesis, elevated previously reduced GSH levels allowing tissue preservation in spinal cord [119]. Analysis of the antioxidant status of a self-healing cutaneous wound at different times after wounding demonstrated that the levels of small molecule antioxidants (GSH, vitamin C & E) in injured tissue decreased by 60-70% as compared to normal skin and only GSH levels were recovered completely 14 days post-wounding [120]. The same group found that glutathione and vitamin E levels in wound tissue of aged rats were lower as compared to young rats, which could explain the delayed wound healing observed in the aged rats. In streptozotocin-induced diabetic rats, the 7-day wound tissue had lower levels of GSH (in contrast to elevated levels of vitamin E) which indicates that reduced levels of GSH could be responsible for delayed wound healing [121].

Among diabetic patients with foot ulcers, the wound edge tissue as compared to control tissue had lower levels of GSH and cysteine, whereas elevated levels of mixed protein disulfides. Lower GSH levels were found in wound tissues of diabetic mice as compared to non-diabetic mice [122]. Hydrocortisone-treated immunocompromised rats also showed reduced levels of GSH, vitamin C and E in both normal and wounded skin (2 days post-wounding) as compared to immunocompetent rats. 7 days post-wounding, levels of vitamin C and E in wound tissue of immunocompromised were similar to that of immunocompetent rats, but GSH level remained depleted even after 2 weeks [123] When rats were depleted of GSH using L-buthionine-(*S,R*)-sulfoximine (BSO), an inhibitor of rate-limiting enzyme in biosynthesis of GSH (γ-glutamylcysteine synthetase), there was a reduction in wound bursting strength as compared to untreated animals [124]. The same group also demonstrated that GSH levels are significantly lower in ischemic skin flaps, but preconditioning enhances skin flap survival by increasing activity of glutathione reductase and maintaining GSH levels [125]. All these results considered together indicate that depletion of small molecule antioxidants disturb the redox state of the wound and result in an impaired healing response. Restoring the redox balance in the wounds by application/delivery of small molecule antioxidants would be a viable strategy to improve the healing response.

Topical application of glutathione monoester (GME), a drug used to increase intracellular GSH content, using carboxymethylcellulose (CMC) vehicle in a diabetic mice wound model resulted in significantly faster healing [122, 126].

Table 2-3 Role of Small Molecule Antioxidants in Wound Healing

Small Molecule Antioxidants	Administration Route	Wound Healing Parameters Affected	Mechanism	[Ref]
Glutathione	Topical application of glutathione monoester, administration of OTC	Faster healing	Restoring cellular redox potential by suppressing oxidative stress	[119, 122]
Vitamin E	Oral	Faster wound closure	Suppressed lipid peroxidation	[127]
Ascorbic acid (Vitamin C)	Oral, Topical	Increased proliferation of fibroblasts and improved collagen synthesis	Allows normal collagen hydroxylation (of proline residues) and is required to reduce Fe^{3+} In human dermal fibroblasts, improved cell motility as a result of increased expression of uPA, hyaluronan-mediated motility receptor and IL-6 expression	[128-131]
Curcumin	Topical	Faster wound closure, increased migration of fibroblasts and myofibroblasts resulting in higher collagen deposition	Reduced lipid peroxidation Upregulation of levels of TGF-β1 and uPA Anti-inflammatory properties - In cultured A549 cells, suppressed H_2O_2 and TNF-α induced release of NF-κβ, AP-1, IL-8 and increased GSH biosynthesis	[132-134]

Dietary supplementation of diabetic rats with palm vitamin E (70% tocotrienols and 30% tocopherols) extract (PVE) and α-tocopherol in an excisional wound model showed that PVE was more effective at enhancing wound healing and inducing antioxidant enzyme levels in the wounds of diabetic rats as compared to α-tocopherol. However, both antioxidants were able to reduce lipid peroxidation in healing wounds, as measured by lower MDA levels [127]. The difference in the potencies of PVE and α-tocopherol could be attributed to the higher percent tocotrienols content of PVE or preferential pharmacokinetic distribution of tocotrienols in skin. Orally administered tocotrienols have better distribution in skin (15% tocotrienols distributed in the skin as compared to 1% tocopherols) and in some conditions tocotrienols have been reported as more potent antioxidants against lipid peroxidation than tocopherols [135-137]. Although the reasons for impaired wound healing in diabetic mice are not completely understood, an altered VEGF mRNA expression as a result of lipid peroxidation is one of the characteristics of wound healing defect among diabetic mice. Inhibition of lipid peroxidation in diabetic mice by systemic treatment with raxofelast, a hydrophilic vitamin E-like inhibitor of lipid peroxidation, normalized VEGF mRNA expression and secretion resulting in improved wound healing and angiogenesis [138, 139]. This effect of raxofelast was not seen in non-diabetic mice [139].

Curcumin (diferuloylmethane), a yellow pigment present in the Indian spice turmeric, is a polyphenolic antioxidant that also interacts with several cell signaling proteins and thereby exert its anti-cancer, anti-inflammatory, anti-angiogenic, etc. effects [140-142]. Enhancement of wound healing by curcumin has been demonstrated in several studies [132]. Topical application of curcumin in full thickness excision wound model

resulted in increased cellular proliferation and collagen synthesis at the wound site and making wound heal faster. Curcumin exerted antioxidant effect at the wound site by decreasing lipid peroxidation and topical treatment resulted in increased activity of antioxidant enzymes SOD, catalase and GPx [143]. Biopsies of curcumin-treated animal wounds showed increased migration of fibroblasts, myofibroblasts, macrophages, improved neovascularization and higher collagen deposition at wound site. Immunohistochemical, in situ hybridization and polymerase chain reaction analysis showed an increase in transforming growth factor-β1 (TGF-β1) levels and TGF-β1 mRNA expression, indicating that curcumin-treatment induced endogenous production of TGF-β1 in the wound of both diabetic and non-diabetic mice [144, 145]. TGF-β1stimulates fibroblast proliferation and enhances fibroblast production of collagen and fibronectin, thereby playing an important role in production of extracellular matrix [146]. TGF-β1 has also been suggested to induce epidermal keratinocytes to express integrins that facilitate the migratory component of re-epithelialization [147]. Madhyastha et. al. have observed curcumin-induced and JNK and p38 MAPK mediated upregulation of urokinase plasminogen activator (uPA) gene expression, and that uPA upregulation is important in promoting fibrinolysis, matrix remodeling and cell migration, two mechanisms that are vital for wound healing [133, 148]. Faster wound closure and enhanced collagen deposition in curcumin-treated wounds could be a result of curcumin-induced TGF-β1 production and uPA upregulation. In cultured alveolar epithelial cells (A549), curcumin suppressed H_2O_2-induced and TNF-α-induced NF-κβ, activator protein-1 (AP-1) and IL-8 release, exerting its anti-inflammatory properties. In the same study, curcumin-treatment of A549 cells resulted in an increased GSH biosynthesis and

glutamylcysteine ligase catalytic subunit mRNA expression, suggesting that antioxidant properties of curcumin do not depend only on its free radical scavenging ability [134].

Beneficial effects of vitamin C (ascorbic acid) on wound healing in humans was reported by Ringsdorf and Cheraskin [128]. Topical application of vitamin C in a incisional wound model resulted in faster wound healing marked by reduced number of macrophages, increased proliferation of fibroblasts and new vessels, and thicker and more organized collagen fibers in the wounds [129]. Intraperitoneal administration of vitamin C prior to γ-radiation resulted in elevated wound contraction in a dose-dependent manner and improved healing of the wounds after whole body exposure to γ-radiation [149]. Ascorbic acid can regulate the extra cellular matrix synthesis by inducing increased collagen synthesis in human dermal fibroblasts. Stimulatory effect of vitamin C on collagen production results from its action in allowing normal collagen hydroxylation and restoring efficient collagen secretion [130]. Enzymatic mechanism suggested for hydroxylation of collagen (proline residues) occurs through a reactive iron-oxygen complex (the ferryl ion) and that ascorbic acid is required to reduce Fe^{3+} formed during the reaction [150]. Long term treatment of human dermal fibroblasts with L-ascorbic acid 2-phosphate (AA2P), a stable vitamin C derivative, resulted an increase in cell motility in context of wound healing. Microarray analysis showed that AA2P treatment increased the expression of uPA, upregulated the hyaluronan-mediated motility receptor which is required for fibroblast migration in the context of wound healing and IL-6, which also promotes cell motility and matrix remodeling during wound healing [131].

Studies with other small molecule antioxidants like quercetin, allopurinol, retinoids (e.g. vitamin A, tretinoin) and uric acid have shown enhanced wound healing

and improved collagen content at wound site indicating that scavenging free radicals has a beneficial effect on overall wound healing process [151-154].

2.3.2.2 Role of Antioxidant Enzymes in Wound Healing

Table 2-4 provides a summary of effect of antioxidant enzymes on wound healing outcomes and their mechanism of action.

2.3.2.2.1 SOD

Importance of SOD in wound healing can be inferred from the finding that SOD1 deficiency resulted in a delayed wound healing response [155]. Steiling et. al. have studied spatial and temporal expression of different antioxidant enzymes during cutaneous wound repair and found that SOD1 and SOD2 mRNA levels were upregulated during early phase of wound repair when the oxidative burst occurs. *In situ* hybridization and immunofluorescence data indicated that Cu/ZnSOD is expressed in basal cells of the hyperproliferative epithelium at wound edge and in the granulation tissue. SOD2 was expressed in both, basal as well as suprabasal cells of hyperproliferative epidermis [156]. Contrary to this data, Shukla et. al. had reported reduced activity of SOD after cutaneous injury and that SOD activity was not recovered even after 14 days [120]. This inconsistency in the mRNA expression and enzyme activity reported in the two studies could be a result of loss of enzymatic activity of SOD at wound site due to oxidative environment at the wound site [157, 158].

Intravenous administration of SOD in an ischemic skin injury model resulted in a reduction in edema and increased the wound breaking strength and collagen synthesis at wound site [152]. Delayed healing in streptozotocin-induced type 1 diabetic mice was

Table 2-4 Role of Antioxidant Enzymes in Wound Healing

Antioxidant Enzymes	Administration Route	Wound Healing Parameters Affected	Mechanism	[Ref]
Catalase	Overexpression of catalase by adenoviral gene delivery, topical application	Impaired wound angiogenesis, closure and slowed tissue remodeling Improved dental pulp tissue healing in	Low concentrations of H_2O_2 mediate wound angiogenesis by VEGF expression	[116, 159]
SOD	Intravenous SOD and SOD mimetic, cutaneous gene therapy of MnSOD	Reduced wound edema, increased collagen synthesis and new blood vessel formation	Reduced hyperglycemia-induced ROS	[152, 160, 161]
Peroxiredoxin	Transgenic over expression of Prdx6	Enhancement of wound closure in aged mice and reduced number of apoptotic cells after UVA/UVB irradiation	Prdx6 deficient endothelial and inflammatory cells are more susceptible to ROS treatment Prdx6 knockout mice showed severe hemorrhage in granulation tissue	[162, 163]

restored by a single regimen of cutaneous gene therapy of MnSOD, marked by reduced superoxide levels and increased cutaneous MnSOD and NOS activity [161]. The same group also demonstrated that poor wound healing in diabetic mice is a result of decreased MnSOD expression and activity in endothelial progenitor cells (EPCs), which normally assist angiogenesis at wound site. By restoring diabetic EPC function after ex vivo MnSOD gene transfer prior to their transplantation at the wound site resulted in an enhanced and accelerated wound healing. Enhanced wound healing effect was also observed by increasing the number of transplanted diabetic EPCs [164]. Also, transgenic diabetic mice that overexpress MnSOD or treatment of diabetic mice with SOD mimetic corrected post-ischemic defects in neovascularization, oxygen delivery, chemokine expression and normalized tissue survival [160]. These results taken together demonstrate that scavenging superoxide can correct impaired wound healing process.

2.3.2.2.2 Catalase and Glutathione Peroxidase

Catalase and GPx at the wound site keep a check on the levels of H_2O_2 generated by SOD from superoxide anion. Steiling et. al. showed that catalase and GPx were coexpressed along with SOD in the wound. Along with Cu/ZnSOD and MnSOD, only the levels of selenoenzymes GPx (SeGPx) mRNA were upregulated during early phase of wound repair where as catalase and phospholipid hydroperoxide GPx (PhGPx) mRNA levels did not alter after injury. Like SOD, catalase and GPx mRNA expressions were also prominent in the hyperproliferative endothelium but were found in lower levels in the granulation tissue. Similar expression pattern of SOD, catalase and GPx suggests that H_2O_2 produced by SOD is detoxified by catalase and GPx before it could react with transition metal ions to generate deleterious hydroxyl radicals [156]. However, Shukla et.

al. have shown that catalase activity in the healing wounds decreased during the first week post wounding and activity level of catalase was recovered to its original level at 2 weeks post-wounding [120]. Again as mentioned above, the discrepancy in the mRNA expression of catalase and the activity of catalase could be a result of enzyme inactivation or translational failure to code protein to due to the oxidative environment at the wound site.

Unexpectedly, catalase overexpression by adenoviral gene delivery impaired wound angiogenesis, closure and slowed tissue remodeling [116]. H_2O_2 by itself or H_2O_2 generated by overexpression of SOD1 via gene transfer induces VEGF expression in wound related cells [165-167] and low concentration of H_2O_2 present at the wound was important, mediating angiogenesis by up-regulating VEGF expression. However, in a separate study by Alacam et. al., topical application of catalase as a pulp-capping agent improved long-term (after 90 days) dental pulp tissue healing in a canine injury model [159].

2.3.2.2.3 Peroxiredoxins

Kümin et. al. studied expression of peroxiredoxins post injury in a full-thickness excisional wound model and found enhanced expression of Prdx6 and moderate increase in expression of Prdx4 as compared to unaltered expression of Prdx1 and Prdx2 [168]. Levels of Prdx6 mRNA were highest at day 1 after injury, remained elevated till day 7 and levels reduced back to normal skin level 14 days post wounding when the wound was completely healed [169]. Using an *in situ* hybridization technique, it was found that *in vivo*, Prdx6 mRNA was highly expressed by keratinocytes of the hyperproliferative epidermis of skin wounds, although other cells in the granulation tissue also expressed

Prdx6 mRNA [170]. Since wound healing response was associated with altered Prdx6 levels as compared to other five peroxiredoxins, Kümin et. al. have studied effect of Prdx6 overexpression and underexpression on wound healing [162, 168]. Although Prdx6 knockout mice develops normally, they were found to be more susceptible to oxidative stress injury induced by intraperitoneal injection of paraquat, suggesting that Prdx6 aides in the regulation of superoxide mediated oxidative stress. Also, macrophages from these Prdx6 knockout mice had lower survival rates against oxidative insult induced by H_2O_2, t-butyl hydroperoxide and paraquat [171]. Even though Prdx6 expression was predominant in the hyperproliferative epidermis of skin, cutaneous injury to the Prdx6 knockout mice resulted in normal wound epithelialization indicating that other antioxidant enzymes in these cells can compensate for absence of Prdx6. However, severe hemorrhage in the granulation tissue of the knockout mice was observed and the extent of hemorrhage correlated with the oxidative damage to the granulation tissue as indicated by presence of oxidized proteins and nitrotyrosine positive cells. At the ultrastructural level in the wound tissue of Prdx6 knockout mice, endothelial cells appeared to be damaged and their rate of apoptosis was also enhanced. Increased susceptibility of cultured endothelial cells to oxidative stress after siRNA-mediated knock-down of Prdx6 confirmed sensitivity of endothelial cells to loss of Prdx6. Wound healing studies in the bone marrow chimeric mice indicate that Prdx6-deficient inflammatory and endothelial cells contribute to the hemorrhage observed in the granulation tissue. This study also revealed the ROS mediated cross-talk between hematopoietic cells and resident cells at the wound [168]. Overexpression of Prdx6 in transgenic mice did not affect their skin morphogenesis and homeostatis. Keratinocytes

cultured form Prdx6 overexpressing mice showed enhanced resistance to ultraviolet A (UVA) and menadione-induced oxidative damage. Upon skin injury to these transgenic mice, enhanced wound closure was observed in aged animals, suggesting that overexpression of Prdx6 protected the skin from age related accumulative oxidative damage which is responsible for poor wound healing in aged animals [162].

2.3.3 "Antioxidant Materials" for Wound Healing

As described, antioxidants clearly play an important role in ROS mediated inter-cellular and intra-cellular signaling and pro-healing effects of several antioxidants. However, sub-optimal delivery of antioxidants to the wound site has complicated their use as a regenerative medicine strategy. Antioxidants could be delivered at wound site via oral route (or dietary supplementation), intravenously or direct dermal application to the wound. Several studies have shown that oral administration of antioxidants has a beneficial effect on wound healing [127, 172]. However, unfavorable pharmacological distribution of these antioxidants means that large doses are required for the antioxidants to reach a therapeutic concentration at the wound site, and the wound healing effect if any would be slow. Large doses of antioxidants for prolonged period could also result in other side effects. Also, oral delivery of AOE has been at best marginally effective [173]. All these drawbacks make oral delivery a less attractive option for wound healing applications. Direct application of antioxidants on the wound (e.g. topical application) seems to be an easier and effective way of antioxidant delivery to the wound site. However, direct application of antioxidants is limited by, i.) rapid clearance, ii.) stability and iii.) choice of material used to deliver antioxidants.

Loading antioxidants into a synthetic scaffold, a film or a porous 3D network, that acts as a diffusion barrier could be used for slow and controlled release of antioxidants from the scaffolds. Full thickness dermal wounds in rats that were treated with curcumin and quercetin incorporated collagen films showed increased wound reduction and enhanced cell proliferation as compared to control and collagen treated animals [151, 174]. Incorporation of curcumin in electrospun nanofiber mats of cellulose acetate and poly(ε-caprolactone) (PCL) resulted in a sustained release of curcumin over ~ 3 days [175, 176]. Fibroblasts cultured on curcumin-loaded PCL nanofibers showed resistance to H_2O_2 induced oxidative stress and mouse macrophages cultured on curcumin-loaded PCL nanofibers reduced LPS induced IL-6 expression, a marker of inflammation. In a streptozotocin-induced diabetic mice wound model, curcumin-loaded PCL nanofibers had a pro-wound healing effect as evidenced by increased rate of wound closure [175]. Hydrogels, three dimensional network of hydrophilic polymers, can be used for immobilizing antioxidant enzymes to prevent inactivation of enzymes otherwise caused by direct application. Study by Chiumiento et. al. where they loaded carboxymethylcellulose (CMC) hydrogels with SOD and treated the rat wounds with CMC-SOD found that CMC-SOD reduced the time necessary for wound healing. Also, CMC-SOD had a proliferative effect on primary human fibroblasts [177].

Effectiveness of scaffold based antioxidant therapy would also depend on the biomaterial used for the synthesis of the scaffold, since in some settings biomaterials could themselves induce an inflammatory response from the host tissue [178]. This inflammatory response is often the result of local accumulation of the polymer degradation byproducts or leachouts, inducing cellular oxidative stress [179-182]. One of

the approaches to suppress biomaterial induced inflammatory response could be to conjugate small molecule antioxidants like ascorbic acid, vitamin E, GSH, gallic acid, catechin, etc. to the polymer ('antioxidant polymers') [183-186]. Conjugation of low molecular weight superoxide dismutase mimetic (SODm) to implanted biomedical materials like ultra-high molecular weight polyethylene (UHMWPE), poly(etherurethane urea) and tantalum metal suppressed both chronic and inflammatory responses to the implants as evident by fewer neutrophils (after 3 days), fewer foreign body giant cells (FBGCs) (after 28 days) and inhibition of fibrous capsule formation [187]. Also, incorporation of NAC in poly(methyl methacrylate) (PMMA) bone cement reduced cytotoxicity of PMMA by scavenging free radicals and increasing GSH levels in osteoblasts, resulting in increased bone formation with higher strength [188]. Antioxidant polymers could not only be used to improve biocompatibility, but could also serve as a means of delivering antioxidants at the wound site. Some of the above mentioned examples of antioxidant polymers [184, 186] are limited by low percentage of antioxidant content as compared to the bulk material. If designed appropriately by increasing their percent antioxidant content and controlling the degradation rate (rate of release of antioxidants), antioxidant polymers can be used effectively for antioxidant delivery at the wound site.

2.4 Role of Oxidative Stress in Biocompatibility of Biodegradable Materials

Over the decades, biocompatibility has evolved from simply meaning an inert material [189, 190], which does not induce any deleterious tissue response, to the William's definition, "the ability of a biomaterial to perform its desired function without eliciting any undesired effect, but generating a beneficial cellular or tissue response"

[191]. This shift in definition has accompanied our ever increasing understanding of the biological response to materials, which depends on the physiochemical properties, including shape, surface chemistry and, for degradable materials, the rate of degradation and degradation products. The summation of these properties can result in responses varying from the chronic inflammatory foreign body giant cell response to fibrous encapsulation to complete tissue integration [192, 193].

Recent studies have demonstrated that even materials, which are classically considered biocompatible and FDA approved (e.g., poly(lactic acid)), can induce a pathological response. For instance, the degradation products of poly(lactic acid) have been shown to induce the oxidative stress response [179, 193, 194]. Monomers like bisphenol-glycidyl-methacrylate and 2-hydroxy-ethyl methacrylate, which are commonly used additives in dental bonding agents and resin composites, induce ROS production in human dental pulp cells and pulp fibroblasts leading to pulpal inflammation [195-197]. Detection of biomaterial-induced ROS is currently being used to characterize the inflammatory host tissue response to the biomaterial, in both *in vitro* and *in vivo* models [198, 199]. It is believed that control over this oxidative stress is a logical means of tuning the biological response to materials, improving their apparent biocompatibility.

2.5 Vascular Oxidative Stress

Vascular oxidative stress has been implicated as a key mechanism in the pathogenesis of many disease states (**Table 2-1**) [200] and is characterized by a dysfunctional endothelium, which is a key target for antioxidant therapy. Oxidative stress in the endothelium can be initiated and/or propagated due to exposure of EC to pro-oxidants circulating in blood (oxidants released by activated leukocytes and platelets or

oxidized low-density lipoproteins) [201], oxidants produced by cellular milieu (extracellular matrix, other vascular cells) or oxidants generated by endothelial cells themselves [200]. VOS results in endothelial production of oxidants and expression of various inflammatory cytokines, which then influence the expression of inflammatory signals such as cell adhesion molecules (CAM) like ICAM-1, VCAM-1, etc [12, 14] (discussed in detail in **Section 2.3.1**). These CAMs facilitate endothelial-leukocyte interactions which further damages endothelial cells (EC) by releasing more oxidants [200, 202]. Oxidative stress and inflammatory response thus operate in vicious cycle to damage endothelium and result in a diseased state.

2.5.1 Challenges in Delivery of Antioxidants to Suppress Oxidative Stress

Both, small molecule oxidant scavengers (e.g. tocopherol, glutathione, etc.) and antioxidant enzymes (e.g. SOD, catalase, etc.), have their own unique set of delivery challenges. Small molecule antioxidants are well tolerated, stable for long term storage, resistant to complex and/or aggressive formulation processing methods and relatively inexpensive. However, these small molecule scavengers typically reduce free radicals and other oxidizing species in stoichiometric ratios, being consumed in the process [203, 204]. Hence, large sustained doses are expected to be required in order to observe a significant clinical effect.

Besides their high potency, antioxidant enzymes are also highly selective, allowing for a more targeted approach to antioxidant therapy not possible with small molecule antioxidants. However, antioxidant enzymes are relatively fragile and expensive, limiting the set of conditions which can be used for their formulation [173].

Further, they are prone to proteolytic and pH dependant inactivation, which can limit their therapeutic duration [205, 206].

2.5.2 Nanocarriers for Vascular Delivery of Antioxidants

As mentioned in **Section 2.1**, the success of antioxidant therapy for treatment of vascular oxidative stress depends on sufficient delivery of antioxidants to the endothelium and the duration for which the delivered antioxidants stay active. While the exact requirements needed depend upon the disease state being considered, nanoscale drug carriers are a promising avenue for achieving these goals. The following section reviews some of the existing nanocarrier startegies for antioxidant delivery and then explains the need for antioxidant polymers as a novel strategy for treatment of vascular oxidative stress.

2.5.2.1 Liposomes

Liposomes, one of the first and most widely studied carrier for drug delivery applications, are membrane vesicles formulated using naturally derived phospholipids or synthetic amphiphiles. Amphiphiles when dispersed in aqueous medium, self-assemble in a spheroidal membrane type arrangement where the hydrophobic lipid part of the molecules associate with each other whereas the hydrophilic heads are exposed to the aqueous phase, resulting in entrapment of aqueous phase in the spherical core. Extrusion and sonication are the most commonly used methods for the formulation of liposomes in the size range of 50 nm to 10 μm or more. Size of liposomes formulated using extrusion is determined by the pore size of the polycarbonate filter used for extrusion.

Spherical aqueous core and the lipid membrane domain can be used for loading hydrophilic and hydrophobic drugs respectively. Drug loading in the liposomes is determined by the equilibrium partitioning of the drug inside and outside the liposome. Since partitioning decreases with increase in MW of drug, liposomes are more suited for encapsulating low molecular weight hydrophilic drugs into the aqueous compartment. Some of the water-soluble antioxidants that can be loaded into liposomes include glutathione, N-acetyl cysteine (NAC) and ascorbic acid (vitamin C). Intratracheal liposomal delivery of NAC provided more pulmonary protection in a 2-chloroethyl ethyl sufide (CEES) injury model as compared to free NAC[207]. As opposed to large hydrophilic capacity, liposomes have a relative low hydrophobic capacity (~ 10-20% for 100 nm liposome) for drug loading. Nonetheless, this can be used for loading hydrophobic antioxidants like α-tocopherol (vitamin E) [207-209], resveratrol [210], curcumin [211] and flavonoids (e.g. quercetin, catechin) [212]. Liposomes improve the bioavailability of such hydrophobic compounds. Loading of large hydrophilic enzymes into liposomes is rather difficult. Freeze/thaw, freeze drying, pH gradient and electrostatic attraction have been used to improve the loading of antioxidant enzymes into liposomes [213-216].

Several liposomal formulations of vitamin C, vitamin E and other small molecule antioxidants have been successfully used for dermal applications in the cosmetic industry [217, 218]. Liposomes have also been commercially used as delivery vehicles for various pharmaceutics [219-221]. However, their use for the delivery of antioxidants through intravenous route has been limited due to their poor mechanical stability, poor circulation half-life and their rapid clearance through reticuloendothelial system (RES) [218, 222].

2.5.2.2 Solid Lipid Nanoparticles

Solid lipid nanoparticles (SLN) are another lipid based carrier like liposomes, only difference being the lipids used (triglycerides and waxes) that are solid at room and physiological temperature. SLN are formulated either using high pressure homogenization or emulsification techniques at elevated temperatures with/without surfactants [223, 224]. Lipids used for SLN formulation are naturally derived and are likely to be well tolerated. The large hydrophobic core of SLN makes them a suitable delivery vehicle for carrying high loads of hydrophobic small molecule antioxidants. Several lipophilic small molecule antioxidants like vitamin E, baicalin, retinol, quercetin, curcuminoids and resveratrol were successfully loaded into SLN [225-230]. However, the harsh formulations conditions (e.g. high temperature and high shear) of SLN are not suitable for loading antioxidant enzymes which may lose activity during formulation.

2.5.2.3 Polymer Nanoparticles

Biodegradable polymeric nanoparticles are a logical choice for delivery of antioxidant enzymes. Through the encapsulation of enzymes within a diffusion limiting polymer shell, the enzyme can be protected from premature proteolytic inactivation. Further, through tuning of the substrate diffusion properties of the encapsulating material, it is possible to impact the selectivity of the loaded enzyme [231]. Finally, as the enzyme is functional in the loaded state, the duration of activity can be controlled through the degradation rate of the polymer, with release of drug presumably possessing only transient activity.

Poly(lactic acid) (PLA), poly(lactic acid-co-glycolic acid) (PLGA) and poly(ε-caprolactone) have been formulated into nano and microparticles for controlled release of

drugs [232, 233]. Amphiphilic di-block copolymers (e.g. PEG-PLA, PEG-PLGA) can provide native "stealth" properties to polymer nanoparticles as well sites for conjugating targeting moieties. Nanoparticles of amphiphilic polymers can be synthesized using solvent evaporation, polymer micellization or multiple emulsification steps [234-236]. However, not all formulation settings can be used to load enzymes. For instance, single step solvent extraction techniques typically result in poor protein loading, as the hydrophobic particles exlude the hydrophilic protein. Further, the use of aqueous miscible solvents (e.g., acetone, ethanol, methanol), can result in enzyme inactivation. Using a unique temperature swing double emulsion methods, polymer nanoparticles were formulated to achieve active catalase loading [206, 237]. These carriers were able to prolong enzymatic activity in a proteolytic environment, with 25% of the loaded enzyme mass remaining stably active after 24hours incubation, compared to free enzyme which lost >90% activity within 1 hour. This method was found to be amendable to a variety of enzymes. Interestingly, enzymes whose substrates were slowly diffusing through the polymer shell possessed no measurable activity following proteolytic incubation, suggesting the ability for the carrier to augment the observed specificity of the loaded enzyme [231].

2.5.2.4 Polymersomes

Polymersomes (or polymer vesicles), synthetic polymer based analogs of phospholipid liposomes, are another class of polymer nanocarriers, which are composed of polymer amphiphiles that self-assembled into bilayer like structures (e.g., PEG-PLA, PEG-PBD(poly butadiene), PEG-poly(propylene-sulfide)-PEG) [238, 239] (for detailed review, refer to [240]). Like liposomes, polymersomes have large internal aqueous

domain that can be used for loading hydrophilic drugs. Thicker membrane of polymersomes (~8 nm as compared to ~3 nm for liposomes) make them a more robust carrier that can resist membrane deforming forces which disrupt the liposomal membrane [238]. Also, owing to the higher PEGylation density of polymersome surface, polymersomes have a two-fold higher circulation life (20-30 hrs in rats) as compared to liposomes [241]. Polymersomes have been used to load significant amounts of hydrophilic and hydrophobic anticancer drugs into aqueous core and membrane respectively [242-244]. Polymersomes can be used for simultaneous loading of both water-soluble and water-insoluble small molecule antioxidants for a robust antioxidant therapy. However, more rigorous encapsulation conditions (e.g. high temperature, pressure) for polymersome formulation can result in loss of enzyme activity which make polymersomes a non-ideal candidate for loading antioxidant enzymes [5, 245].

2.5.2.5 Polymer Nanocapsules

Encapsulation of a single protein molecule in polymeric shells, called "single-protein nanocapsules", is one of the novel approaches applied for protein delivery [246]. In this approach, several proteins, including SOD, were covalently functionalized with vinyl groups followed by free radical polymerization in the presence of other diacrylate monomers which resulted in encapsulation of single protein molecules in a nanometer thick (~ 5 nm) polymer shell. Surface properties and degradation rates of polymer shells was controlled by choosing appropriate monomers. SOD nanocapsules prevented cell death in a *in vitro* paraquat injury model, suggesting that the polymer shells are permeable to the substrate molecules (e.g. $O_2^{\cdot -}$) and protect the enzyme from proteolytic degradation [246].

Polymer nanocapsules having large aqueous cores synthesized from (allyloxy)12cucurbit[6]uril, a rigid disk-shaped molecule, is another potential approach for protein delivery[247]. Even though their applicability for delivery of antioxidants has not been studied, work done by Kim et al. on developing a polymer nanocapsule incorporating disulfide bridges that can degrade in a reducing environment could be very applicable for release of antioxidant enzymes triggered by reduced environment in the host cell [248].

2.5.4 "Antioxidant Polymers" for Vascular Delivery of Antioxidants

As discussed above, for small molecule antioxidant therapy to be successful, large sustained doses at the injury site are required. However, small molecule antioxidants have a concentration dependant anti- or pro-oxidant effect, where delivery of small molecule antioxidants in excess (e.g. burst release from nanocarriers) can induce an undesired pro-oxidant effect in host tissue [249-251]. Hence, nanocarriers for small molecule antioxidants should be designed for delivery of significant amounts, but at a gradual and controlled rate.

This makes delivery of small molecule antioxidants challenging as most of the carriers can achieve a maximum loading of ~35% for small molecule drugs [252-254]. As a result, in order to achieve sufficient antioxidant levels, large carrier masses may be needed, which may induce unwanted immunogenicity. Further, the passive loading of free small molecule drugs into nanocarriers can often result in limited control of drug release profiles [255]. Incorporating small molecule antioxidants covalently in a biodegradable polymer backbone permits a mechanism to overcome both of these limitations, by 1) enhancing the total mass of drug in the nanocarrier and 2) allowing

chemical cleavage to control the release rate. Many small molecule antioxidants have reactive groups like phenols and thiols, which can be easily functionalized and incorporated into polymers using polyester, polyanhydride or poly(β-amino ester) chemistry [256]. This approach provides that added benefit of protecting the labile center from premature oxidation.

Several approaches have been pursued to covalently conjugate small molecule antioxidants to polymers and proteins. For instance, Vitamin E was conjugated to poly(acrylic acid) to synthesize a water-soluble carrier for vitamin E that suppressed oxidative stress in sperm cells *in vitro* [183]. Antioxidant polymers with glutathione, ascorbic acid, gallic acid and catechin conjugated to PEG, poly(methyl methacrylate) and gelatin have also been synthesized and shown to have antioxidant properties *in vitro* [184-186]. However, these antioxidant polymers are limited by their low relative mass of antioxidant compared to the bulk material. There is need for antioxidant polymers with high "% antioxidant loading" that can be formulated into nanoparticles allowing for vascular delivery of these antioxidants.

2.6 Conclusion – Rationale for Antioxidant Polymers

Oxidative stress plays a critical role in wound healing, biocompatibility of materials and other vascular diseases. Translation of small molecule antioxidant therapy for treatment of oxidative stress into clinical success depends on i.) delivery of antioxidants in significant amounts, ii.) gradual release of antioxidants (i.e. control over rate of release) and iii.) minimizing undesired immunogenicity from carrier/delivery agent. Antioxidant polymers, where small molecule antioxidants are incorporated into a biodegradable polymer backbone, is an emerging area of research which may have huge

impact in the field of biomaterials. As demonstrated, antioxidant polymers have potential to address some of the problems related to the treatment of non-healing wounds, improving biocompatibility of materials and treatment of vascular oxidative stress through controlled delivery of small molecule antioxidants.

This dissertation describes synthesis, characterization and evaluation of antioxidant polymers to suppress oxidative stress. Taking advantage of polymer chemistry, phenolic antioxidants were polymerized into polyesters and poly(β-amino esters). *In vitro* degradation characteristics of synthesized antioxidant polymers and their ability to suppress oxidative stress injury in the cells were studied. Also, effect of antioxidant polymers on the redox state of the cells in absence of injury agent was characterized.

Chapter 3. Research Goals

3.1 Introduction

In this dissertation, antioxidant polymers are developed which upon degradation release active antioxidant scavenger molecules. These polymers are formulated either into polymer nanoparticles or hydrogels to study their degradation characteristics, cytotoxicity and ability to suppress oxidative stress in *in vitro* cell culture models. By delivering small molecule antioxidants in a controlled manner, it may be possible to treat a variety of diseases where oxidative stress plays a critical role in the pathophysiology of the disease. The robustness of this proposed small molecule antioxidant therapy will depend on the tunability of antioxidant polymers to deliver various antioxidants at different rates, which often vary depending on the disease.

3.2 Objectives and Significance

The overall hypothesis of this work is :

Antioxidant polymers can be synthesized that upon biodegradation release active antioxidants which can then scavenge free radicals to protect cells/tissues from oxidative stress injury.

In order to test this hypothesis, research was planned in three distinct stages, described in the following sections as specific aims, each to test a specific hypothesis.

3.2.1 Specific Aim 1: Synthesis and characterization of poly(trolox ester)

A. Synthesis of poly(trolox ester) and its characterization using Fourier Transformed Infrared Spectroscopy (FTIR), ^{1}H and ^{13}C Nuclear Magnetic

Resonance (NMR) Spectroscopy and Gel Permeation Chromatography (GPC).

B. Formulation of poly(trolox ester) nanoparticles with control over their size.

C. Study *in vitro* degradation of poly(trolox ester) nanoparticles, determine antioxidant activity of degradation products and determine their cytotoxicity.

3.2.1.1 Hypothesis #1

Trolox can be polymerized into a poly(ester) form using carbodiimide based condensation reaction and degradation products of poly(trolox ester) will have antioxidant potential to scavenge free radicals without exerting any cytotoxic effects.

3.2.1.2 Significance and Outcome

Experiments carried out to test this hypothesis are explained in C**hapter 4**. Using Steglich esterification reaction, poly(esters) of trolox with two different molecular weights, PTx-1000 and PTx-2500 were synthesized. FTIR and ^{13}C NMR characterization confirmed successful esterification reaction to synthesize PTx-1000 and PTx-2500. GPC analysis was used to determine molecular weight of synthesized polymers. Single emulsion technique was employed to formulate polymer nanoparticles with controlled size. Poly(trolox ester) nanoparticle degrade very slowly by hydrolysis. However, they are susceptible to enzymatic degradation and degradation products have radical

scavenging ability as measured using a *in vitro* assay. Poly(trolox ester) nanoparticles had very little to no cytotoxicity up to a concentration of 1 mg/ml.

3.2.2 Specific Aim 2: Investigate Effect of Poly(trolox ester) on Oxidative Stress in the Cells, Both in the Presence and Absence of Injury Agent

A. Study the protective effect of poly(trolox ester) nanoparticles against metal nanoparticle induced oxidative stress injury.

B. Study the concentration dependant effect of trolox and poly(trolox ester) nanoparticles on the redox state of the cells.

C. Use protein oxidation as a marker of oxidative stress to determine effect of poly(trolox ester) nanoparticles on the redox state of the cells.

3.2.2.1 Hypothesis #2

Poly(trolox ester) nanoparticles suppress oxidative stress in the cells, both in presence and absence of oxidative injury, and can be used to modulate redox state of the cell.

3.2.2.2 Significance and Outcome

Chapter 5 describes the experiments carried to test this hypothesis. DCF fluorescence was successfully used to monitor oxidative stress levels in the cells. Treatment with poly(trolox ester) nanoparticles protected cells from the metal nanoparticle induced oxidative stress injury. In the absence of injury, poly(trolox ester) nanoparticles suppressed background oxidative stress levels in the cells as measured by DCF fluorescence as well as by protein carbonyl measurements. Monitoring oxidative stress in the cells using DCF fluorescence revealed concentration dependant prooxidant

and antioxidant effect of trolox, whereas measurement of redox state using cellular protein oxidation products did not exhibit this effect of trolox. This emphasizes the importance of delivery route in modulating redox state of the cell using slow degrading poly(trolox ester) nanoparticles.

3.2.3 Specific Aim 3: Develop a flexible polymer chemistry that could be extended to variety of antioxidants and could be tuned for their degradation rate.

A. Apply non-free-radical polymerization poly(β-amino ester) chemistry to synthesize polyphenolic antioxidants based poly(antioxidant β-amino esters) (PABAE).

B. Investigate degradation characteristics of PABAE and determine antioxidant activity of PABAE degradation products.

C. Investigate cytotoxicity of PABAE degradation products and their effect on cellular oxidative stress levels in absence and presence of injury.

3.2.3.1 Hypothesis #3

Polyphenolic antioxidants can be incorporated into PABAE hydrogel which undergo hydrolytic degradation and their degradation products have antioxidant activity capable of suppressing oxidative stress in the cells.

3.2.3.2 Significance and Outcome

The non-free-radical polymerization poly(β-amino ester) chemistry described in **Chapter 6** was successfully used to incorporate acrylate functionalized quercetin and curcumin into a PABAE network. This polymerization scheme can be extended to all polyphenolic antioxidants and allows tuning of the rate of polymer degradation by

appropriate choice of co-monomers and ratio of these co-monomers. **Chapter 7** describes cytotoxicity of PABAE degradation products and their effect on oxidative stress levels in the cells which were similar to the effects of the corresponding free form antioxidants.

Chapter 4. Synthesis and Characterization of Poly(trolox ester)

Based on the research article published in :

> P.P. Wattamwar, Y. Mo, R. Wan, R. Palli, Q. Zhang and T.D. Dziubla, "Antioxidant Activity of Degradable Polymer Poly(trolox) to Suppress Oxidative Stress Injury in the Cells", Advanced Functional Materials, 2010, 20, 147-154.

4.1 Introduction

While it is thought that degradable materials can evade long term compatibility issues through degradation, recent studies found that the local accumulation of acids (which are by-products of biodegradation) and monomer/oligomer leachouts, may trigger inflammatory response leading to further oxidative stress [179-181, 193-196]. Attempts have been made to attenuate biomaterial induced oxidative stress by synthesizing polymers (e.g. polyketals) that would result in neutral degradation products [257]. Studies have shown that the conjugation of antioxidant molecules to various polymers can suppress oxidative stress [188, 258, 259]. For example, vitamin E along with carbohydrate-targeting protein and solubility enhancers were conjugated to acrylate/methacrylate backbone to synthesize a water soluble antioxidant polymer. Cellular uptake of these polymers resulted in a slow release and accumulation of vitamin E over a period of 8 days [258]. Oligomers of glutathione and poly(ethylene glycol), where glutathione was linked to poly(ethylene glycol) (600 g/mol) using disulfide linkages, self-assembled to form aggregates (~300 nm) which protected cells from H_2O_2 based oxidative stress injury [259]. In other examples, ascorbic acid and polyphenols were conjugated to gelatin and methacrylic acid to result in non-biodegradable polymers that had antioxidant functionality [184, 185]. However, these functional materials are

limited in their heterogeneity and low relative mass of antioxidant compared to the bulk material. Taking a cue from the pioneering work in anti-inflammatory polymers of aspirin [260], in this work, we synthesized a new biodegradable polymer, poly(trolox ester), having native antioxidant activity. Trolox, a synthetic and water soluble analogue of Vitamin E **(Figure 4-1)**, released as degradation product of the polymer could theoretically attenuate the biomaterial oxidative stress by scavenging ROS like superoxide anion, hydroxyl radical and RNS like peroxynitrite [261-263].

As an alternative to pendant conjugation strategies, trolox, a water-soluble analogue of vitamin E, was polymerized through a polycondensation reaction mediated by Stagelich esterification. As the condensation pairs used result in a zero length conjugation bond, the resulting biodegradable poly(trolox ester) possesses 100% antioxidant mass. Using a single step solvent extraction method, it is possible to formulate poly(trolox ester) into nanoparticles of sizes 100-250nm. We report here that the formulated polymer nanoparticles undergo enzymatic degradation resulting in degradation products that have ability to scavenge radicals and that these nanoparticles were found to have little to no cytotoxicity at concentrations up to 1mg/ml.

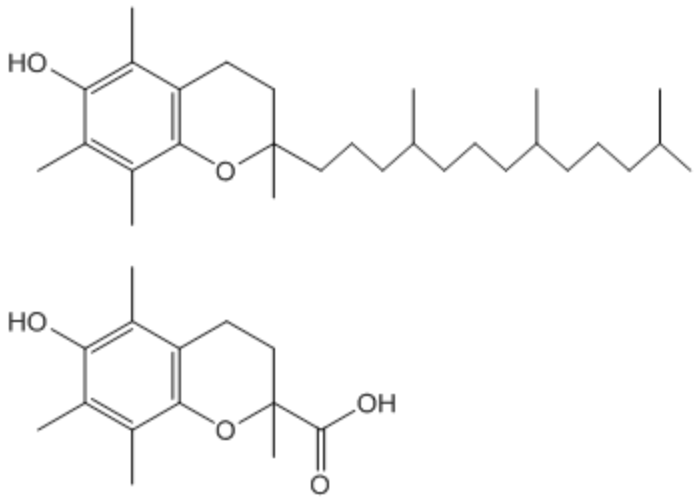

Figure 4-1. Chemical Structure of Vitamin E (top) and Trolox.

4.2 Materials and Methods

4.2.1 Synthesis of PTx-1000

For PTx-1000, a carbodiimide and 4-(dimethylamino)pyridine (DMAP) based reaction was used (**Figure 2**) [264]. Molecular sieves (4 Å pore size) were added to dichloromethane (DCM) and stirred overnight under inert atmosphere to capture any water present in the solvent. Using line transfers, anhydrous DCM (60 ml per 1 g of trolox) was transferred to a reaction vessel loaded with trolox and DMAP (0.5 molar equivalent of trolox). Solution of trolox and DMAP in DCM was warmed till it became clear. In a separate vessel, *N*,*N*′-dicyclohexylcarbodiimide (DCC) was dissolved in anhydrous DCM at a stock concentration of 40 mg/ml. This DCC solution was added to the trolox/DMAP solution under continuous stirring until DCC was 10% in molar excess of trolox. The reaction mixture was stirred in the dark for 24 hrs under a continuous slow argon purge. After this reaction, the precipitated dicyclohexyl urea was removed by vacuum filtration. The filtrate was dried under vacuum using a roto-evaporator (Rotovapor R II, Buchi, Switzerland). The resultant yellowish powder was re-dissolved in acetone and subjected to ultrafiltration. Ultrafiltration was performed to remove unreacted compounds and catalyst from the polymer product using a solvent-resistant stirred cell with a 3 kDa MWCO Ultracel YM/PL ultrafiltration membrane (Millipore, USA). Acetone was evaporated from the retentate and the resultant solid polymer mass was subjected to vacuum overnight to remove residual solvent. PTx-1000 was stored under dark at room temperature.

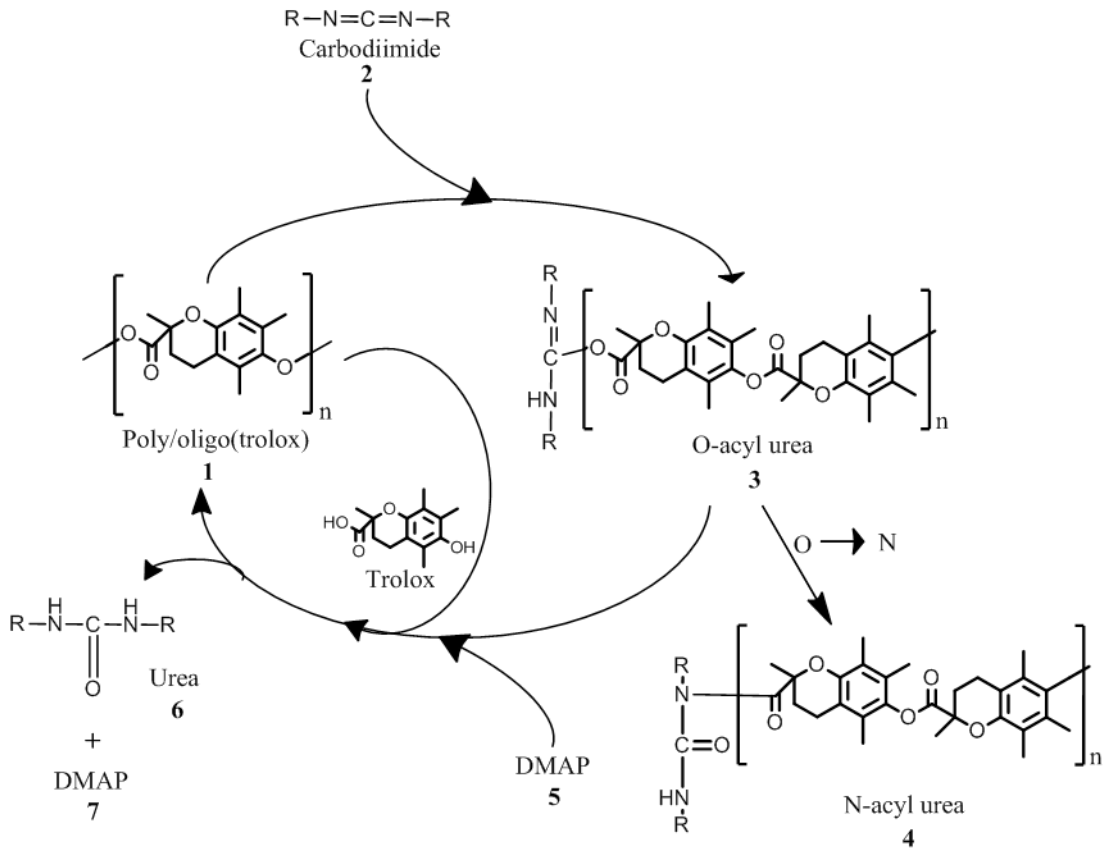

Figure 4-2. Trolox Polymerization Scheme

Trolox (**1**, n=1**)** undergoes an esterification reaction to form poly(trolox ester) (**1**). Carbodiimide (**2**) reacts with the terminal carboxylic acid group of **1** to form an active intermediate O-acyl urea (**3**). Catalyst DMAP (**5**) then traps this intermediate and reacts with the phenolic group of trolox/poly(trolox ester) (**1**) to form an ester. This new product (**1**) has a carboxyl group that can repeat this process allowing for the growth of the polymer. Urea (**6**) is a by-product that precipitates out in reaction mixture where as N-acyl urea (**4**) is an undesired side-product formed by rearrangement of **3**. It is theorized that the formation of **4** results in the terminal capping of this reactive end group and prevents further polymer chain growth. *(This reaction mechanism is adapted from Wiener and Gilon [264].)*

4.2.2 Synthesis of 4-(Dimethylamino)pyridinium 4-toluenesulfonate (DPTS)

DPTS was synthesized following the procedure as described in detail by Moore and Stupp [265]. Dry p-toluenesulfonic acid (PTSA) was obtained by subjecting a solution of PTSA in toluene to azeotropic distillation using a Dean-Stark trap. Separately, an equimolar amount of DMAP was dissolved in toluene and then added to the dry solution of PTSA in benzene under continuous stirring. The resulting suspension of DPTS was stirred for a while and then cooled to room temperature. DPTS suspension in toluene was vacuum filtered and was recovered as solid powder. DPTS was further purified by dissolving it in boiling DCM at saturation conditions. DCM solution was stored overnight at -20ºC. The resultant needle shaped white crystals were recovered by vacuum filtration. Using differential scanning calorimetry, melting point of DPTS (MW = 294 g mol^{-1}) was found to be 176 ^{0}C, which is similar to previously reported melting point of 165 ^{0}C [265].

4.2.3 Synthesis of PTx-2500

A carbodiimide-DPTS based reaction was employed for PTx-2500 synthesis [265]. DCM was dried overnight over calcium hydride. Anhydrous DCM (27 ml per 1 g of trolox) was then distilled into a two neck round bottom flask loaded with equimolar amounts of trolox and DPTS. Reaction mixture was turbid to begin with since trolox concentration was above its saturation concentration. N,N'-diisopropylcarbodiimide (DIC) (1.5 molar equivalents of trolox) was weighed and added as a neat reagent using a syringe. The reaction mixture was stirred under dark and inert conditions for 24 hrs. Inert conditions were maintained by purging argon through reaction vessel. After 24 hrs, DCM was evaporated off from reaction mixture using a roto-evaporator and solid mass was

dissolved in acetone. The insoluble diisopropyl urea was removed by vacuum filtration and the filtrate was subjected to ultrafiltration as described in PTx-1000 synthesis. PTx-2500 was obtained as yellowish dry powder and was stored in the dark at room temperature.

4.2.4 Characterization of Synthesized Polymers

Synthesized polymers were characterized using Fourier Transformed Infrared (FTIR) spectroscopy, ^{13}C Nuclear Magnetic Resonance (NMR) spectroscopy and Gel Permeation Chromatography (GPC). FTIR measurements were performed on a Digilab Stingray system consisting of a FTIR 7000e stepscan spectrometer (Varian Inc.). ^{13}C NMR spectra were obtained using a Varian Gemini 200 MHz NMR spectrometer. A Shimadzu Prominence LC-20 AB HPLC system installed with a waters 2410 refractive index detector was used to calculate molecular weight using GPC. 300 x 7.5 mm PLgel 3 μm mixed-E column (Polymer Laboratories), 300 x 7.8 mm Waters Styragel HR-1 and HR-2 colums were used in series for separation. Polystyrene standards (Polymer Laboratories) in the molecular weight range of 20,000 to 500 Da were used (with tetrahydrofuran as eluent) to develop a linear range of calibration for molecular weight determination.

4.2.5 Nanoparticle Formulation and Characterization

PTx-1000 and PTx-2500 are both insoluble in water, allowing them to be processed as nanoparticles. A single emulsion procedure was employed for nanoparticle formulation. Polymer was dissolved in acetone at a known concentration. This acetone solution was then added to a pluronic F-68 solution in phosphate buffered saline (PBS) while vortexing at 1400 rpm. In all the formulations, the final concentration of acetone in

the surfactant solution was 10 % v/v. Concentration of surfactant solution and concentration of polymer in acetone were varied to control the size of nanoparticles. The particle solution was left open under stirring conditions overnight to let the acetone evaporate off. Formulated nanoparticles were subjected to ultrafiltration to remove excess surfactant from nanoparticle suspension. Ultrafiltration was performed using a 100 kDa MWCO Ultracel YM/PL membrane in a stirred cell. Particle size was measured before and after the ultrafiltration using dynamic light scattering on a Malvern Zetasizer Nano (Westborough, MA). Nanoparticles free of excess surfactant were used for all the further studies.

4.2.6 *In Vitro* Degradation of Poly(trolox ester)

Poly(trolox ester) nanoparticles were diluted to a final concentration of 1 mg/ml in PBS at pH of 7.4 with and without the enzyme carbonic anhydrase (CA). CA was dissolved in PBS at a concentration of 2 mg/ml and the nanoparticle suspension was incubated in a shaker bath at 37 ^{0}C. 150 μL of aliquots were removed at different time points and were immediately analyzed for their antioxidant activity and size.

4.2.7 *In Vitro* Assay for Measurement of Antioxidant Activity

Antioxidant activity of samples from degradation studies was measured using a 2',7'-dichlorofluorescein (DCF) based fluorescent assay. An azo initiator 2,2'-azo-bis(2-aminopropane)-HCl (AAPH) that undergoes thermal degradation was used to mimic the peroxyl radical formation *in vivo*. Procedure described by Aldini et. al. was followed for hydrolysis of 2',7'-dichlorodihydrofluorescein diacetate (DCF-DA) [266]. In brief, 500 μL of 1 mM DCF-DA stock solution in ethanol was added to 2 ml of 0.01 N NaOH solution and stirred for 20 min under darkness. Solution was then neutralized by adding 2

ml of 0.01 N HCl solution. Hydrolysis of DCF-DA results in 2',7'-dichlorodihydrofluorescein (DCFH) which is then diluted in PBS to a final concentration of 10 or 20 μM. The diluted DCFH solution was stored in ice under darkness and was used for further measurements within 4 hrs after preparation. To a well in a 96-well microplate, 50 μL of sample was added to 200 μL of DCFH solution. Fluorescence measurement was started when 20 μL of 270 mM AAPH in PBS was added to the well. Peroxyl radicals generated from AAPH and unscavenged by antioxidants oxidize DCFH to result in fluorescent compound DCF. Varian Cary Eclipse fluorescence spectrophotometer was used for all fluorescence measurements. Assay was performed on a 96 well plate using a Varian microplate reader. Excitation and emission wavelengths were 502 nm and 525 nm respectively and slit width was 10 nm. Data was acquired using Cary Eclipse software from Varian. Assay was always calibrated using known trolox concentrations and the antioxidant potential of the sample was determined in terms of molar active trolox equivalents.

4.2.8 Cytotoxicity of Poly(trolox ester) Nanoparticles

Mouse pulmonary microvascular endothelial cells (MPMVEC) were isolated from mouse lungs as described previously [267]. MPMVEC were cultured in Dulbecco's modified eagle medium (DMEM) supplemented with 10% fetal bovine serum, 1% nonessential amino acids and penicillin/streptomycin in a 96 well microplate overnight. Polymer nanoparticles at a concentration of 10 mg/ml in PBS were diluted in DMEM to different concentrations and added to the wells. 24 hrs after adding the nanoparticles, the cell viability was determined by CellTiter 96 AQ_{ueous} Non-Radioactive Cell Proliferation Assay by incubation with 3-(4,5-Dimethylthiazol-2-yl)-5-(3-carboxymethoxyphenyl)-2-

(4-sulfophenyl)-2H-tetrazolium (MTS) / phenazine methosulfate (PMS) mixture at 37 ^{0}C for 3 hrs. MTS is reduced by dehydrogenase enzymes in metabolically active cells to a blue colored soluble formazan product. The absorbance of the formazan was then measured at 490 nm using a microplate reader (Synergy HT, BioTek, Vermont).

4.3 Results and Discussion

4.3.1 Synthesis and Characterization of Poly(trolox ester)

A carbodiimide based polymerization reaction was used for the synthesis of poly(trolox ester) **(Figure 4-2)**. Initial trolox concentration was 16.7 mg/ml. The molar ratio of the reactants, DCC:trolox and DMAP:trolox, was 1.1 and 0.5, respectively. GPC results revealed the product to be oligomeric (i.e. $\leq$ 7 mers, See **Figure 4-3)**. Average molecular weight of the oligomers, referred to as PTx-1000, was M_N = 830 and M_W = 1156 and possessed a polydispersity index of 1.4. Increasing the DCC:trolox and DMAP:trolox ratios to 1.5 and 1 respectively did not increase average molecular weight of oligomer (results not shown). As shown in **Figure 4-2**, esterification of trolox using a carbodiimide involves the formation of an active intermediate O-acyl urea. This intermediate can undergo molecular rearrangement (O$\rightarrow$N migration) to form N-acyl urea which results in terminal capping of reactive carboxylic group thereby preventing further polymer chain growth. *[The peak at 171.75 in ^{13}C NMR spectra of PTx-1000 could be related to the N-acyl urea peak]*.

The rate of N-acyl urea formation depends on the pKa of the trolox carboxyl acid group (pKa = 3.89) [268] and solvent pH and can be suppressed by acid catalysis [265]. The reaction medium pH was lowered by using PTSA. A DMAP:PTSA ratio of 1:1 was maintained using separately synthesized DPTS. Initial trolox concentration was 37 mg/ml

in DCM and the ratio of DIC:trolox and DPTS:trolox was 1.5 and 1, respectively. Acid catalysis resulted in a polymer, referred as PTx-2500, with an average molecular weight of M_N = 1294 and M_W = 2520 which results in polydispersity index of 1.9. As shown in **Figure 4-3**, PTx-2500 possesses a significant fraction of higher molecular weight chains, up to 10,000 MW. The peaks at wavelengths of 1747 cm^{-1} (ester carbonyl stretch) in the IR spectrum (**Figure 4-4**) and 172.5 ppm in the ^{13}C NMR spectrum (**Figure 4-5**) are indicative of ester bonds in PTx-1000 and PTx-2500.

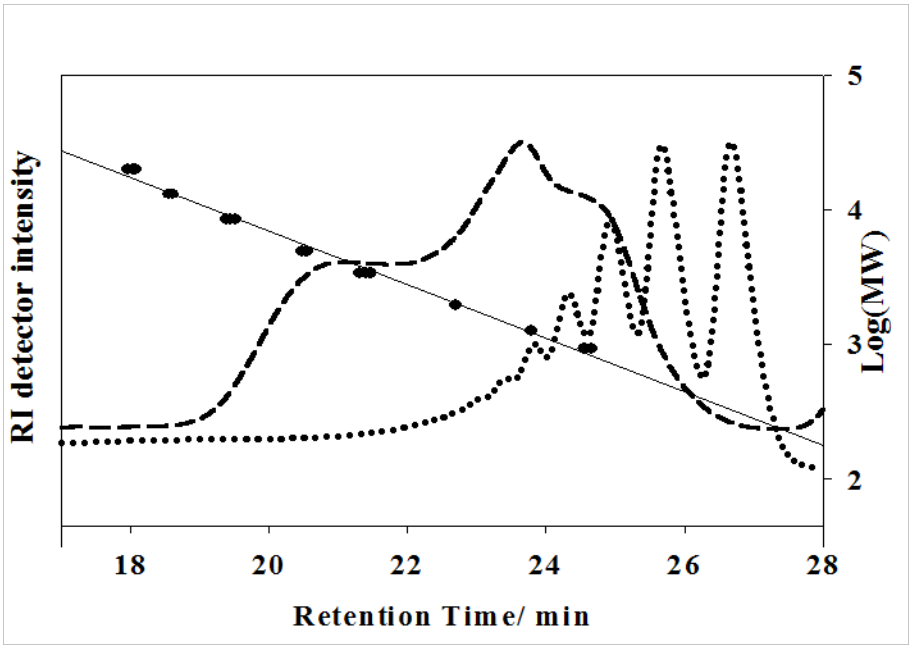

Figure 4-3. GPC analysis of PTx-1000 and PTx-2500

Chromatograms of synthesized and purified PTx-1000 and PTx-2500 obtained from GPC analysis. Presence of several peaks in PTx-1000 chromatogram indicates that synthesis resulted in oligomers of trolox (M_N = 830 and M_W = 1156).

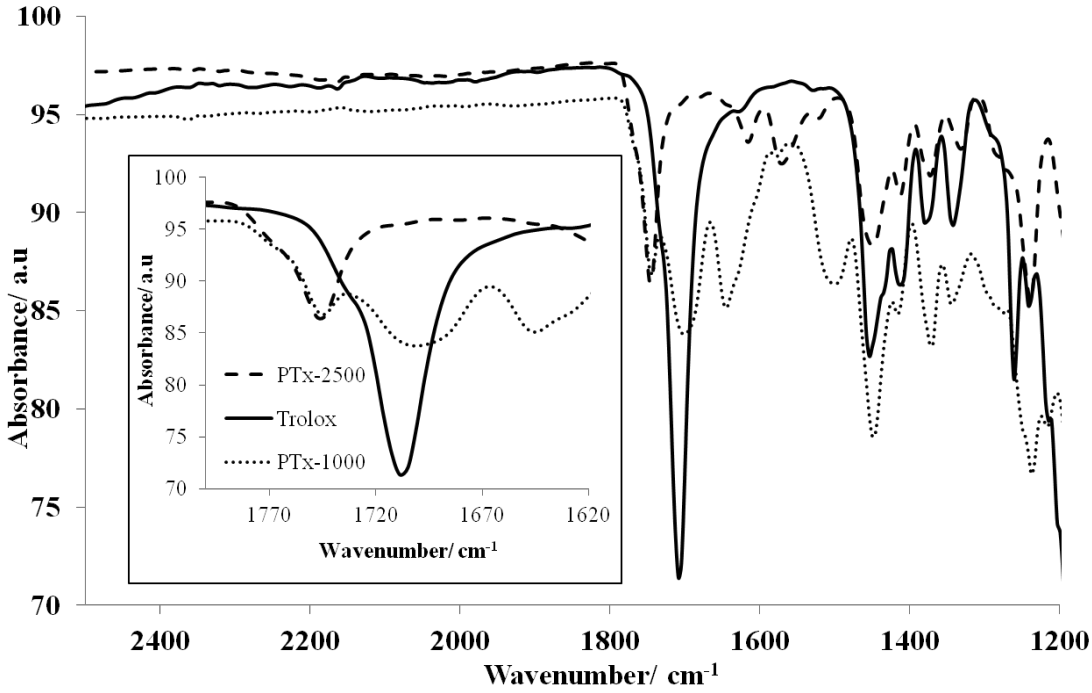

Figure 4-4. FTIR Spectra of Trolox, PTx-1000 and PTx-2500.

In the inset, peak at ~ 1747 cm^{-1} indicates presence of ester bond.

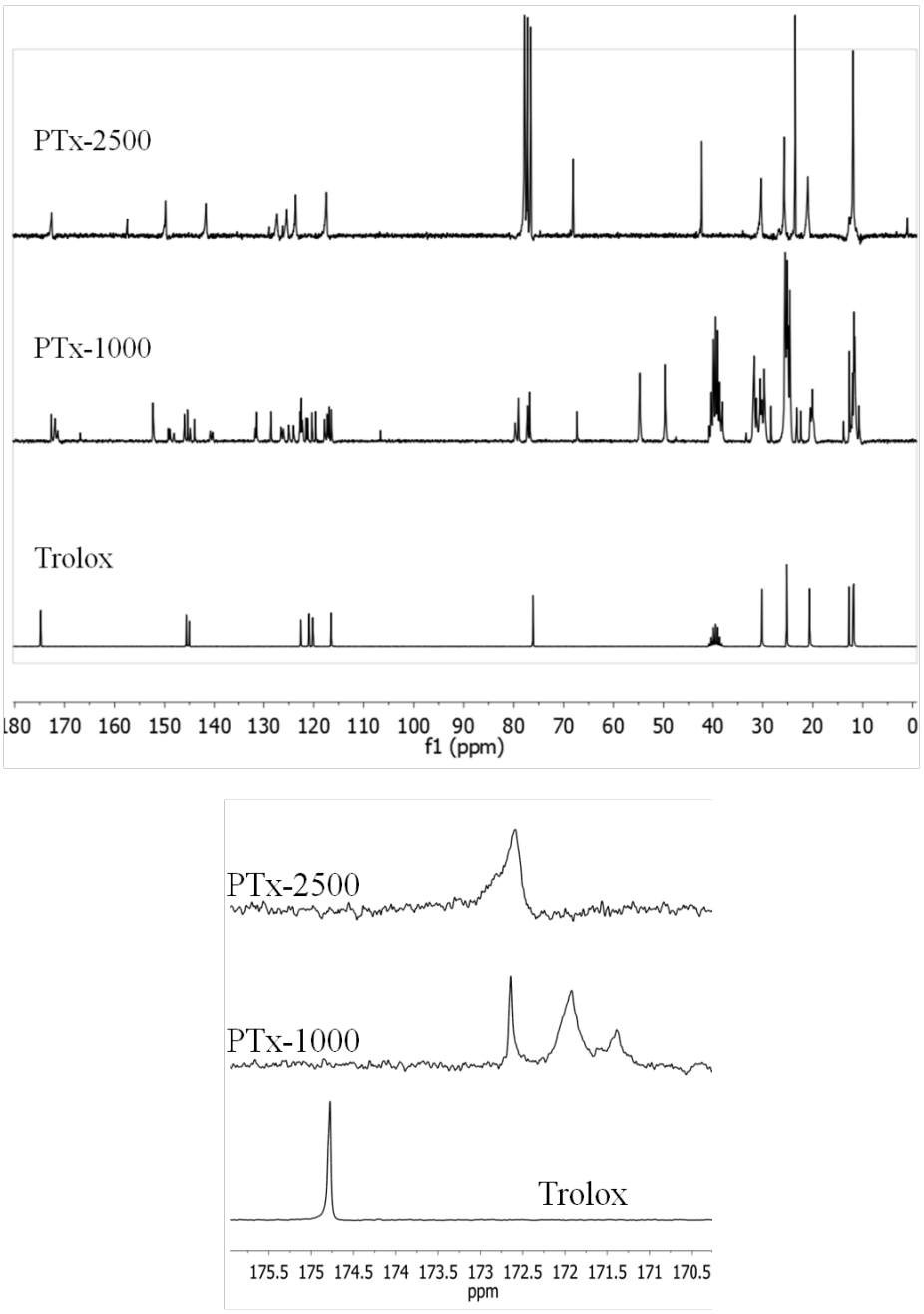

Figure 4-5. ^{13}C NMR Analysis of Trolox, PTx-1000 and PTx-2500

(Top) ^{13}C NMR spectra of trolox, purified PTx-1000 and PTx-2500.

(Bottom) Peak at 174.77 ppm in trolox spectrum is characteristic of carbonyl bond in a carboxylic acid. Peaks at 172.75 ppm is related to carbonyl bond in trolox ester. *[Peak at 172 ppm in PTx-1000 spectra can be related to the N-acyl urea present in PTx-1000].*

4.3.2 Poly(trolox ester) Nanoparticle Formulation and Characterization

In order to study feasibility of antioxidant polymers for targeted vascular delivery of antioxidants, which is the long-term goal of the project, polymer nanoparticles were formulated using a single step emulsion technique. Pluronic F-68 was used as a surfactant to prevent nanoparticle aggregation. Size of poly(trolox ester) nanoparticles was controlled by varying the concentration of polymer in acetone during the single emulsion technique. To obtain PTx-1000 nanoparticles, a 1 wt% pluronic F-68 solution in phosphate buffered saline (PBS) was used. As PTx-1000 concentration in acetone was increased from 5 mg/ml to 25 mg/ml, size of the resultant nanoparticles changed from 120 nm to 220 nm (**Figure 4-6**). However, when a 1 wt% pluronic F-68 solution was used for PTx-2500 nanoparticle formulation, it resulted in formation of many micron sized particles. This can be attributed to the increased viscosity of PTx-2500 solution in the organic solvent owing to its higher molecular weight. In order to minimize the formation of micron sized particles, surfactant concentration was increased from 1 wt% to 4 wt%. Before size measurement, PTx-2500 nanoparticle solutions were subjected to filtration using a 1 μm syringe filter to remove small fractions of micron sized particles. As PTx-2500 concentration in acetone was increased from 2.5 mg/ml to 7.5 mg/ml, size of the resultant nanoparticles changed from 170 nm to 230 nm (**Figure 4-6**). Immunotargeted intracellular delivery of nanocarriers to endothelium is size-dependant, and has been shown to be optimum for nanocarriers in range of 100-300 nm. Taking this into consideration, since a common size range of 180 – 220 nm for PTx-1000 and PTx-2500 nanoparticles was achieved, PTx-2500 nanoparticles at concentrations lower than 2.5 mg/ml were not formulated.

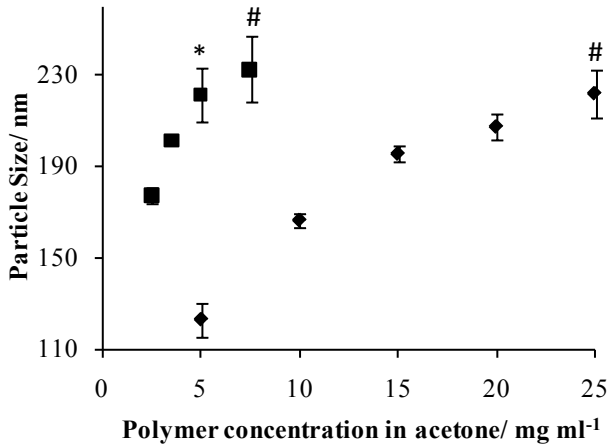

Figure 4-6. Tuning Particle Size by Changing the Concentration of Polymer in Organic Solvent.

PTx-1000 (diamonds) and PTx-2500 (squares) nanoparticles were formulated using a single emulsion technique. Polymers were dissolved at different concentrations in acetone. Acetone solution was then added drop-wise to pluronic F-68 solution in PBS. Surfactant solution concentration used for PTx-1000 and PTx-2500 nanoparticle formulation was 1 wt% and 4 wt% respectively. In all the formulations, final acetone concentration in PBS was limited to 10%. Resulting particles were diluted 10 times and particle size was measured by dynamic light scattering (DLS) using a Malvern Zetasizer Nano. ($M \pm SD$, $n=3$). * represents that the data point is significantly different from previous data point in series with whereas # represents that the data point is not significantly different from previous data point in the series with $p<0.05$.

4.3.3 *In Vitro* Degradation of PTx-1000 and PTx-2500 Nanoparticles

Antioxidant activity of poly(trolox ester) was verified by an *in vitro* degradation study. PTx-1000 (160 nm) and PTx-2500 (195 nm) nanoparticles at a concentration of 1 mg/ml were incubated in PBS (pH 7.4) at 37 ^{0}C with and without the enzyme carbonic anhydrase (CA). In absence of CA, except for a small initial spike, no increase in the antioxidant activity of the nanoparticle suspension could be detected. However, results from *in vitro* oxidative stress studies suggested that PTx-1000 and PTx-2500 might be susceptible to enzymatic degradation. The enzyme, CA, was studied because it is known to have esterase activity to hydrolyze phenyl esters [269], and is localized in the cytosol as well as in/on the plasma membrane of a cell [270, 271]. As such, it is a likely candidate for *in vitro* degradation of nanoparticles. Indeed, in the presence of the enzyme CA, the antioxidant activity of the nanoparticle suspension increased from 0 μM to 70 μM over a period of 100 hrs (**Figure 4-7**).

As we have observed that incubation of pure trolox in PBS loses its antioxidant activity with time, it is possible that some of the antioxidants released as the degradation products of poly(trolox ester) can undergo natural oxidation during the incubation period meaning that the measured antioxidant activity is an underestimation of actual antioxidant activity of nanoparticle suspension. Incubation of PTx-1000 and PTx-2500 nanoparticles at 37 ^{0}C resulted in a significant increase in their size over the time. However, in the presence of CA, increase in the size was slightly higher as compared to the size increase during non-enzymatic incubation (**Figure 4-7**). As degradation of poly(trolox ester) nanoparticles proceeds, its hydrophilicity will increase resulting in the swelling of particles. Release of antioxidants and swelling of nanoparticles confirms that

PTx-1000 and PTx-2500 are more susceptible to enzymatic degradation as compared to hydrolytic degradation.

4.3.4 Cytotoxicity of Poly(trolox ester) Nanoparticles

Biocompatibility of the degradable polymer typically depends on the toxicity of its degradation and leachable products which are either oligomers or monomers. To study the biocompatibility of the poly(trolox ester) polymers, mouse pulmonary microvascular endothelial cells (MPMVEC) were exposed to PTx-1000 (195 nm) and PTx-2500 (215 nm) nanoparticles at concentrations ranging from 3.9 μg/ml to 1000 μg/ml and cell viability was measured by CellTiter 96 AQ_{ueous} using a Non-Radioactive Cell Proliferation Assay (MTS assay, Promega, Madison, WI) **(Figure 4-8)**. Exposure of endothelial cells to PTx-1000 nanoparticles at concentrations up to 500 μg/ml did not result in any significant cytotoxic effects. When the concentration was increased to 1000 μg/ml, the cell viability dropped marginally to 87.9 $\pm$ 3.5 % as compared to the control. PTx-2500 nanoparticles did not have any significant cytotoxic effects in the concentration range studied.

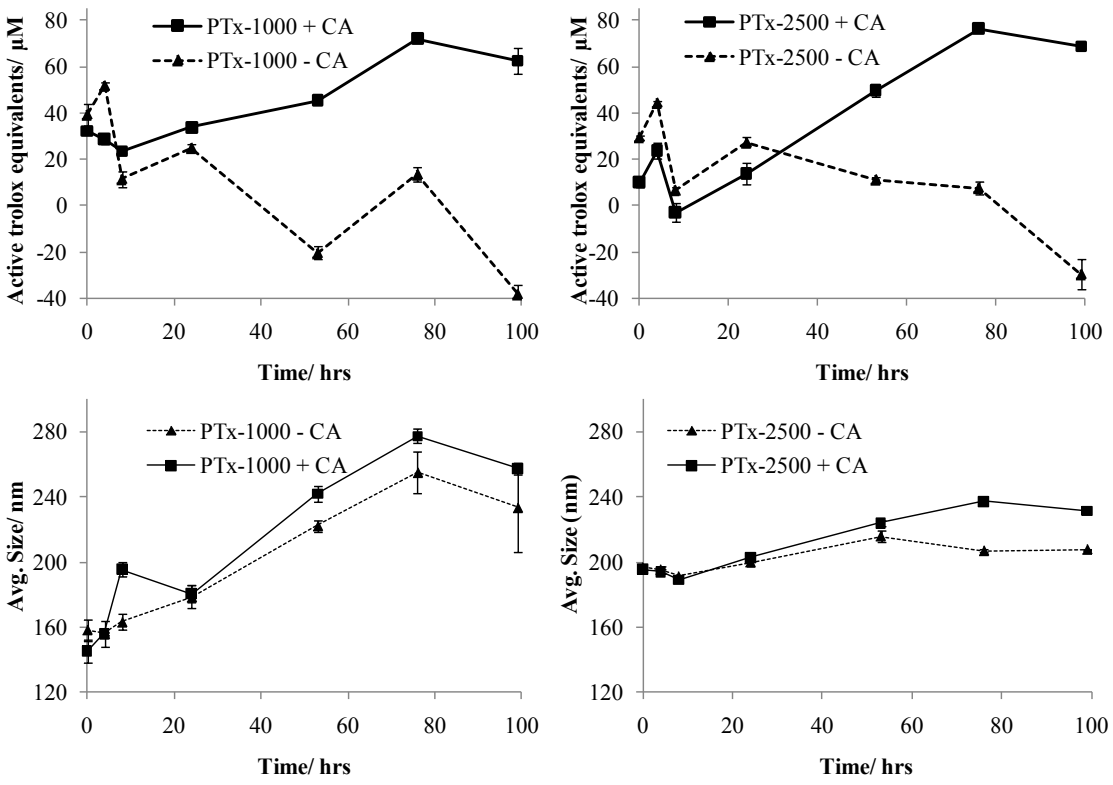

Figure 4-7. Enzymatic Degradation of Poly(trolox ester) Nanoparticles

Poly(trolox ester) nanoparticles were suspended in PBS at 37 ^{0}C at concentration of 1 mg/ml with(squares) and without(triangles) the enzyme CA. Aliquots were removed at different time points and were immediately used to measure antioxidant activity. Size of nanoparticles in all the suspensions was also measured at different time points. One-way ANOVA was performed on all the trends. All the trends were significant with $p<0.05$.

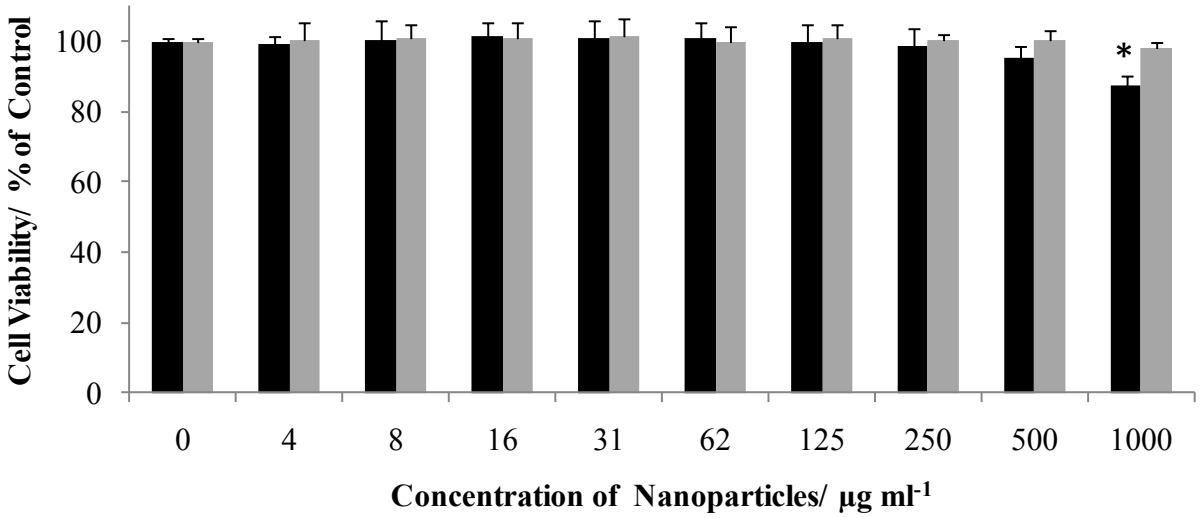

Figure 4-8. Cytotoxicity of Poly(trolox ester) Nanoparticles

MPMVEC cultured in a 96 well plate were exposed to PTx-1000 (black) and PTx-2500 (grey) nanoparticles for 24 hrs. After 24 hrs, cell viability was measured using MTS assay. (M $\pm$ SD, n=3). Cells without exposure were used as control. * represents significant difference from the control with $p<0.05$.

4.4 Conclusion

In conclusion, trolox was polymerized successfully using carbodiimide based esterification reaction to result in two polymers of different molecular weights. Nanoparticles of PTx-1000 and PTx-2500 were formulated using single emulsion method with a control over their size. Formulation of poly(trolox ester) into nanoparticles will allow its characterization for drug delivery applications. *In vitro* degradation studies suggests that poly(trolox ester) is more susceptible to enzymatic degradation as compared to hydrolytic degradation. Also, degradation products of poly(trolox ester) have radical scavenging ability as determined by an *in vitro* assay. Poly(trolox ester) nanoparticles had very little to no cytotoxicity up to concentration of 1 mg/ml and will be characterized for their antioxidant activity in *in vitro* cell culture models.

Chapter 5. Effect of Poly(trolox ester) on Oxidative Stress in Cells

Based on the research articles published in :

P.P. Wattamwar, Y. Mo, R. Wan, R. Palli, Q. Zhang and T.D. Dziubla, "Antioxidant Activity of Degradable Polymer Poly(trolox) to Suppress Oxidative Stress Injury in the Cells", Advanced Functional Materials, 2010, 20, 147-154.

P.P. Wattamwar, S.S. Hardas, D. Allan Butterfield, K.W. Anderson and T.D. Dziubla, "Tuning of the Pro-oxidant and Antioxidant Activity of Trolox Through the Controlled Release from Biodegradable Poly(trolox ester) Polymers", Journal of Biomedical Materials Research Part A, 2011, 99A, 184-191.

5.1 Introduction

It is well known that, depending upon the setting, the degradation of biodegradable materials can result in a localized inflammatory response [272], which is often the result of accumulated degradable byproducts, inducing cellular oxidative stress [181, 182, 273, 274]. This observation has led to several groups developing antioxidant coupled biomaterials as a way of inhibiting localized biomaterial related inflammation [184, 186, 187, 256, 258, 275]. While this work has demonstrated an ability to suppress inflammation, little is known about the chemical targets in which these materials augment oxidative stress. For instance, the chronic inflammatory foreign body giant cell response is characterized by macrophages releasing a plethora of digestive enzymes and oxidative species like superoxide radical ($O_2^{\cdot -}$). The enzyme superoxide dismutase (SOD) converts $O_2^{\cdot -}$ in to hydrogen peroxide (H_2O_2). H_2O_2 can then react with transient, redox active reduced metal ions (Fe^{2+}, Cu^{+}, etc.) to form hydroxyl radicals ($OH^{\cdot}$). $O_2^{\cdot -}$ can also react with nitric oxide (NO) to form peroxynitrite ($ONOO^{-}$). These reactive oxygen species

(ROS) and reactive nitrogen species (RNS), respectively, can further react with and oxidatively damage cellular proteins and lipids thereby producing oxidative stress markers such as protein carbonyl, 3-nitrotyrosine (3NT) and 4-hydroxy-2-trans-nonenal (HNE) [276, 277]. The latter can covalently bind to Cys, His, and Lys residues on proteins via Michael addition, changing the structure and function of protein [278]. However, small molecule antioxidants can terminate different reactive species, e.g., water soluble antioxidants like gallic acid, vitamin C, trolox etc. eliminate radicals generated in the cytosolic cellular compartment, while hydrophobic antioxidants like vitamin E (tocopherol), β-carotene, etc. reduce lipid peroxidation. As such, antioxidants can modulate the redox state of the cell by controlling the levels of ROS and RNS [200]. Modulation of this redox state can induce various cell responses like cell proliferation, differentiation, inflammation, apoptosis, etc. [32-35]. Despite this control, of the tools available for designing biomaterials to modulate cellular/tissue behavior (e.g. growth factor release, cytokine/drug release, structural cues), redox status remains an underdeveloped yet exciting mechanism for controlling cellular response to biomaterials. As such, a knowledge of which chemical targets are affected can provide insight into which settings an oxidation sensitive biomaterial is most useful.

As described in the previous chapter, we had synthesized poly(trolox ester), a biodegradable polymer of trolox that upon degradation results in release of active antioxidant trolox [256]. Trolox [(±)-6-Hydroxy-2,5,7,8-tetramethylchromane-2-carboxylic acid], a synthetic and water-soluble analogue of α-tocopherol (Vitamin E), has been shown to have antioxidant protective effect against oxidative stress injury [35, 279-281]. In this work, we report that poly(trolox ester) provides protection against

cellular oxidative stress in an *in vitro* model where cobalt nanoparticles were used to induce cellular oxidative stress. However, the free antioxidant, trolox, is known to possess a concentration dependent antioxidant and pro-oxidant effect [282-284]. In the current study, it was found that the toxicity of trolox resulting from its pro-oxidant effect can be reduced by the slow release of trolox through biodegradation of poly(trolox ester). Further, it was found that the method of delivery altered what chemical target was protected from oxidation. Specifically, there was a dose-dependent suppression of protein oxidation (as monitored by protein carbonyl formation) for poly(trolox ester) nanoparticles and not free soluble trolox. This work details the importance of oxidized product analysis and highlights the advantages that the mechanism of delivery can have upon the therapeutic response. This result emphasizes the unique potential for antioxidant polymers like poly(trolox ester) in a variety of biomedical applications, including wound healing, improving implant response and tissue engineering applications.

5.2 Antioxidant Mechanism of Trolox – Reactions of Trolox with Free Radicals

While proposing to use trolox as a scavenger of biological oxidants, it is necessary to know their kinetics of scavenging which would determine their scavenging efficiency. Even though scavenging kinetics are much slower compared to enzymatic degradation of oxidants, they are fast enough to provide protection of biologically sensitive molecules. This section describes mechanism and kinetics of scavenging of biological oxidants by trolox. Except for phytyl chain in Vitamin E, trolox and Vit E are similar and hence their reactions with the free radicals are similar.

When small antioxidant molecules react with ROS, there is a transfer of the radical with the formation of less-reactive antioxidant-derived radical as shown below in reaction (1).

$$AH + R^{\bullet} \rightarrow A^{\bullet} + RH \quad (1)$$

The antioxidant-derived radical is less reactive and has a life time longer than that of the oxidant initially scavenged. The reduction potentials of oxidants and antioxidants indicate stability of their radicals, where a higher reduction indicates a less stable radical and vice versa (**Table 5-1**) [285]. Trolox has a reduction potential lower than several biological free radicals and can be used as a potential antioxidant against these radicals.

Reactions of trolox with ROS and RNS are summarized in **Figure 5-1**. Trolox is susceptible to $OH^{\cdot}$ attack at various sites. Either, abstraction of phenolic hydrogen as shown in reaction (2) or addition to the phenolic ring to form an $OH^{\cdot}$ adduct, as shown in reaction (3) and (5). $OH^{\cdot}$ adduct then yields phenoxyl radical ($TxO^{\cdot}$) by elimination of water molecule (reaction (4) and (6)), which is a acid/base-catalyzed process. Reaction (7) represents overall formation of $TxO^{\cdot}$ with a rate constant k_7 determined as 6.9×10^9 dm^3/ mol/s [262].

Pulse radiolysis studies of the reaction of trolox with $O_2^{\cdot -}$ indicate that trolox does not react with superoxide anion [261, 262]. However, electron spin resonance studies have shown that trolox can be oxidized by $O_2^{\cdot -}$ (reaction (8)), although in these studies, involvement of H_2O_2, protonated form of $O2^{\cdot -}$, is a possibility. The reaction rate of k_8 = 1.7×10^4 dm^3/ mol/s has been reported [262]. Also, it has been reported that superoxide anion can react with the trolox phenoxyl radical by the reaction (9). The

Table 5-1 One-electron Reduction Potentials of Some Oxidants and Antioxidants.

All listed potentials were obtained at pH 7[285].

Species	Redox Couple	E^0 (mV)
Hydroxyl radical, $OH^{\cdot}$	H^+ / H_2O	2310
Aliphatic alkoxyl radical, $LO^{\cdot}$	H^+ / LOH	1600
Peroxynitrite, $ONOO^-$	ONOOH / $NO^{\cdot}$	1400
Alkyl peroxyl radical, $LOO^{\cdot}$	H^+ / LOOH	1000
Polyunsaturated fatty acid radical, $L^{\cdot}$	H^+ / LH	600
α-tocopheroxyl radical, $T\text{-}O^{\cdot}$	H^+ / T-OH	500
Trolox radical, $T\text{-}O^{\cdot}$	H^+ / T-OH	480
H_2O_2	$H^+ / H_2O, OH^{\cdot}$	320
Ascorbate radical, $Asc^{\cdot}$	H^+ / Ascorbate monoanion	282
$O_2^{\cdot -}$	$O_2 / O_2^{\cdot -}$	-330

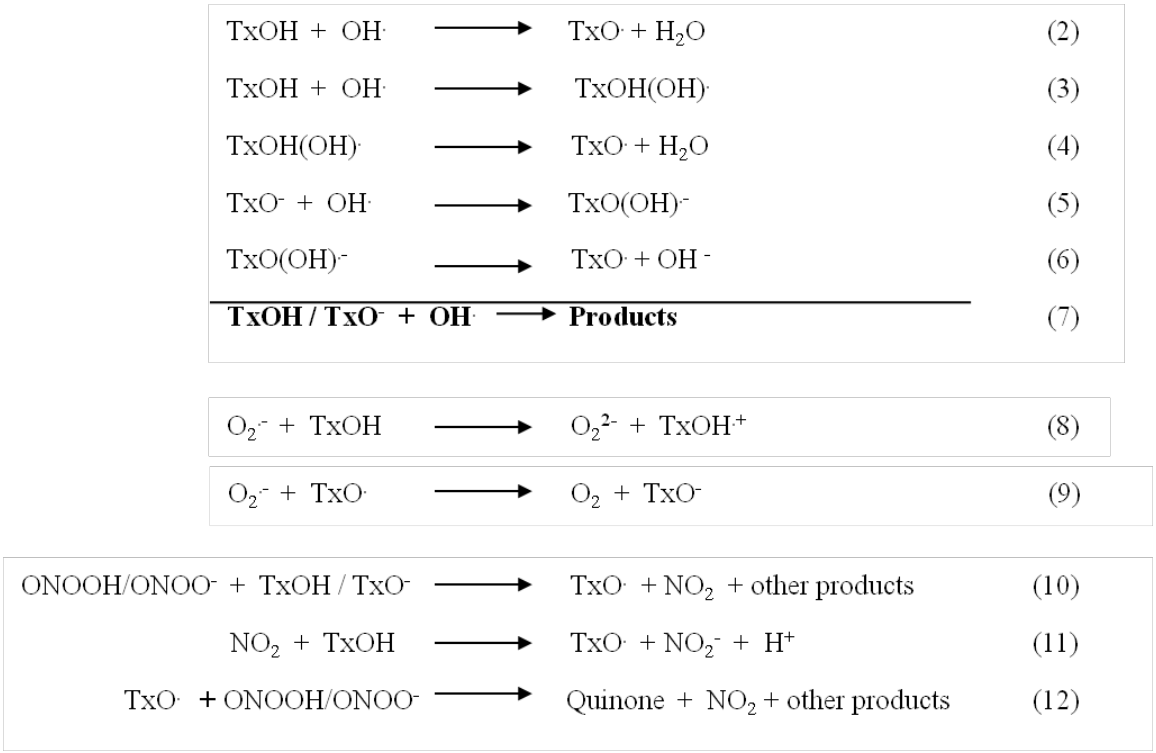

Figure 5-1. Reactions of Trolox with ROS and RNS.

(Reactions 2-7) Reactions of trolox with hydroxyl radical. (2) Hydrogen abstraction from phenolic group to form phenoxyl radical. (3) & (5) Addition of $OH^{\cdot}$ to phenolic ring to form a $OH^{\cdot}$ adduct. (4) & (6) $OH^{\cdot}$ adduct further forms phenoxyl radical by elimination of water molecule. (7) Represents the overall formation of phenoxyl radical under a range of pH. Reactions (3) and (4) represent reactions at neutral pH, whereas reactions (5) and (6) represent reactions at basic pH. TxOH : Trolox, $TxO^{\cdot}$: Trolox phenoxyl radical, $TxOH(OH)^{\cdot}$: $OH^{\cdot}$ adduct with Tx

(Reactions 8 and 9) Reactions of trolox with $O_2^{\cdot -}$

(Reactions 10-12) Reactions of trolox with RNS. $TxOH/TxO^{-}$: Trolox in protonated and deprotonated form, $ONOOH/ONOO^{-}$: peroxynitrite in protonated and deprotonated form, NO_2: Nitrite radical, $TxO^{\cdot}$: Trolox phenoxyl radical

reaction rate k_9 for reaction (9) has been reported as (4.5 $\pm$ 0.5) x 10^8 $M^{-1}{\cdot}s^{-1}$ [261]. Reaction (9) can be seen as a reaction for scavenging $O2^{\cdot-}$ as well as for regeneration of TxOH.

Reactions of trolox with reactive nitrogen species (RNS) like $ONOO^-$ and NO_2 are shown at the bottom of **Figure 5-1**. Trolox can undergo both one electron and two electron oxidation reactions depending on the concentration of peroxynitrite present. All the reaction rates depend on pH of solution due to prototropic equilibria of both trolox and peroxynitrite. In the range of pH 5.9 – 11, k_{10} and k_{12} have been reported as 8.3 – 3.4 x 10^4 and 6.4 – 1.6 x 10^3 $M^{-1}{\cdot}s^{-1}$ respectively. At neutral pH, rate constant k_{11} has been reported to be < 10^5 $M^{-1}{\cdot}s^{-1}$ [263].

Pro-oxidant effects of Vitamin E, Vitamin C and trolox have been reported previously [283, 286, 287], where antioxidant radicals react with low density lipoproteins (LDL), resulting in further generation of lipid radicals. It was observed that trolox behaves like a prooxidant only when radicals were generated using metal ions like Cu^{2+} or Cr(VI). Many of these transient metal ions are present *in vivo.* Trolox always acts like an antioxidant when peroxyl radicals were generated. It can be argued that, in presence of metal ions, trolox acts to reduce metal ions leading to excess generation of trolox phenoxyl radical. In absence of metal ions and oxygen, trolox phenoxyl radical undergoes a disproportionation reaction and a associated intramolecular cyclization (**Figure 5-2**) at a significant rate [288]. Vitamin E acted as a prooxidant only under high concentrations and exerted a better antioxidant effect at low concentrations [289]. In absence of oxygen, Vitamin E phenoxyl radical undergoes dimerization reaction [290]. Therefore,

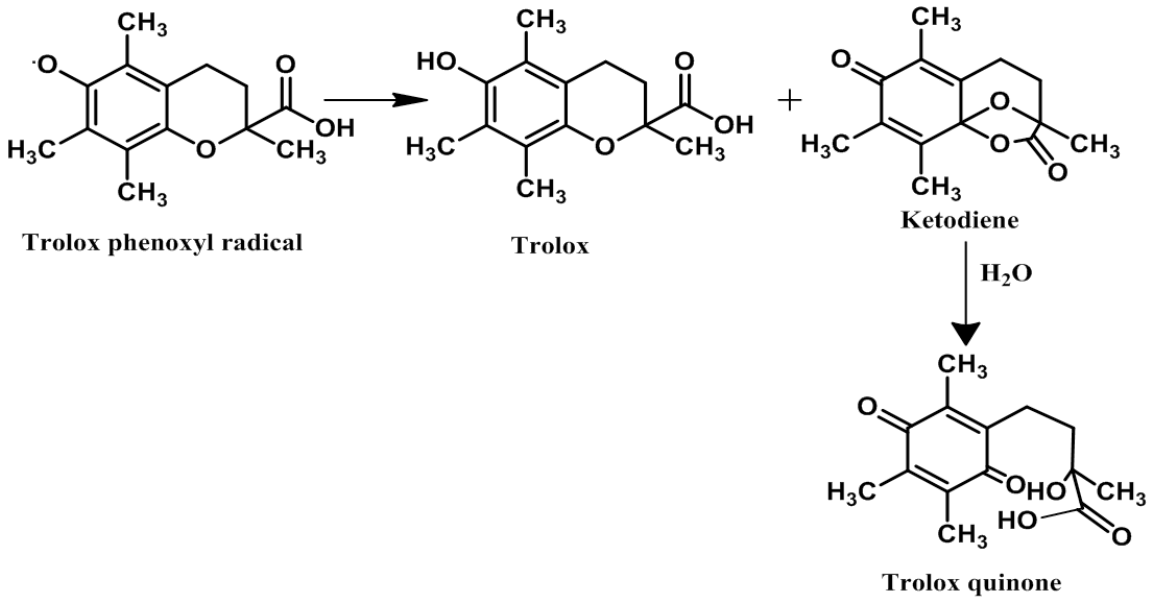

Figure 5-2. Decay Reactions of Trolox Phenoxyl Radical [288].

$TxO^{\cdot}$ disproportionates by a second-order, pH dependent process to give trolox and a unstable ketodiene intermediate. In a second reaction, ketodiene intermediate undergoes a slow pH dependent hydrolysis to form trolox quinone. The disproportionation reaction rate constant ranges from $10^9 – 10^4$ $M^{-1}{\cdot}s^{-1}$ and decreases with increase in pH and maximum decrease occurs between pH 2- 9. The reaction rate constant of intermediate decomposition ranges between 0.9 – 0.02 $M^{-1}{\cdot}s^{-1}$ in a pH range of 2 – 10 and it increases with pH [288].

antioxidant or prooxidant capacity of both trolox and Vitamin E depends on their concentrations and physiological conditions.

5.3 Materials and Methods

5.3.1 Materials

All reagents were used as received without any further purification. (±)-6-Hydroxy-2,5,7,8-tetramethylchromane-2-carboxylic acid (Trolox), 3-(4,5-Dimethyl-2-thiazolyl)-2,5-diphenyl-2H-tetrazolium bromide (MTT) and Pluronic F-68 were purchased from Sigma-Aldrich (St. Louis, MO). 2',7'-dichlorodihydrofluorescein diacetate (DCF-DA) and Live/Dead® cell viability assay were purchased from Invitrogen (Carlsbad, CA). All solvents were either obtained from Sigma-Aldrich or Fisher Scientific. Anti-nitrotyrosine antibody, Anti-dinitrophenylhydrazine (DNPH) protein antibody and HNE anti-body were purchased from Intergen (Purchase, NY) and Millipore (Billerica, MA).

5.3.2 Poly(trolox ester) Nanoparticle Formulation

PTx-1000 and PTx-2500 nanoparticles were formulated as previously described [256]. Briefly, polymer solution in acetone (10 mg/mL PTx-1000 and 2 mg/mL PTx-2500) was added to a pluronic F-68 solution in PBS while stirring. The resulting nanoparticle solution was left open overnight under stirring conditions to allow evaporation of the acetone. To remove excess surfactant, the nanoparticle suspension was centrifuged at 22000 rpm for 2 hrs. Supernatant was discarded and the pellet was resuspended in 40 mL phosphate buffered saline (PBS). Centrifugation was repeated two more times and cell media was used for final resuspension of the pellet. Nanoparticle size

was measured using dynamic light scattering on a Malvern Zetasizer Nano (Westborough, MA). Nanoparticles free of excess surfactant and of size 180-200 nm were used for all the studies.

5.3.3 *In Vitro* Cell Protection Against Oxidative Stress

Human leukemic monocyte lymphoma cells (U937) were obtained from American Type Culture Collection (ATCC) (Rockville, MD) and cultured in RPMI 1640 medium (Mediatech Inc., Manassas, VA) supplemented with 10% fetal bovine serum and penicillin/streptomycin. 96 well microplate was seeded with U937 cells at a seeding density of 70000 cells/well and cultured overnight. DCF-DA at a concentration of 5 μM was added and one hour later, polymer nanoparticles were added. Another hour later, oxidative stress was induced in the cells by adding cobalt nanoparticles (Nano-Co). 12 hrs later, fluorescence was measured from top at an excitation wavelength of 485 nm and emission wavelength of 528 nm using multi-detection microplate reader. Percent protection from injury by the antioxidant polymer was calculated by the following equation.

$$\%protection = \frac{Fluorescence_{injured} - Fluorescence_{sample}}{Fluorescence_{injured} - Fluorescence_{control}}$$

5.3.4 Cell Line

Human umbilical vein endothelial cells (HUVECs) were purchased from Lonza. Cells were cultured in EGM-2 medium with 2% fetal bovine serum at 37 ^{0}C in a humidified atmosphere of 5% CO_2 (v/v). All the studies with HUVECs have been conducted with cells from passage 3 to 5 and at 90% confluency.

5.3.5 Measuring Oxidative Stress in Cells Using DCF Fluorescence

HUVECs were seeded onto a 96-well plate at a density of 25000 cells/cm^2 and incubated at 37 ^{0}C in a humidified atmosphere of 95% air and 5% CO_2. After 24 h, medium in each well was replaced by 100 μL of treatment solution [trolox solution or poly(trolox ester) nanoparticle suspension in media] and 100 μL of 10 μM DCF-DA solution in media. Fluorescence was then measured at various time points using a bottom-reading GENios Pro fluorescence spectrophotometer (Tecan, Switzerland) at excitation and emission wavelengths of 485 nm and 535 nm, respectively. Well plates were incubated at 37 ^{0}C throughout the study and briefly taken out of the incubator for fluorescence measurements at each time point.

5.3.6 Cytotoxicity of Trolox, Poly(trolox ester) Nanoparticles and Nanoparticle Leachouts

Cytotoxicity of trolox was determined using a standard MTT assay according to manufacturer's protocol. Active reductase enzymes in the cell convert MTT into a colored formazan product which is then measured using UV spectrophotometry. HUVECs were seeded onto a 96-well plate at a density of 25000 cells/cm^2. After 24 h, media in the wells was removed and replaced by trolox solution in cell media. Freshly prepared 250 mM trolox stock solution in DMSO was diluted in cell media to prepare trolox solutions. Another 24 h later, trolox solution was removed and cells were washed twice with 200 μL PBS. 200 μL of 0.5 mg/mL MTT solution in PBS was then added to each well and the 96-well plate was incubated at 37 ^{0}C. After 5 h, MTT solution was gently removed from the wells and 100 μL of DMSO was added to dissolve the formazan

product. The absorbance intensity was recorded at 570 nm for formazan and at 690 nm for background using a Cary-50 Bio UV-Visible spectrophotometer equipped with a Cary 50 MPR microplate reader (Varian, Santa Clara, CA).

Toxicity of poly(trolox ester) nanoparticles to mouse pulmonary microvascular endothelial cells (MPMVEC) as measured by MTS assay (modification of MTT assay) has been reported previously [256]. Hence, in this study, cytotoxicity of PTx-1000 and PTx-2500 nanoparticles was determined using Live/Dead Viability Assay (Molecular Probes) according to manufacturer's protocol. HUVECs were seeded onto a 24-well plate at a cell density of 25000 cells/cm^2. After 24 h, cell media was replaced with 0.5 mL of nanoparticle suspensions in cell media. After another 24 h, nanoparticle solution was removed from each well and cells were washed twice with 2 mL of PBS. Cells were then stained with two-color fluorescence Live/Dead assay. They were then imaged via fluorescence microscopy where the live cells fluoresced green and the dead cells fluoresced red. The live and dead cells were counted using NIS-Elements software (Nikon Instruments, Melville, NY). The cell viability was then calculated as the number of live cells over the total number of live and dead cells.

To study the cytotoxicity of nanoparticle leachouts, HUVECs were seeded onto a 24-well plate at a cell density of 25000 cells/cm^2. After 24 h, media was taken out of each well. Cell media (250 μL) was added to the well and a porous insert (Nunc^{TM} cell culture insert with 0.02 μm pore size Anapore^{TM} membrane) was placed in each well. Another 250 μL of media or nanoparticle suspension was added to the insert. Cell viability was measured after 24 h using Live/Dead assay as described above.

5.3.7 Measurement of Protein Carbonyls, 3-nitrotyrosine (3NT) and Protein Bound 4-hydroxy-2-trans-nonenal (HNE) as Markers of Oxidative Stress

HUVECs were seeded on to a 6-well plate at a cell density of 25000 cells/cm^2. 24 h later, cell media from the well was replaced by 2 mL of treatment solution in media. Twenty-four h after the treatment, solution above the cells was removed and cells were washed twice with chilled PBS. Cells were then scraped and centrifuged. Cell pellet was then lysed using a cell lysis buffer, the latter prepared by mixing RIPA buffer (pH = 8.0) and protease inhibitor cocktail (Amresco, Solon, OH) using manufacturer's protocol.

Levels of protein carbonyl, 3NT and HNE were measured by slot blot technique [291, 292]. Briefly, for protein carbonyl levels, each sample was derivatized by incubating with 5µL of 12% SDS and 10mM solution of 2,4-dinitrophenylhydrazine (DNPH) in 2N HCl for 20 min at room temp followed by a 7.5 µL addition of a neutralization solution (2M Tris in 30% glycerol). The sample was then used for slot blot analysis. Whereas, for 3NT and protein bound HNE levels, samples were denatured in 5µL of 12% SDS solution and Laemmli sample buffer. Specific antibodies were used against protein carbonyl, 3NT or HNE protein modifications and colorimetric technique was used for detection as described previously [291, 292].

Statistical analysis

Treatment comparisons were made using analysis of variance (ANOVA) followed by post hoc Student's t-test. Contrasts were considered significantly different at $P < 0.05$. Data are reported as mean $\pm$ standard errors.

5.4 Results

5.4.1 Nano-Co Induced Oxidative Stress Injury and Protection from Poly(trolox ester) Nanoparticles

To measure the effect of Nano-CO treatment on oxidative stress levels in U937 cells, DCF fluorescence was measured as percent of control (0 μg/ml Nano-Co) (**Figure 5-3**). DCF fluorescence increased with increase in Nano-Co concentration and for Nano-Co concentrations of 2.5 and 5 μg/ml, DCF fluorescence was maximum at 12 h, after which DCF fluorescence started decreasing.

To study the protective effect of poly(trolox ester) nanoparticles, human U937 monocytes were exposed to PTx-1000 (180 nm) and PTx-2500 nanoparticles (215 nm) 1 hr prior to inducing oxidative stress by exposure to Nano-Co particles. PTx-1000 and PTx-2500 nanoparticles at concentrations of 160 and 320 μg/ml, where they have no severe cytotoxic effect, were studied. Oxidative stress was measured by measuring DCF fluorescence after treatment with Nano-Co **(Figure 5-4)**. Without the addition of Nano-Co to the cells, incubation of PTx-1000 and PTx-2500 nanoparticles with the cells for 12 hrs reduced the background oxidative stress in the cells by 40% and 25% respectively. Pre-incubation of cells with poly(trolox ester) nanoparticles prior to adding Nano-Co, suppressed the oxidative stress in the cells by 40-50% in case of PTx-1000 nanoparticles and 25-40% in case of PTx-2500 nanoparticles.

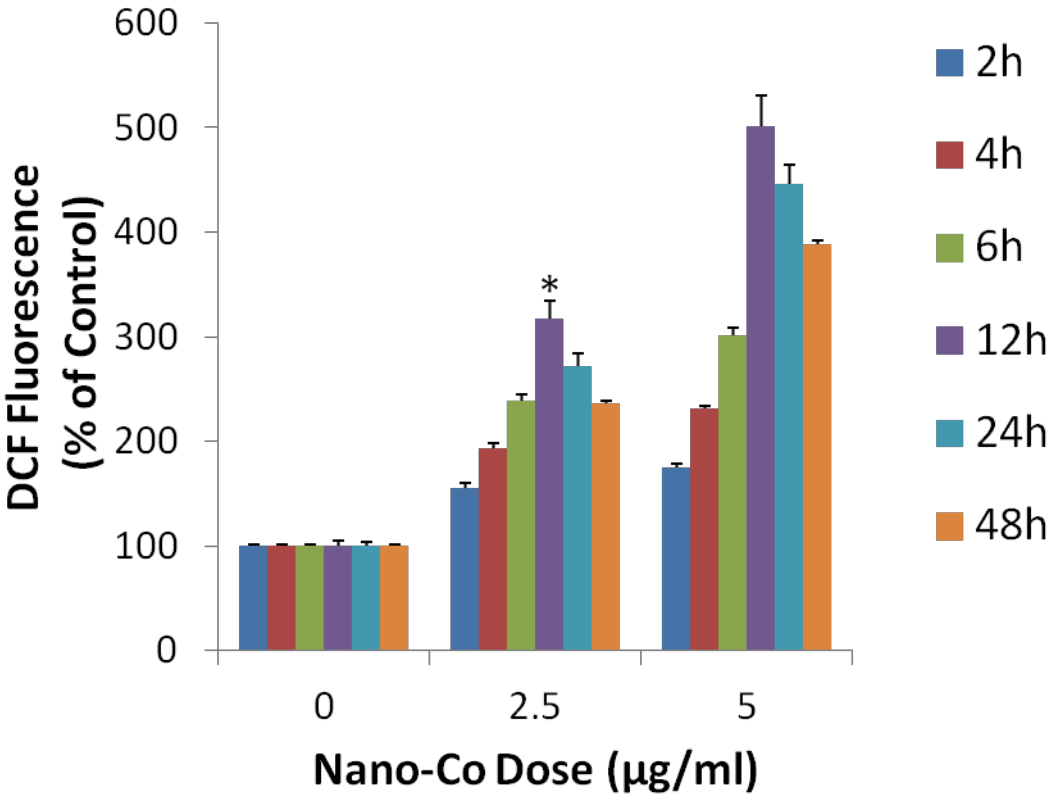

Figure 5-3. Oxidative Stress Injury Model.

U937 cells were treated with Nano-Co at concentrations of 2.5 and 5 µg ml^{-1}. DCF fluorescence, a marker of oxidative stress in the cells, was measured at different times. For both the concentrations of Nano-Co, cells experience maximum oxidative stress after 12 hrs of Nano-Co addition. (M $\pm$ SD, n=3). * represents significant difference from 6h and 24h data points with $p<0.05$.

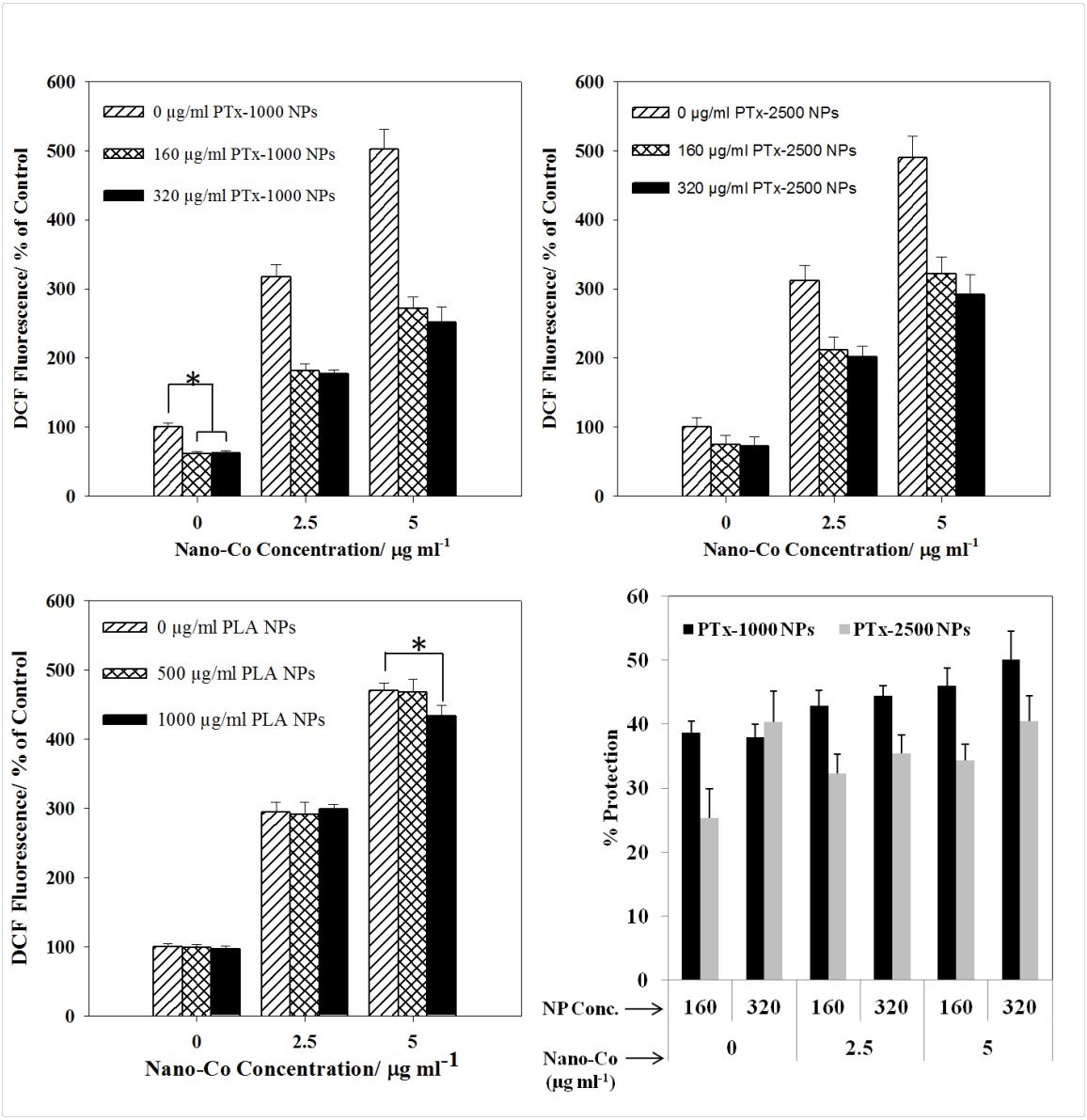

Figure 5-4. Cell Protection Against Oxidative Stress by Poly(trolox ester) Nanoparticles.

One hour after adding DCF to the U937 cells, PTx-1000 nanoparticles (top left) and PTx-2500 nanoparticles (top right) were added to the cells at concentrations of 160 and 320 µg ml^{-1} and PLA nanoparticles (bottom left) were added to the cells at concentrations of 500 and 1000 µg ml^{-1}. Another hour later Nano-Co was added at concentrations of 2.5 and 5 µg ml^{-1}. 12 hrs after the addition of Nano-Co, DCF fluorescence was measured. % Protection of cells from the oxidative stress injury using PTx-1000 and PTx-2500 nanoparticles at different concentrations (bottom right). (M $\pm$ SD, n=3). * represents significant difference from respective control values with $p<0.05$.

5.4.2 Effect of Trolox and Poly(trolox ester) Nanoparticles on Background Oxidative Stress in the Cells

Effect of trolox on the oxidative stress levels in the cells was measured using DCF fluorescence (used as a marker of oxidative stress) in HUVECs (Fig. 1). Fluorescence intensities as percent of control at 27 h time are compared in **Figure 5-5**. Trolox at lower concentrations suppresses oxidative stress in the cells as indicated by reduced fluorescence as compared to the control. At concentrations of trolox from 50 to 125 µg/mL, the DCF fluorescence in the cells is lower than control, but higher as compared to fluorescence at 25 µg/mL. DCF fluorescence increases with increasing trolox concentration in the range of 50 to 1000 µg/mL, where the fluorescence at 1000 µg/mL is almost eight times that of the control (0 ug/ml trolox).

In a similar study, PTx-1000 and PTx-2500 nanoparticles followed by DCF-DA solution were added to HUVECs and fluorescence was measured after 27 h (**Figure 5-6**). In the case of PTx-1000 nanoparticles, DCF fluorescence at 27 h decreases with increasing nanoparticle concentration up to 1000 µg/mL. At concentrations of 2000 and 4000 µg/mL of PTx-1000 nanoparticles, an increase in the fluorescence is observed compared to the fluorescence at 1000 µg/ml. DCF fluorescence is increasingly suppressed with an increase in PTx-2500 nanoparticle concentration.

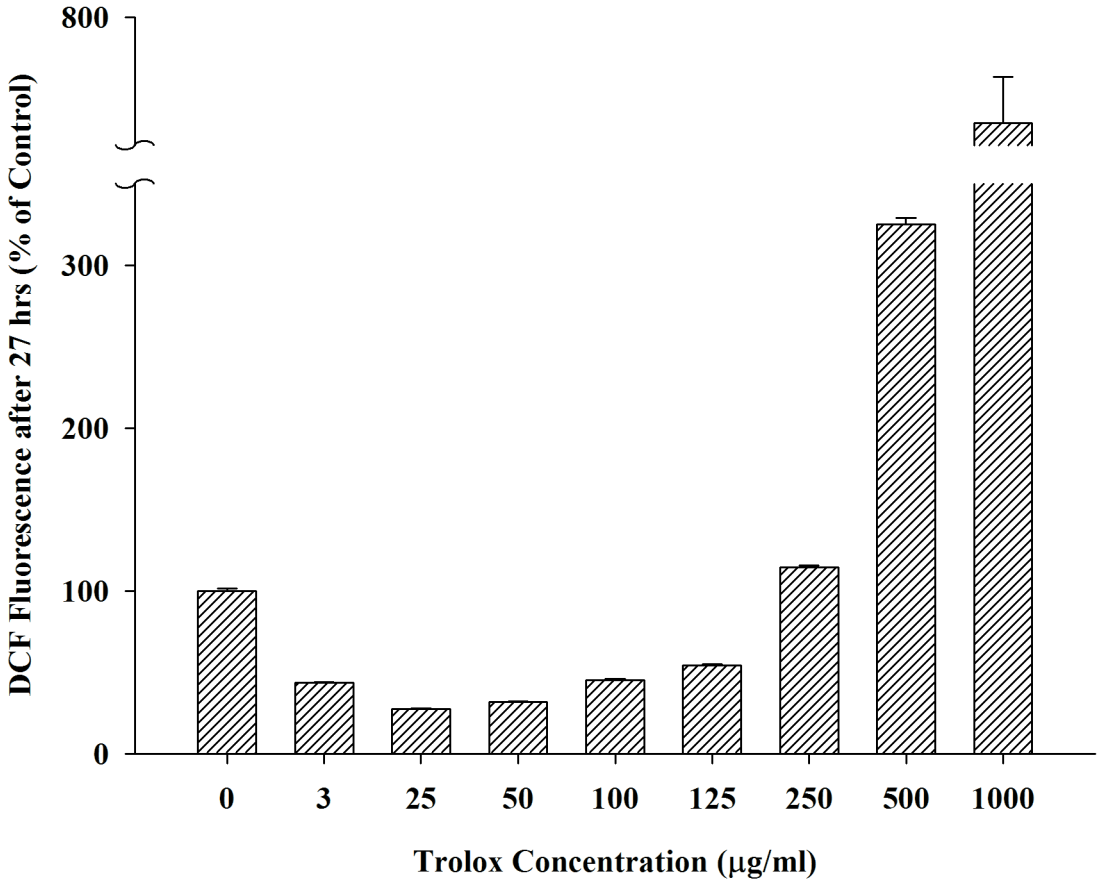

Figure 5-5. Effect of Trolox on Oxidative Stress Level in HUVECs.

Trolox solution in HUVEC media was added at different concentrations to HUVECs cultured in a 96-well plate. Fluorescence was measured after 27 h using a bottom reading fluorescence spectrophotometer set at 485/535 nm excitation and emission. (n=5, M±SE)

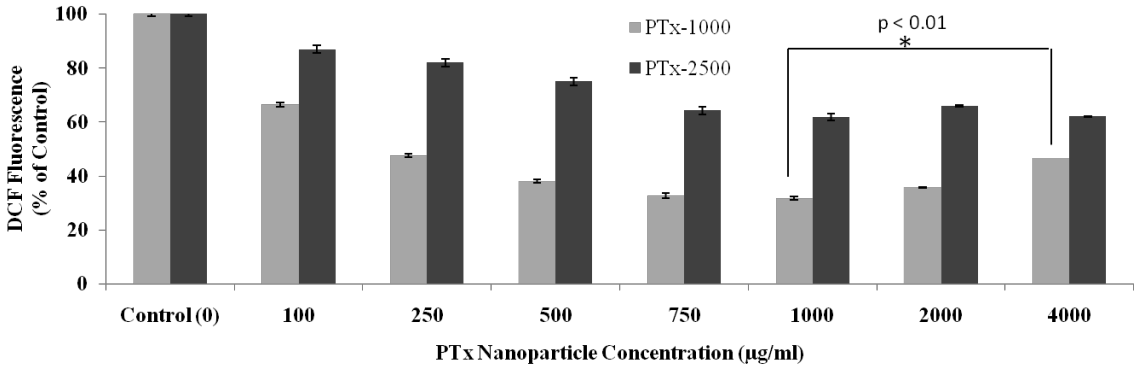

Figure 5-6. Effect of Poly(trolox ester) Nanoparticles on Oxidative Stress in HUVECs.

PTx-1000 (grey) and PTx-2500 (black) nanoparticles suspended in EGM-2 media at different concentrations were added to HUVECs cultured in 96-well plate and fluorescence measured after 27 h is compared with control. ANOVA analysis of data indicates that the trends are significant for both PTx-1000 and PTx-2500 nanoparticles. (n=5, M±SE)

5.4.3 Cytotoxicity of Trolox, Poly(trolox ester) Nanoparticles and Their Leachouts

HUVECs were treated with trolox solutions of different concentrations for 24 h and the cell viability was measured using MTT assay (**Figure 5-7**). Trolox at concentrations up to 500 μg/mL does not have any significant toxicity as compared to the control. However, cell viability at 1000 μg/mL significantly decreased to just above 70%.

To study the cytotoxicity of poly(trolox ester) nanoparticles, PTx-1000 and PTx-2500 nanoparticles were added to HUVECs at different concentrations and cell viability was measured after 24 h using Live/Dead assay (**Figure 5-8**). In the concentration range studied here, cell viability did not change significantly as compared to control.

In order to study the cytotoxicity of poly(trolox ester) nanoparticle leachouts, poly(trolox ester) nanoparticles suspended at concentration of 1 mg/mL were physically separated from HUVECs using a porous membrane support with pore size of 20 nm. Viability of the HUVECs exposed to poly(trolox ester) leachouts did not change significantly as compared to control (**Figure 5-9**).

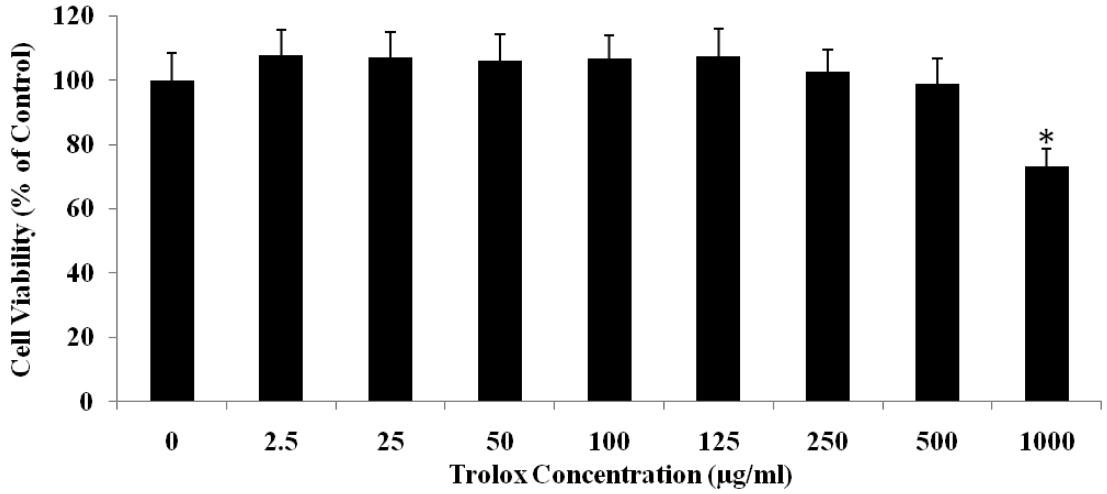

Figure 5-7. Cytotoxicity of Trolox.

HUVECs were treated with trolox at different concentrations for 24 h. Cell viability was measured using MTT assay. Trolox has significant (*) cytotoxicity only at 1000 µg/mL concentration ($p < 0.05$). (n=5, M$\pm$SE)

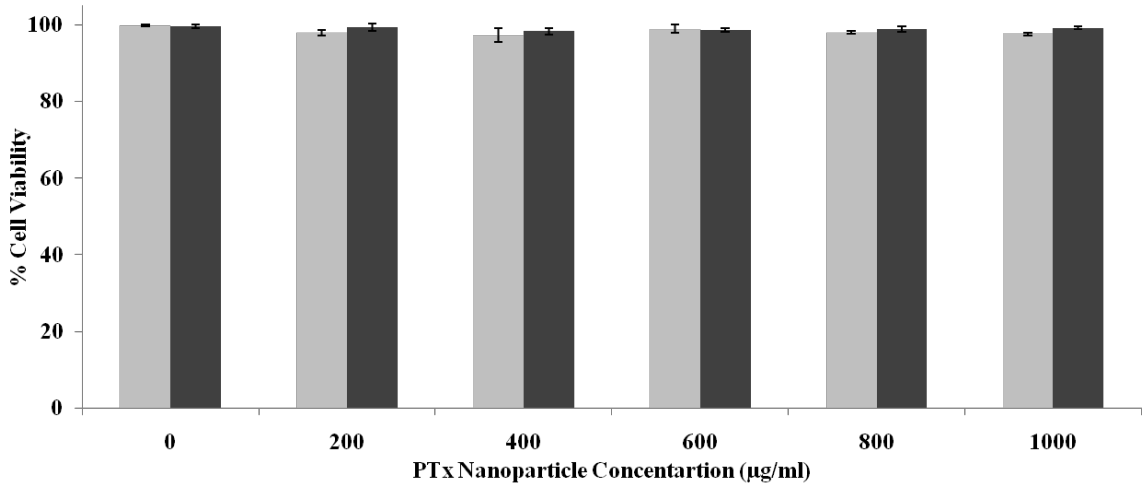

Figure 5-8. Cytotoxicity of Poly(trolox ester) Nanoparticles.

HUVECs were treated with PTx-1000 nanoparticles (grey) and PTx-2500 nanoparticles (black) for 24 h. Cell viability was measured using the Live/Dead assay. One-way ANOVA was performed and the trends were insignificant with $p < 0.05$. PTx-1000 and PTx-2500 nanoparticles do not have any significant toxicity to HUVECs. (n=3, M$\pm$SE)

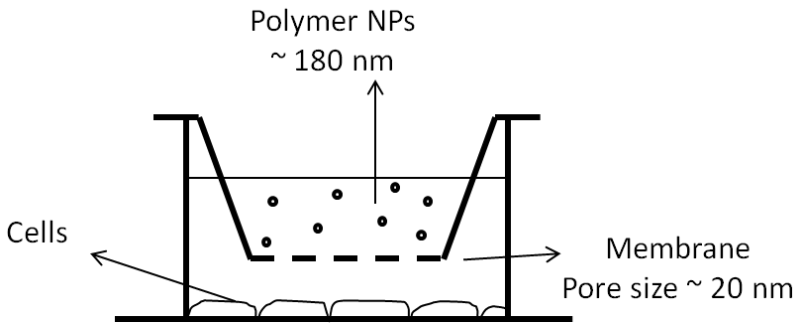

(A)

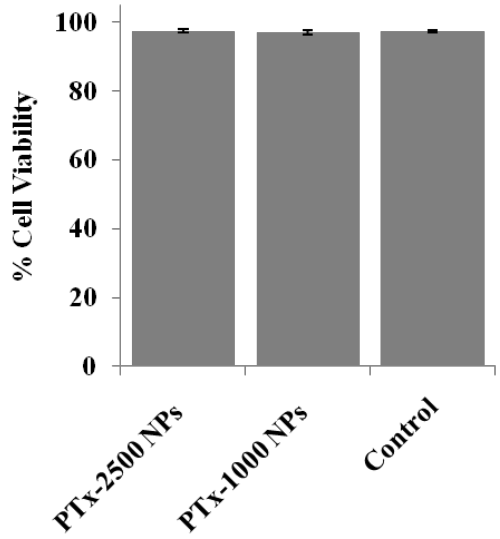

(B)

Figure 5-9. Cytotoxicity of Poly(trolox ester) Leachouts.

(A) Schematic showing nanoparticles separated from cells by porous membrane

(B) HUVECs were treated with PTx-1000 and PTx-2500 nanoparticle leachouts for 24 h. Poly(trolox ester) nanoparticles at concentration of 1 mg/mL were suspended in EGM-2 media on a porous insert above confluent HUVECs cultured in 24-well plates. Cell viability was measured using the Live/Dead assay. (n=3, M±SE)

5.4.4 Oxidized Cellular Proteins (protein carbonyl, 3-NT and HNE levels) as Markers of Oxidative Stress

HUVECs were exposed to free trolox, PTx-1000 and PTx-2500 nanoparticles for 24 h. After three washes with phosphate buffered saline solution, cells were lysed and cellular protein was collected as described in methods section. Protein samples were then analyzed for protein carbonyl (**Figure 5-10A**), 3-NT (**Figure 5-10B**) and protein-bound HNE (**Figure 5-10C**) levels. Treatment of HUVECs with trolox did not show any significant difference from control in any of the three markers. Protein carbonyl content decreased as compared to control for cells treated with PTx-1000 and PTx-2500 nanoparticles at concentrations of 1 mg/ml. At lower concentrations (0.1 mg/ml) of PTx-1000 and PTx-2500 nanoparticles, there was no significant change in protein carbonyl content. Nanoparticle treatments did not show any significant difference from control for 3-NT and protein-bound HNE levels, though a non-significant trend in 3-NT levels suggests that there were two measures of oxidative stress which were observed to be lower for the PTx-1000 nanoparticles.

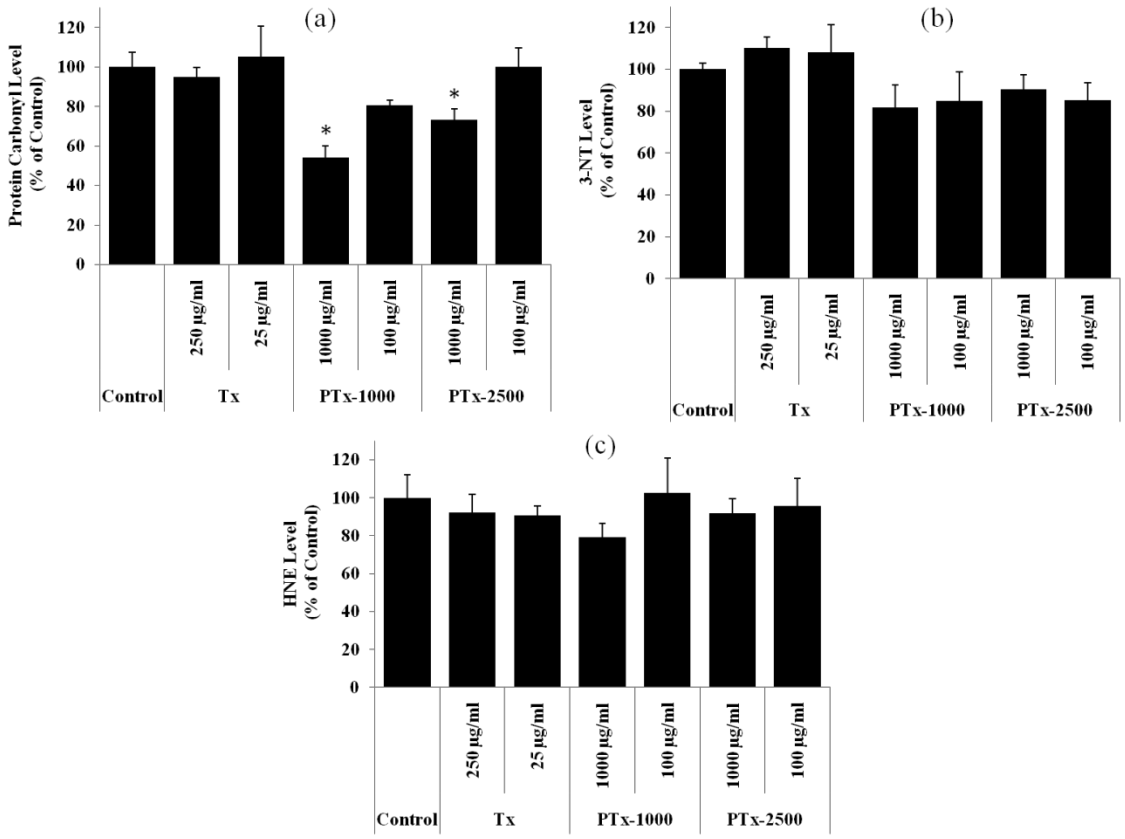

Figure 5-10. Monitoring Oxidative Stress Levels in HUVECs.

Cells were treated with free trolox, PTx-1000 and PTx-2500 at two different concentrations for 24 h. Cells were then lysed and collected protein was analyzed for a.) protein carbonyl content, b.) 3-NT levels and c.) protein-bound HNE levels using immunochemical methods. One-way ANOVA was performed on all the data sets. The trend is significant only for the protein carbonyl levels, but not for 3-NT and HNE levels. (n=3, M$\pm$SE)

5.5 Discussion

In vitro degradation studies of poly(trolox ester) nanoparticles had found that degradation products of PTx-1000 and PTx-2500 nanoparticles had radical scavenging activity. In order to confirm this result, PTx-1000 and PTx-2500 nanoparticles were tested in an *in vitro* oxidative stress-based cell injury model. It is known that exposure of cells to metal and metal oxide nanoparticles could induce a range of biological responses including cytotoxicity and inflammation, often mediated by oxidative stress mechanisms [293-295]. In this study, oxidative stress injury was induced in the monocytes with exposure to cobalt nanoparticles (Nano-Co). It has been shown previously that addition of Nano-Co leads to ROS generation in U937 cells [294]. A time-dependent and dose-dependent effect of only Nano-Co was studied to find the time and concentration at which maximum ROS generation was observed. DCF fluorescence which is indicative of oxidative stress injury in the cells, is maximum at 12 hrs after exposure to Nano-Co and increases with increase in Nano-Co concentration (**Figure 5-3**). Therefore to study the extent of protection provided by poly(trolox ester) nanoparticles, oxidative stress in cells was monitored 12 hrs after induction of injury.

Poly(trolox ester) nanoparticles suppressed the Nano-Co induced oxidative stress in the cells by 40-50% in case of PTx-1000 nanoparticles and 25-40% in case of PTx-2500 nanoparticles (**Figure 5-4**). It is hypothesized that lower degree of protection by PTx-2500 nanoparticles can be a result of slower release of trolox from PTx-2500 nanoparticles. Also, protection provided by poly(trolox ester) nanoparticles was independent of the dose of nanoparticles. This could be explained by the inability of trolox monomer to completely suppress the oxidative damage caused by Nano-Co injury.

Dose-dependent effect of trolox monomer in the presence of Nano-Co injury shows that trolox at a concentration of 50 μg/ml suppressed DCF fluorescence by 45% (**Figure 5-11**). In a control set of experiments, poly(lactic acid) (PLA) nanoparticles with an average size of 280 nm were added to the cells prior to adding Nano-Co particles and PLA nanoparticles were unable to suppress oxidative stress in the cells (**Figure 5-4**). PLA nanoparticles were formulated using similar single-step emulsion technique as used for poly(trolox ester) nanoparticle formulation.

It was observed that, without the addition of Nano-Co to the cells, incubation of trolox, PTx-1000 and PTx-2500 nanoparticles with the cells for 12 hrs reduced the background oxidative stress in the cells by 50%, 40% and 25% respectively (**Figure 5-4 and Figure 5-11**). While further studying this effect of trolox and poly(trolox ester) nanoparticles on background oxidative stress in the HUVECs, it was found that trolox has a concentration dependant antioxidant and pro-oxidant effect (**Figure 5-5**).

This concentration dependent biphasic behavior of antioxidants in both *in vitro* and *in vivo* settings has been illustrated in the literature [249, 250, 280, 282-284, 296-298]. In a healthy cell/tissue, there is a balance between the rate at which ROS and RNS are generated and the rates at which antioxidant defense mechanisms terminate the reactive species. Any change in the antioxidant reservoir concentration or rate of generation of free radicals can change the redox state of the cell/tissue. A change in redox state can induce different cellular responses ranging from cellular apoptosis to cell differentiation [34, 299, 300]. This two-way antioxidant and pro-oxidant effect can be used in tissue engineering applications to control the oxidative stress level in the cells and

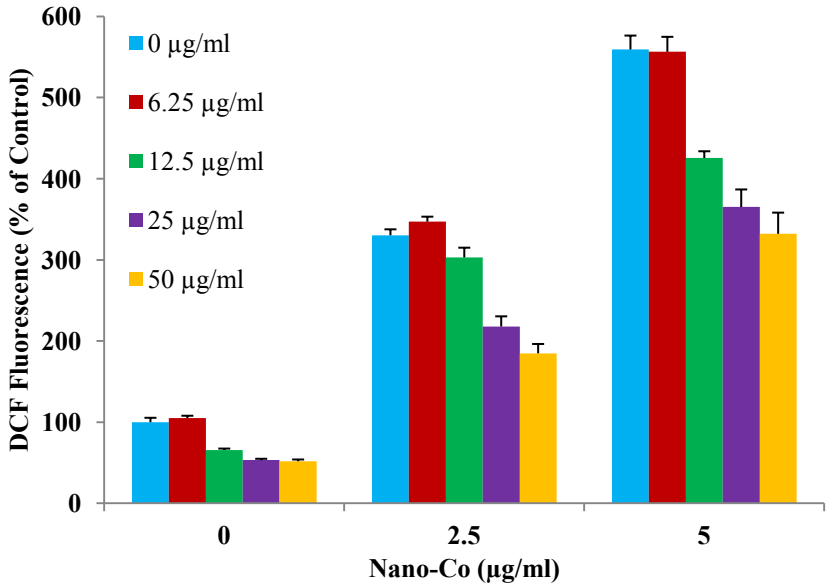

Figure 5-11. Cell Protection Against Oxidative Stress by Trolox Monomer.

One hour after adding DCF to the U937 cells, trolox was added to the cells at concentrations of 6 – 50 µg/ml. Another hour later Nano-Co was added at concentrations of 2.5 and 5 µg ml^{-1}. 12 hrs after the addition of Nano-Co, DCF fluorescence was measured. (M $\pm$ SD, n=3).

thereby modulate cell response. Polymers composed of antioxidants linked through hydrolysable bonds provide a means of controlling release of these antioxidants and thereby affect the redox state of the cell.

Phenolic antioxidants (A-OH) like trolox can react with and terminate free radical species ($R^{\cdot}$) resulting in a stable phenoxyl radical ($A\text{-}O^{\cdot}$). In a normal cell/tissue, various small molecule antioxidants exert antioxidant effects synergistically where other antioxidants with reduction potential lower than $A\text{-}O^{\cdot}$ can regenerate A-OH. The mechanisms by which antioxidants can act as pro-oxidants vary depending on that particular antioxidant and its environment. Some of the mechanisms that could result in pro-oxidant effects are depletion of glutathione [249, 297], the presence of reduced transition metal (Fe, Cu) ions [250, 296, 301], blocking several biomolecular targets like kinases and other proteins, etc. Even though the biphasic effect of trolox represented by the U-shaped bar graph in **Figure 5-5** has been reported in the literature [284, 302-304], the exact mechanism for its pro-oxidant activity is not known. Trolox (T-OH) can react with a free radical ($R^{\cdot}$) to from trolox phenoxyl radical ($T\text{-}O^{\cdot}$) and R-H. The resulting $T\text{-}O^{\cdot}$ is more stable as compared to $R^{\cdot}$ and can trap another free radical to give a trolox quinone [261, 263, 305]. If trolox is present in excess as compared to the rate of generation of free radicals, the system will have equivalent amount of trolox converted into trolox phenoxyl radical which can in turn oxidize species that have lower redox potential.

DCF fluorescence is a widely used model to study oxidative stress injury. DCF-DA (2',7'-dichlorodihydrofluorescin diacetate), a non-fluorescent ester form of the dye, is taken up by the cells and cleaved to non-fluorescent DCFH (2',7'-

dichlorodihydrofluorescin) by active esterases in the cell. DCFH can then react with free radicals to result in fluorescent DCF (2',7'-dichlorofluorescin) a marker of oxidative stress in the cells. DCF fluorescence data in **Figure 5-5** suggest that the critical trolox concentration for HUVECs at which trolox starts showing pro-oxidant effects is approximately between 25 to 50 µg/mL.

Even though the DCF fluorescence model is simple and widely used, it is an indirect and general marker of overall oxidative stress in the cell and does not provide information regarding which specific oxidative species are responsible for oxidation of DCFH [306-309], nor what cellular components are at risk of damage. Indeed, DCFH can not only be oxidized by variety of oxidative species like $ONOO^-$, OH^-, lipid peroxides, thiol radicals, etc., but could also be oxidized by antioxidant radicals ($T\text{-}O^\cdot$). DCF fluorescence data should therefore be interpreted with caution. As compared to the DCF fluorescence, markers of oxidative stress like protein carbonyl, 3NT and protein-bound HNE are direct evidence of damage occurred to proteins, enzymes and lipids at cellular levels and are quantitative. Also, 3-NT and protein-bound HNE are markers specific for protein damage by RNS and lipid peroxidation, respectively. Generalized protein oxidation can be detected through monitoring the extent of protein carbonyl content contained within the cell, with an increase indicating an elevation in protein oxidation. Proteins obtained after treatment of HUVECs with free trolox, PTx-1000 and PTx-2500 nanoparticles were analyzed for their protein carbonyl, 3-NT and protein-bound HNE content. Both PTx-1000 and PTx-2500 nanoparticles at 1 mg/mL showed a significant difference in protein carbonyl content, suggesting a unique anti-oxidant protective effect. Neither antioxidant nor pro-oxidant effect of free trolox was observed using any of the

three markers, suggesting that the DCF fluorescence increase observed may be a "false positive", further emphasizing the importance of secondary validation when monitoring cellular oxidative stress.

The advantage of having antioxidant polymers like poly(trolox ester) is that they can be used to deliver antioxidants in gradual and controlled manner as compared to initial pulse dose of antioxidants. Our previous work on poly(trolox ester) suggests the polymer undergoes enzymatic degradation to release active antioxidants [256]. As shown in **Figure 5-6**, treatment of HUVECs with PTx-1000 and PTx-2500 nanoparticles resulted in suppression of DCF fluorescence in a concentration dependent manner. To rule out the possibility of this suppression of fluorescence as result of cell death, cytotoxicity of trolox monomer, PTx-1000 and PTx-2500 nanoparticles was determined. As shown in **Figure 5-7**, trolox has significant cytotoxicity at concentration of 1000 μg/ml. While toxicity of trolox at higher concentrations was thought to be a result of its pro-oxidant effect as observed by DCF fluorescence studies, the lack of oxidative products (**Figure 5-10**) suggest an alternate mechanism for this cell death.

PTx-1000 and PTx-2500 have very little to no cytotoxicity to HUVECs as indicated by the cell viability data in **Figure 5-8**. This study conforms with our previous findings regarding poly(trolox ester) nanoparticles having very little to no cytotoxicity to mouse pulmonary microvascular endothelial cells (MPMVEC), where cell viability was measured using the MTS assay [256]. However, cytotoxicity could also result from degradation products or the leachouts from poly(trolox ester) nanoparticles. To determine cytotoxicity of leachouts, poly(trolox ester) nanoparticles were suspended in a porous support above a confluent layer of HUVECs. The porous support (Nunc cell culture

inserts, 0.02 μm Anapore membrane) had a pore size of ~ 20 nm which would prevent nanoparticles of 180-200 nm from interacting with cells. However, water soluble leachouts from nanoparticles can diffuse through the membrane and interact with the cells. Poly(trolox ester) nanoparticle leachouts do not have any significant cytotoxicity as shown in **Figure 5-9**. Insignificant cytotoxicity of poly(trolox ester) nanoparticles and leachouts suggests that the suppression of DCF fluorescence by PTx-1000 and PTx-2500 treatment is a result of the antioxidant effect. The antioxidant effect of poly(trolox ester) was also verified by the protein carbonyl data, where PTx-1000 and PTx-2500 nanoparticles at higher concentrations suppressed protein carbonyl content in HUVECs. PTx-1000 nanoparticles suppress DCF fluorescence more as compared to PTx-2500 nanoparticles. This conceivably can result from a difference in the degradation rate of the polymers and hence trolox being released at difference rates. PTx-1000 is more hydrophilic as compared to PTx-2500 and would degrade faster due to its lower molecular weight. A similar trend was observed where PTx-1000 nanoparticles provided more protection from oxidative stress injury in a *in vitro* model as compared to PTx-2500 nanoparticles (**Figure 5-4**). Increased DCF fluorescence at higher PTx-1000 nanoparticle concentrations of 2000 and 4000 μg/mL indicates the pro-oxidant effect of PTx-1000. Biphasic DCF monitored antioxidant and pro-oxidant behavior of trolox could be recreated using PTx-1000 nanoparticles, where PTx-1000 acts as a pro-oxidant at very high concentrations.

5.6 Conclusions

Poly(trolox ester) has very little to no cytotoxicity and suppresses almost 50% of oxidative stress in the cells induced by nanometals. Also, poly(trolox ester) nanoparticles

affect the redox state of the cells as confirmed by DCF fluorescence and protein carbonyl measurements in HUVECs. The polymer form of trolox possessed a unique ability to suppress protein oxidation not seen with the free trolox samples, emphasizing the importance of delivery route in modulating the potential therapeutic effect of antioxidant drugs. While DCF demonstrated a biphasic antioxidant/pro-oxidant effect of trolox, monitored cellular oxidative stress products did not exhibit this effect. Because of the slow release of trolox through its biodegradation, poly(trolox ester) is an effective means of modulating cellular redox states. This capability has far reaching implications in the use of antioxidant polymers as a means of controlling cell status for a variety of biomedical, pharmaceutical and tissue engineering applications.

Chapter 6. A Single-step Polymerization Method for Poly(β-amino ester) Biodegradable Hydrogels and Their Characterization

Chapter partly based on the research articles published in :

D. Biswal, P.P. Wattamwar, T.D. Dziubla and J.Z. Hilt, "Poly(β-amino ester) Hydrogel Synthesis by Single Step Polymerization Method", Polymer, 2011, 52, 5985-5992.

My contribution in this research article was to synthesize hydrogels,characterize swelling response of synthesized hydrogels in organic solvents and to determine mechanical properties of the gels.

P.P. Wattamwar, D. Biswal, A. Lyvers, D. Cochran, J.Z. Hilt and T.D. Dziubla, "Synthesis and Characterization of Poly(antioxidant β-amino esters) for Controlled Release of Polyphenolic Antioxidants", Acta Biomaterialia (*to be Submitted*)

6.1 Introduction

As described in the previous chapters, poly(trolox ester) is capable of degrading and releasing trolox, resulting in the suppression of cellular oxidative stress. While this work is promising and serves as a antioxidant polymer proof-of-concept, poly(trolox ester) has its own set of limitations, which reduces enthusiasm for their use. Degradation of poly(trolox ester) by hydrolysis is very slow and it requires enzymatic degradation to see functional effects, allowing little to no control over the rate of polymer degradation. As the field of antioxidant polymers emerges, important questions like the choice of antioxidant and the rate at which antioxidants should be released from the polymer still need to be addressed. The answers to these questions will likely depend on the settings in which the antioxidant polymers are intended to be used. For example, acute oxidative stress injury like ischemia-repurfusion requires form of antioxidant polymer suitable for vascular delivery (nanoparticles) that releases antioxidants gradually over a short period

of time (few hours to days). Whereas chronic disorders like non-healing wounds or biomaterial-induced local inflammation require antioxidant polymers in form of scaffolds/films/coatings that release antioxidants locally over a period of few weeks to months. In order to address these questions, there is a strong need for a flexible polymer chemistry platform that can allow for studying the biological response to a biomaterial based upon the type of antioxidant, the release rate and method of exposure (e.g., coating, nanoparticle, implant).

Poly(β-amino esters) (PBAE), synthesized by a conjugate addition reaction of primary/secondary amines with diacrylates, are a class of biodegradable polymers and hydrogels that have hydrolytically cleavable ester groups and a strong pH-dependent degradation rate that has been used for triggered drug/protein release [310-319]. Several research groups have studied vast libraries of acrylate and amine monomers to tune mechanical and degradation properties of PBAE [320, 321]. Much of this work focused on PBAE hydrogels involving a two-step synthesis method: i.) synthesis of a PBAE macromer/oligomer with acrylate end groups, followed by ii.) free radical polymerization of PBAE macromers/oligomers to form a crosslinked PBAE hydrogel. PBAE hydrogels provide a platform whereby appropriate choice of acrylate monomer, amine monomer and the ratio of two monomers, hydrogel properties can be tuned and their effect on tissue engineering and biomaterial applications can be studied [315, 322]. However, the second step of free radical polymerization, which requires use of free radical initiators and accelerators, can cause cellular toxicity during *in situ* polymerization [323]. Further, due to the highly reactive nature of free radicals, free radical polymerization can often be inhibited in the presence of cosolutes (e.g. drugs, porogens, etc.) resulting in poor gel

formation [324, 325]. Moreover, we have observed in our lab that free radical polymerization in the presence of antioxidants (e.g. green tea extracts, vitamin E, etc.) does not result in crosslinked hydrogels, due to the free radical inhibiting effects of these antioxidants.

In this chapter, a modified non-free-radical polymerization poly(β-amino ester) chemistry [326] is presented as a platform to synthesize antioxidant polymers with tunable properties. Reaction kinetics of PBAE synthesis along with effect of different monomers and the ratio of acrylates to amines on the degradation of PBAE have been studied in detail by Biswal et. al. [326]. In the same study, Dipti Biswal had carried out the experiments to study swelling of PBAE in different organic solvents and found that PBAE hydrogels undergo degradation in primary alcohols. My contribution to this research article was to apply the polymer-solvent interaction parameters to understand swelling behavior of PBAE hydrogels in different organic solvents. Also, to understand the ethanol-based degradation mechanism, I characterized the PBAE degradation products using FTIR and taking advantage of this particular characteristic, PBAE was conjugated with ascorbic acid post-synthesis.

6.2 Materials and Methods

6.2.1 Materials

Poly(ethylene glycol) 400 diacrylate (PEG400DA) and diethylene glycol diacrylate (DEGDA) were purchased from Polysciences, Inc. Three primary diamines, 4,7,10-Trioxa-1,13-tridecane diamine (TTD), 2,2’ (ethylenedioxy) bis ethylamine (EDBE), and Hexamethyldiamine (HMD) were obtained from Sigma Aldrich. Quercetin, curcumin, acryloyl chloride, triethylamine and 2,2’-azo-bis(2-aminopropane)-HCl

(AAPH) were all purchased from Sigma-Aldrich. 2',7'-dichlorodihydrofluorescein diacetate (DCF-DA) was purchased from Invitrogen. All organic solvents were obtained from Sigma-Aldrich and Fisher Scientific and used as received.

6.2.2 Synthesis of PBAE

PBAE hydrogels were synthesized by reacting a diacrylate and a primary diamine at 50^{o}C by a one step Michael addition reaction. In a typical experiment, the desired amount of diacrylate (PEG400DA and DEGDA) was mixed with THF solvent (50wt% with respect to total monomer). The primary diamine (TTD, EDBE and HMD) was added to this solution at a set molar ratio to the total diacrylate content. Next, the solution was transferred to a glass plate assembly, and the synthesis was carried out overnight in an oven at 50^{o}C. After reaction, the gels were washed in THF and dried. Different grades of PBAE hydrogels prepared by varying the molar ratio of total acrylate to amine reactive groups (RTAA) from 0.25 to 1.65 are reported in **Table 6-1** [1 mole of diacrylate corresponds to 2 moles of acrylate reactive groups; 1 mole of primary diamine corresponds to total 4 moles of primary/secondary amine reactive groups].

6.2.3 Swelling Response of PBAE

The swelling properties of the resultant hydrogels were evaluated using dimethyl sulfoxide (DMSO), tetrahydrofuran (THF), dichloromethane (DCM) and ethyl acetate (EtOAc) at room temperature. The initial mass of the hydrogel discs were recorded (W_o), and then, the discs were placed in the corresponding solvents at room temperature. The discs were removed from the solvents at a given time, and their masses were recorded in swollen state (W_s). The same solvents were used throughout the swelling studies. The

Table 6-1. List of PBAE Hydrogels Synthesized at Varying RTAA.

Diacrylate	Diamine	RTAA
PEG400DA	TTD	0.6
PEG400DA	EDBE	0.6
PEG400DA	HMD	0.6
PEG400DA	TTD	1.2
PEG400DA	TTD	1.65
DEGDA	HMD	0.6

swelling state of the gel was then characterized by mass swelling ratio as explained before [327].

6.2.4 Calculations for Polymer-Solvent Interaction Parameter

Polymer-solvent interaction parameter was calculated as described by Brandrup and is a sum of enthalpic (χ_H) and entropic (χ_S) components (Equation 1) [328]. χ_H is related to the Hildebrand solubility parameter (δ) and χ_S was considered to be constant at 0.34 (Equation 2). In Equation 2, V_s is molar volume of the solvent and δ_S and δ_P are solubility parameter values for solvent and polymer respectively.

$$\chi = \chi_H + \chi_S \quad (1)$$

$$\chi = \frac{V_S}{RT}(\delta_S - \delta_P)^2 + 0.34 \quad (2)$$

Solubility parameters and the molar volumes of the solvents were obtained from Brandrup and are tabulated in **Table 6-2**, while values for polymers were calculated using the group contribution method as described by Brandrup et. al., where solubility parameter is the square root of cohesive energy density (Equation 3) [328, 329]. Values for cohesive energy and molar volume of different groups for polymers were obtained and are tabulated in **Table 6-3** [329].

$$\delta_{polymer} = \left(\frac{\sum Ecoh_i}{\sum Vm_i}\right)^{1/2} \quad (3)$$

Table 6-2. Solubility Parameter Values of the Solvents.

Solvents	Solubility Parameter (δ) $[(Cal/cm^3)^{1/2}]$	Molar Volume (V_m) (cm^3/mol)
DMSO	12.0	71.3
DCM	9.7	63.9
THF	9.1	79.9
EtOAc	9.1	98.5

Table 6-3. Group Contributions of E_{coh} and V_m [329]

Group	$Ecoh_i$ (J/mol)			Vm_i (cm^3/mol)
	Hayes	Hoftyzer and Van Krevelen	Fedors	
-CH2-	4150	4190	4940	16.1
-O-	6830	6290	3350	3.8
-COO-	14160	3410	18000	18
-NH-	-	-	8370	4.5
-N<	-	-	4190	-9

6.2.5 FTIR Characterization of PBAE Degradation in Ethanol

PBAE hydrogels (PEG400DA-TTD, RTAA=0.6) were degraded completely in water and ethanol. Viscous liquid degradation products were isolated by removing solvents through vacuum drying. FTIR measurements of dry degradation products were obtained using a Digilab Stingray system consisting of a FTIR 7000e stepscan spectrometer (Varian Inc.).

6.2.6 Conjugation of PBAE Hydrogels with Ascorbic Acid

Prior to conjugation with ascorbic acid, PBAE hydrogels (~ 80 mg) (PEG400DA-TTD, RTAA=1.2) were swollen overnight in DMSO. Swollen PBAE hydrogels were then transferred to 3 ml of 26.6 mg/ml ascorbic acid solution in DMSO and incubated at 37 ^{0}C for 48 hrs. Final ratio of ascorbic acid added for conjugation was 100 wt% with respect to PBAE hydrogel. To remove the unconjugated ascorbic acid, hydrogels were incubated in 10 ml of blank DMSO for 12 hrs and this procedure was repeated two more times. Hydrogels were then washed with THF to remove DMSO. Hydrogels were then subjected to vacuum to remove residual solvents and to result ascorbic acid-conjugated PBAE (AA-PBAE).

6.2.7 Release of ascorbic acid from PBAE hydrogels

AA-PBAE were incubated in 10 ml of PBS at 37 ^{0}C. 1 ml of supernatant was removed at every time point. To prevent ascorbic acid oxidation in water, samples were frozen as soon as they were collected. Samples were analyzed using a Shimadzu Prominence LC-20 AB HPLC system installed with a dual-wavelength UV detector. 95:5 acetonitrile:H_2O (with 1% TFA) was used as a eluent with a 4.6 X 150 mm Luna C18

column (Phenomenex, Torrance, CA). Ascorbic acid was monitored at a wavelength of 256 nm.

6.3 Results and Discussions

6.3.1 PBAE Hydrogel Synthesis

As each primary amine is capable of reacting with two acrylate groups, a diamine has tetra-functionality, potentially permitting the synthesis of a crosslinked polymer network (**Figure 6-1**). Since PBAE undergo hydrolytic degradation, to synthesize hydrogels with varying network properties (hydrophilicity, rate of degradation and mechanical properties), two different diacrylates (with different length of PEG units) and three primary diamines (with varying hydrophilicity) were selected to study effect of monomers on PBAE properties.. In order to study effect of RTAA on hydrogel synthesis, the RTAA was varied from excess amine regime to excess acrylate regime, in range of 0.25 to 1.65.

FTIR characterization of PBAE hydrogels and the effect of different monomers and RTAA on the degradation rate and mechanical properties of PBAE are discussed in detail by Biswal et. al. [326].

6.3.2 Swelling Response

The swelling properties of the PBAE hydrogels with RTAA of 0.6 were analyzed. The hydrogels were swollen in DMSO, THF, DCM and EtOAc, in order to study the polymer-solvent interaction. The degree of swelling in different solvents for PEG400DA and DEGDA systems are presented in **Figure 6-2**. It has been observed that for all the systems in THF, DCM and EtOAc maximum swelling is achieved in approximately 2 hrs.

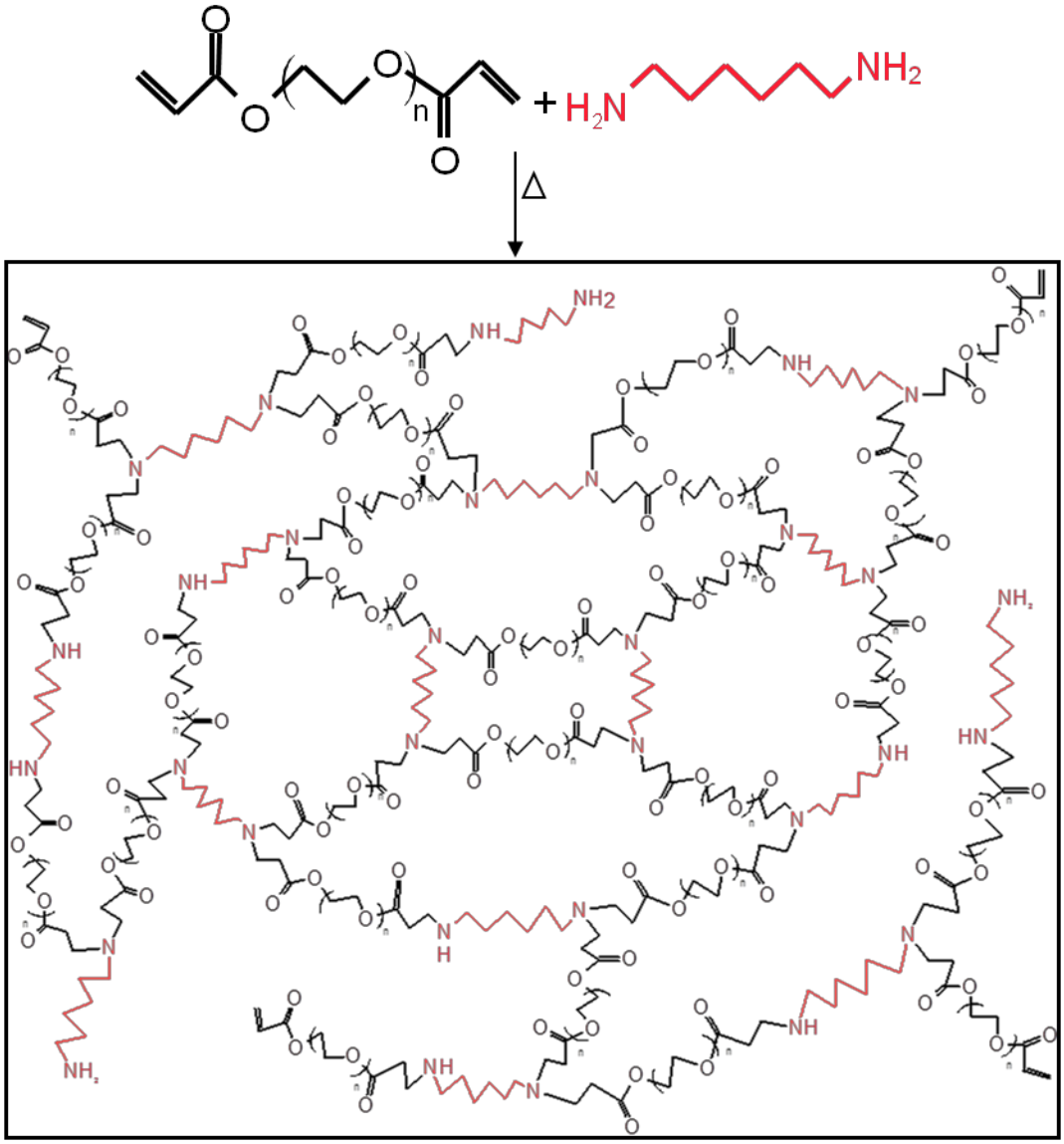

Figure 6-1. Reaction Schematic of PBAE Hydrogel Synthesis Using PEG400DA and HMD.

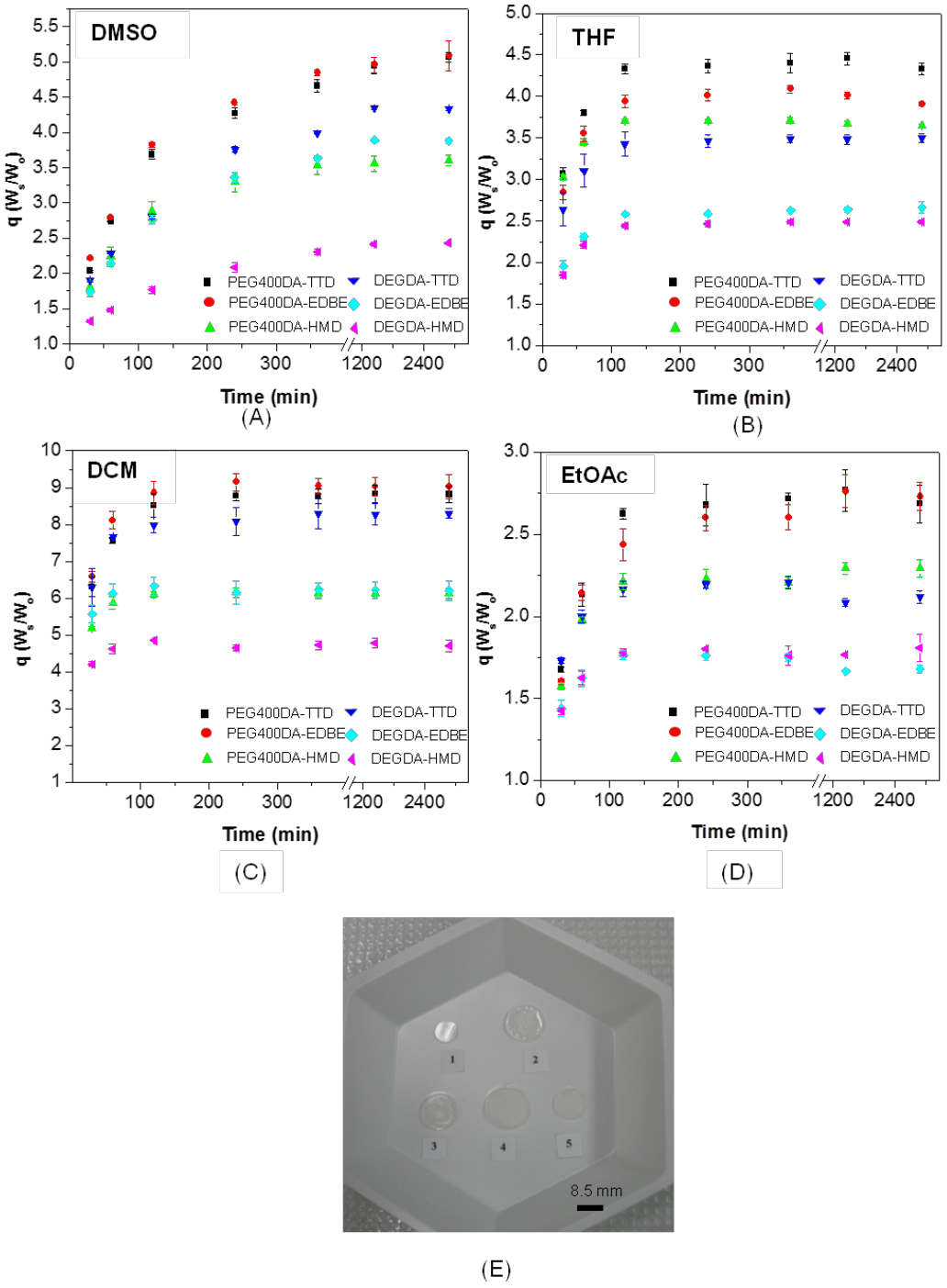

Figure 6-2. Swelling Response of Different Hydrogel Systems.

Swelling response of PBAE hydrogels in (A) DMSO, (B) THF, (C) DCM, and (D) EtOAc; (E) image of PEG400DA-TTD (RTAA of 0.6) swollen gels in different solvents, (1) dry gel, (2) in DMSO, (3) in THF, (4) in DCM, and (5) in EtOAc.

However, in the case of DMSO as solvent, maximum swelling was observed in approximately 6 hrs. For all the systems, a greater degree of swelling was observed in DCM in comparison to the other solvents.

This dependence of the extent of swelling on the polymer/solvent system could be explained by polymer-solvent interaction parameter, which is an indicator of polymer miscibility in the solvent. Similar values of polymer and solvent solubility parameters result in $\chi < 0.5$, which is the Flory-Huggins theory criterion for polymer miscibility in the solvent over the entire concentration range. The solubility parameter (δ_P) depends on polymer molecular structure, and the predicted δ_P values for some of the possible polymeric molecular structures are tabulated in **Table 6-4**. These polymer solubility parameter values were used to determine the polymer-solvent interaction parameter (χ) using equation 2. Depending on the RTAA used, PBAE networks can have some unreacted (residual) secondary amines (**Figure 6-3A**) or completely reacted tertiary amines (**Figure 6-3B**). Swelling studies were carried out for PBAE gels with RTAA=0.6, FTIR analysis of which indicates presence of unreacted (residual) secondary amines in the PBAE gel [326].

Table 6-4. Solubility Parameters for Different PBAE Polymer Networks.

Polymer Molecular Structure		-O-	-COO-	-CH2-	-NH-	-N<	$-CH_3-$	$\Sigma Ecoh_i$ (J/mol)	ΣVm_i (cm^3/mol)	Solubility Parameter (δ_P) $(Cal/cm^3)^{1/2}$
Figure 6-4a	**PEG400DA-TTD**	11	1	30	2	0	0	219790	549.3	9.78
	PEG400DA-EDBE	10	1	26	2	0	0	196680	481.1	9.88
	PEG400DA-HMD	8	1	26	2	0	0	189980	473.5	9.79
	DEGDA-TTD	4	1	16	2	0	0	127180	297.3	10.11
	DEGDA-EDBE	3	1	12	2	0	0	104070	229.1	10.42
	DEGDA-HMD	1	1	12	2	0	0	97370	221.5	10.25
Figure 6-4b	**PEG400DA-TTD**	39	8	90	0	2	0	727630	1734.2	10.01
	PEG400DA-EDBE	38	8	86	0	2	0	704520	1666	10.05
	PEG400DA-HMD	36	8	86	0	2	0	697820	1658.4	10.03
	DEGDA-TTD	11	8	34	0	2	0	357190	726.2	10.84
	DEGDA-EDBE	10	8	30	0	2	0	334080	658	11.02
	DEGDA-HMD	8	8	30	0	2	0	327380	650.4	10.97
Figure 6-4c	**PEG400DA-TTD**	19	4	52	0	2	2	410330	1041.4	9.70
	PEG400DA-EDBE	18	4	48	0	2	2	387220	973.2	9.75
	PEG400DA-HMD	16	4	48	0	2	2	380520	965.6	9.70
	DEGDA-TTD	5	4	24	0	2	2	225110	537.4	10.01
	DEGDA-EDBE	4	4	20	0	2	2	202000	469.2	10.14
	DEGDA-HMD	2	4	20	0	2	2	195300	461.6	10.06

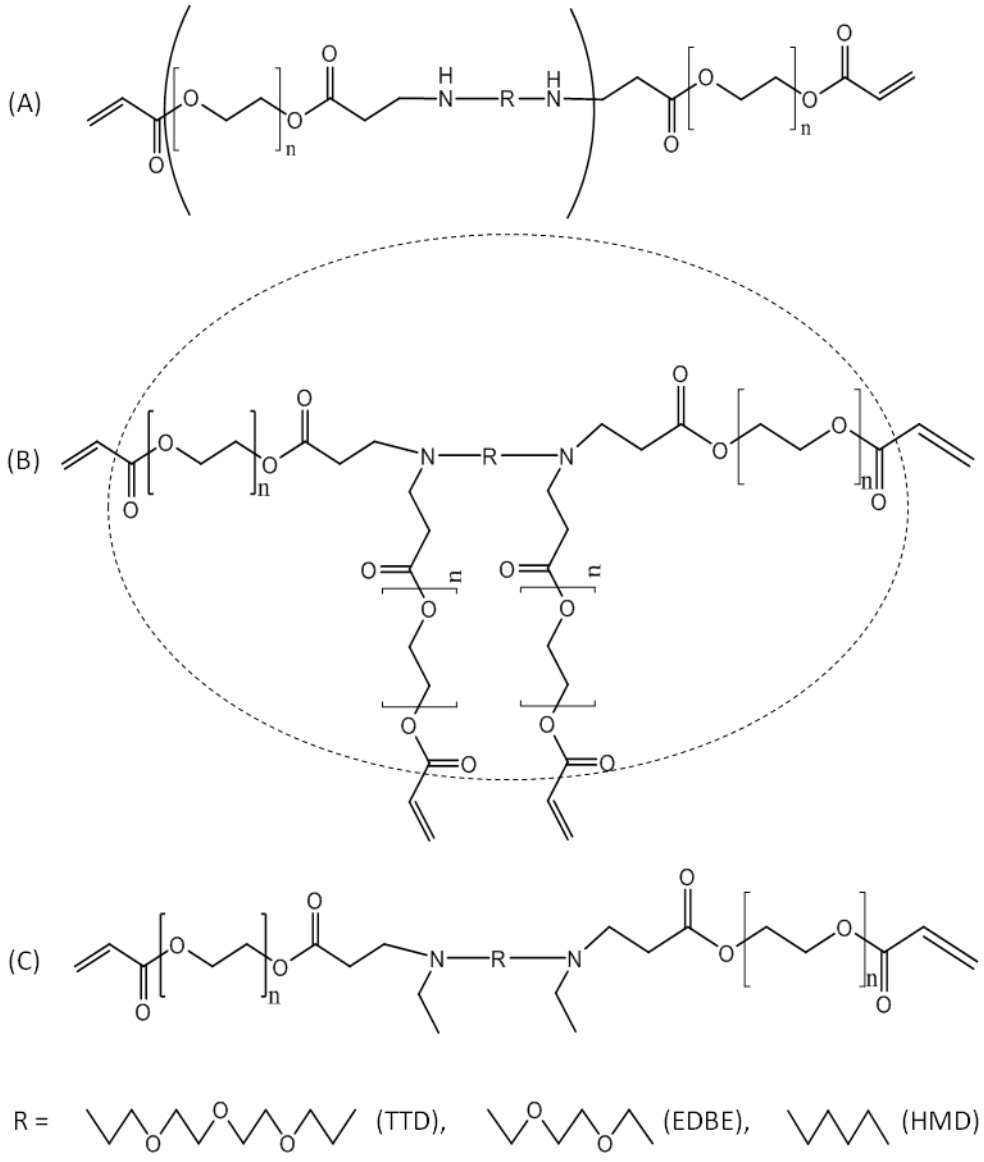

Figure 6-3. Hypothetical Structures for Different Possible PBAE Network.

PBAE network (A) with unreacted secondary diamines, (B) where all the amines are reacted and (C) where secondary amines are capped with an hypothetical ethyl group.

Ideally, equilibrium swelling is inversely proportional to the χ value, where swelling is higher at lower χ. As observed in (**Figure 6-4A and 6-4B),** the degree of swelling for PBAE gels occurred in the order DCM>THF>EtOAc, which can be explained by lower χ values for PBAE-DCM system as compared to PBAE-THF<PBAE-EtOAc. Also, hydrogels synthesized from PEG400DA swell to a greater extent than the corresponding hydrogels made from DEGDA, which can again be explained by lower χ values for PEG400DA based PBAE systems. Swelling, as described by the Flory-Rehner equation, is also a function of M_c (molecular weight between the crosslinks). The higher M_c in case of PEG400DA could also explain increased swelling as compared to DEGDA based PBAE systems. According to the χ values calculated by Ozdemir et al., PEG has a lower solubility in DMSO as compared to THF [330]. The lower solubility of PEG in DMSO should have resulted in the least swelling of PEG-based PBAE in DMSO. However, it was observed that the swelling of PBAE gels in DMSO is comparable to the swelling observed in THF and EtOAc. Predictions of polymer-solvent interaction parameter could deviate in case of polar solvents or polar polymer networks [329]. The highly polar nature of DMSO and its interaction with PEG in the PBAE network could be the reason for the failure to predict χ accurately in case of PBAE-DMSO system.

In order to test the hypothesis that in case of the solvents studied here (DCM, THF, EtOAc and DMSO), PBAE-solvent interaction is mainly determined by PEG density in the PBAE network and not by the presence of secondary/tertiary amines in the network, χ values for a hypothetical polymer network (**Figure 6-3C**) were calculated where secondary amines in the **Figure 6-3A** were ethyl-capped. As shown in **Figure 6-4A** and **6-4C**, χ values for PBAE-solvent systems did not change significantly after

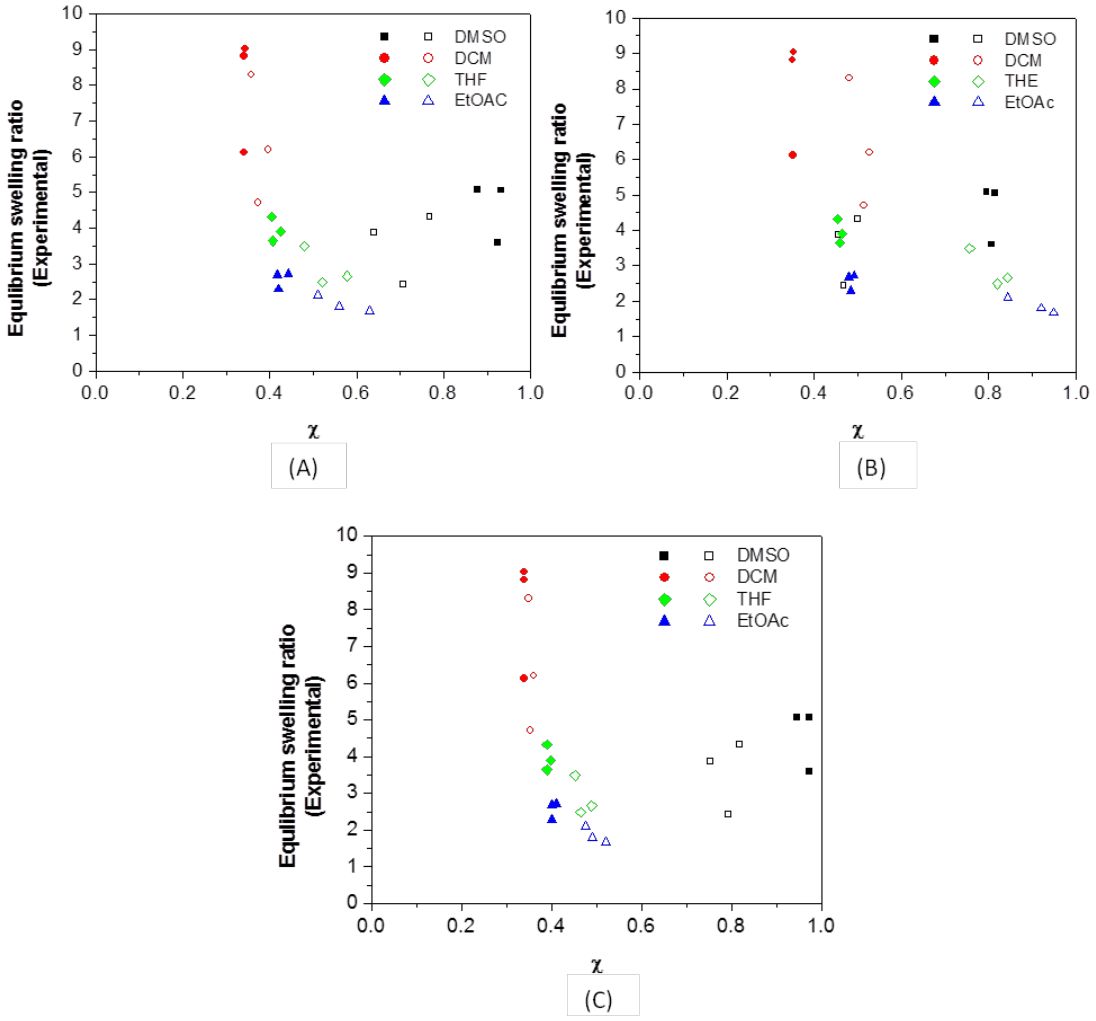

Figure 6-4. Correlation Between Equilibrium Swelling and χ for Corresponding Networks shown in Figure 6-3 (A-C).

Solid markers -PEG400DA systems
Empty markers-DEGDA systems

ethyl-capping secondary amines in the PBAE network. However, by increasing the PEG density in the PBAE network as shown in **Figure 6-4B**, χ values changed significantly for PEG400DA systems which indicates that χ depends mainly on PEG density in the network.

6.3.3 FTIR Characterization of PBAE Degradation in Ethanol

While studying the swelling of PBAE in different solvents, it was observed that PBAE degraded in ethanol. To explore the degradation of PBAE in alcohols, effect of different alcohols (methanol, ethanol, 1-octanol, t-butanol), monomers and RTAA on the rate of PBAE degradation in alcohol were studied in detail [331]. In order to understand the mechanism of PBAE degradation in alcohol, degradation products of PBAE (PEG400DA-TTD, RTAA=1.2) in ethanol were characterized using FTIR (**Figure 6-5**). It has been reported previously that PBAE hydrogels degraded via hydrolysis of ester groups in the crosslinks to lower molecular weight degradation products and kinetic chains of poly(β-amino acids) and diols [321, 332]. The presence of a broad acid peak at 1584 cm^{-1} in the water degradation products of PBAE with decrease of intensity of ester-C=O peak at 1730 cm^{-1} clearly indicates the formation of low molecular weight acids. The transesterification reaction of PBAE with alcohols was also confirmed by the formation of new ester peaks at around 1732cm^{-1} from the ethanol degradation products of PBAE indicates that the degradation occurs via transesterification reaction of ethanol with β-amino ester bonds in PBAE network. The new ester products which were formed during the reaction of ethanol with the PBAE hydrogels, undergo further hydrolysis to form the corresponding acids. The decrease in the intensity of the ester peak at 1732cm^{-1}

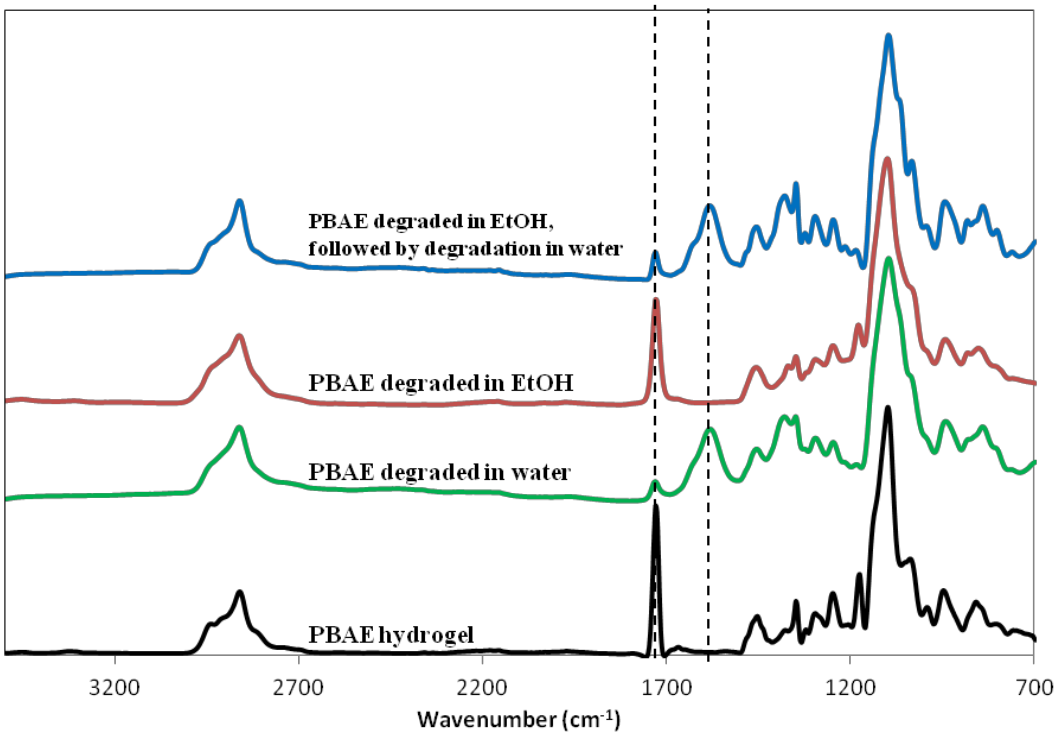

Figure 6-5. FTIR Characterization of PBAE Degradation in Ethanol (EtOH).

and formation of a new peak at around 1584cm^{-1} clearly indicates the hydrolysis of the new ester to the corresponding acid.

6.3.4 Conjugation of PBAE with Ascorbic Acid and Controlled Release of Ascorbic Acid from AA-PBAE

Ascorbic acid (Vitamin C) is a naturally occurring antioxidant and has primary and secondary alcohol groups in the molecular structure (**Figure 6-6**). Taking advantage of alcohol induced transesterification reaction in PBAE network, ascorbic acid was conjugated to the PBAE network. Extent of ascorbic acid conjugation in AA-PBAE could not be analyzed using FT-IR because of the overlapping of characteristic peak of aromatic -C=C- in ascorbic acid.

However, release of ascorbic acid as a function of AA-PBAE degradation was studied. As shown in **Figure 6-7**, ascorbic acid was released gradually over a period of 3 hrs. At the end of AA-PBAE degradation, 3 mg of ascorbic acid was released as analyzed by HPLC. This corresponds to ~3.5 wt% of ascorbic acid loading in AA-PBAE. It was also observed that AA-PBAE degrades slower (~150 min) than corresponding PBAE (PEG400DA-TTD, RTAA=1.2) which degrades completely within 45 mins. The reason for slower degradation rate of AA-PBAE needs to be investigated further. Successful conjugation to ascorbic acid to PBAE provides PBAE as a means of controlled release for drugs with primary alcohol functional groups.

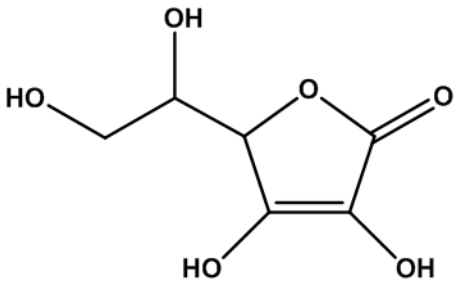

Figure 6-6. Molecular Structure of Ascorbic Acid

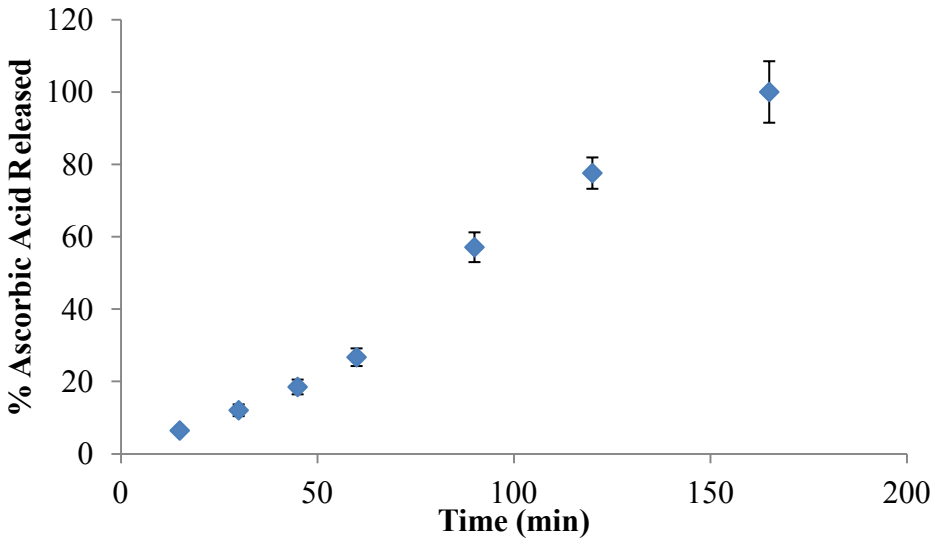

Figure 6-7. Ascorbic Acid Release from AA-PBAE

AA-PBAE were incubated in PBS at 37 ^{0}C and ascorbic acid released in the supernatant was analyzed using HPLC.

6.4 Conclusions

A simple one-step method was developed to synthesize biodegradable PBAE with tunable properties. Theoretical analysis of PBAE swelling proved that swelling is dependent on the PEG density in the PBAE network. Ability of alcohols to degrade PBAE gels was successfully used to conjugate ascorbic acid to PBAE gels which upon degradation in water resulted in controlled release of ascorbic acid.

Chapter 7. Synthesis and Characterization of Poly(antioxidant β-amino esters) for Controlled Release of Polyphenolic Antioxidants

Based on the research article to be submitted to:

P.P. Wattamwar, D. Biswal, A. Lyvers, D. Cochran, J.Z. Hilt and T.D. Dziubla, "Synthesis and Characterization of Poly(antioxidant β-amino esters) for Controlled Release of Polyphenolic Antioxidants", Acta Biomaterialia (*to be Submitted*)

7.1 Introduction

The non-free-radical polymerization poly(β-amino ester) chemistry described in the previous chapter provides a platform to develop and study antioxidant polymers with tunable properties. One of the important advantages of this chemistry is that it can be extended to all polyphenolic antioxidants thereby broadening the scope and properties of antioxidant polymers. In this work, we have synthesized poly(antioxidant β-amino ester) (PABAE) biodegradable hydrogels of two polyphenolic antioxidants, quercetin and curcumin. Acrylate functionalized antioxidants, quercetin multiacrylate (QMA) and curcumin multiacrylate (CMA) were synthesized and reacted with commercially available diacrylate and primary diamine monomer to result in a cross-linked network of PABAE. Degradation rate of PABAE was dependant on content of the hydrophobic antioxidant monomer and can be controlled by appropriate choice of commercially available monomers. PABAE degradation products possessed antioxidant activity and suppressed background oxidative stress levels in the cells, both in absence and presence of injury agent.

7.2 Materials and methods

7.2.1 Materials

Quercetin, curcumin, acryloyl chloride, 4,7,10-Trioxa-1,13-tridecanediamine (TTD), methylthiazolyldiphenyl-tetrazolium bromide (MTT), triethylamine, 2,2'-azo-bis(2-aminopropane)-HCl (AAPH) and hydrogen peroxide (H_2O_2) were all purchased from Sigma-Aldrich. Poly(ethylene glycol) diacrylate (PEG400DA) was purchased from Polysciences, Inc. 2',7'-dichlorodihydrofluorescein diacetate (DCF-DA) was purchased from Invitrogen. All organic solvents were obtained from Sigma-Aldrich and Fisher Scientific and used as received.

7.2.2 Synthesis of Antioxidant Multiacrylates

Antioxidant multiacrylates were synthesized by reacting phenolic antioxidants with acryoyl chloride in tetrahydrofuran (THF) and triethylamine at room temperature for 12 hrs as previously described by Boudreaux et. al. [333] Antioxidants (quercetin or curcumin) were dissolved in THF at a concentration of 100 mg/ml. Triethylamine (Et_3N) was added to the solution at an Et_3N:antioxidant ratio of 4:1 and 2:1 for quercetin and curcumin, respectively. Acryloyl chloride was slowly added to the reaction mixture while being stirred on an ice bath. Initial molar ratio of acryoyl chloride:antioxidant was 4.5:1 and 2.5:1 for quercetin and curcumin, respectively. The reaction was then allowed to proceed at room temperature under dark conditions for 12 hrs. After this reaction, precipitated triethylamine hydrochloride salt was removed by vacuum filtration. Filtrate was subject to vacuum distillation using liquid N_2 trap to remove THF. To remove unreacted acryoyl chloride from the product, the resultant powder was re-dissolved in dichloromethane (DCM) (30 ml) and subsequently extracted with 0.1 M K2CO3 (3 X

120 ml) and DI water (3 X 120 ml), and then dried over $MgSO_4$. Solution was filtered using vacuum filtration and solvent was removed under vacuum using a roto-evaporator (Rotovapor R II, Buchi, Switzerland). Synthesized antioxidant multiacrylates were characterized using FT-IR and ^{1}H-NMR spectroscopy. The resulting powder was stored at -20 ^{0}C until further use.

7.2.3 Synthesis of Poly(antioxidant β-amino esters) Hydrogels (PABAE)

PABAE hydrogels were synthesized by a single step addition of acrylates (PEG400DA and antioxidant multiacrylates) and a primary diamine, TTD, as previously described [326]. **Figure 1** shows a schematic of the crosslinked network in PABAE hydrogels. Briefly, calculated amounts of PEG400DA and primary diamine TTD were mixed in a 2 ml eppendorf tube. This mixture was incubated at 50 ^{0}C for 5 min. Calculated amount of antioxidant multiacrylate dissolved in DCM solvent (50 wt% solvent with respect to total monomer) was transferred to the PEG400DA/TTD reaction mixture, mixed thoroughly and then incubated in an oven at 50 ^{0}C for 24 hrs. PABAE with different antioxidant contents were synthesized and their compositions are listed in **Tables 7-1 and 7-2**. Synthesized hydrogels were then cut into 1 mm thick discs for degradation studies. All discs were washed in THF for 15 min to remove unreacted monomers and dried under vacuum. Different grades of PABAE hydrogels were prepared by varying the molar ratio of antioxidant multiacrylate:PEG400DA between 0 – 20 % while maintaining the ratio of total acrylates to total amines (RTAA) at 1.2.

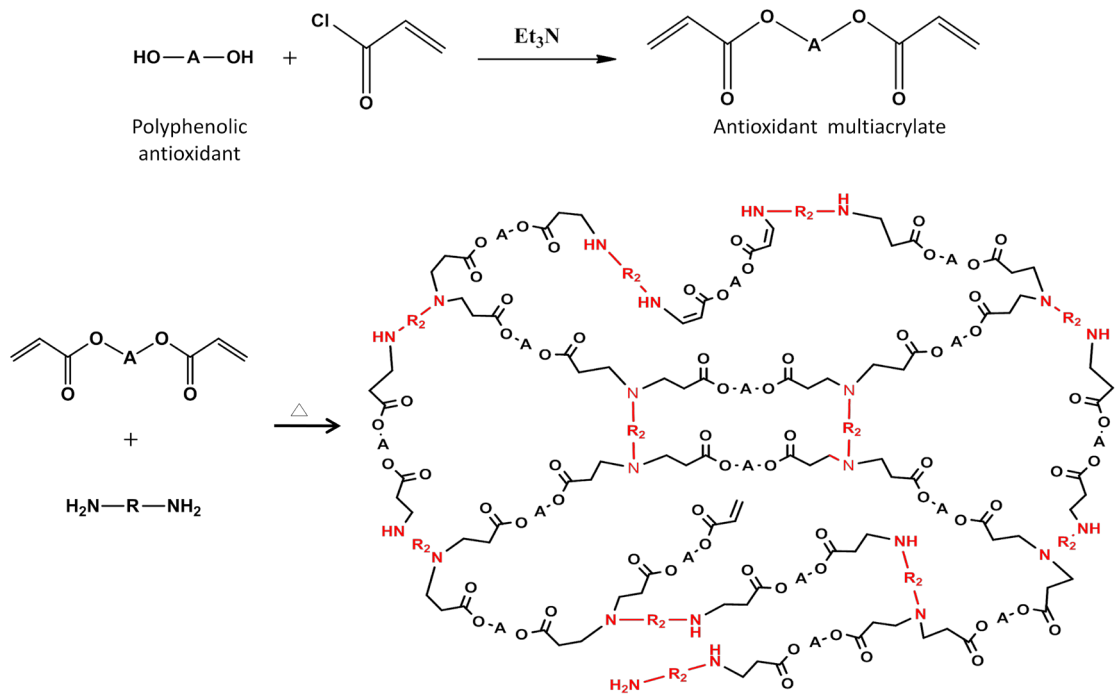

Figure 7-1. A simplified schematic representing synthesis of antioxidant multiacrylates and cross-linked polymer network in PABAE hydrogels.

Table 7-1. Composition of the Synthesized Quercetin PABAE Hydrogels.

Sample Name	wt%			mol%		
	PEG400DA	QMA	TTD	PEG400DA	QMA	TTD
0	84.70	0.00	15.30	70.60	0.00	29.40
5% QMA	79.78	4.28	15.93	66.09	3.48	30.43
10% QMA	74.95	8.49	16.55	61.71	6.86	31.43
20% QMA	65.53	16.71	17.76	53.33	13.33	33.33

Table 7-2. Composition of the Synthesized Curcumin PABAE Hydrogels.

Sample Name	wt%			mol%		
	PEG400DA	CMA	TTD	PEG400DA	CMA	TTD
0	84.70	0.00	15.30	70.60	0.00	29.40
5% CMA	80.67	3.98	15.34	67.06	3.53	29.41
10% CMA	76.63	7.98	15.39	63.53	7.06	29.41
20% CMA	68.48	16.05	15.47	56.47	14.12	29.41

7.2.4 Degradation of PABAE Hydrogels

Degradation studies of PABAE hydrogels were carried out in PBS at 37^0C (pH 7.4). At given time points, each set of gels were removed from the PBS, flash frozen in liquid nitrogen and freeze dried in order to remove residual water. The fraction of mass remaining was calculated from the ratio of the recorded final dry mass (W_d) and initial (W_o) values.

7.2.5 *In Vitro* Assay for Measuring Antioxidant Activity of PABAE Degradation Products

Antioxidant activity of the PABAE degradation products was measured using a DCF fluorescence-based assay as described previously [256]. AAPH undergoes thermal degradation and was used to mimic the peroxyl radical formation *in vivo*. Hydrolysis of DCF-DA results in non-fluorescent DCF which was then diluted in PBS to a concentration of 10 μM. To a well in 96-well plate, 100 μL of sample (solution of PABAE degradation products in PBS) and 100 μL of 10 μM DCF solution was added. Fluorescence measurement was started when 20 μL of AAPH solution was added to the well-plate and DCF fluorescence kinetics was monitored for 4 hrs using a Varian Cary Eclipse fluorescence spectrophotometer (excitation at 502 nm, emission at 525 nm). Assay was calibrated using known concentrations of both quercetin and curcumin, and the antioxidant potential of the quercetin/curcumin PABAE degradation products was reported as molar active quercetin/curcumin equivalents.

7.2.6 Cell Line

Human umbilical vein endothelial cells (HUVECs) were purchased from Lonza and cultured in EGM-2 media with 2% fetal bovine serum at 37 ^{0}C in humidified atmosphere of 5% CO_2. HUVECs in passage 3 to 5 were used for all the studies.

7.2.7 Measuring Oxidative Stress in the Cells After Exposure to PABAE Degradation Products

PABAE hydrogels were incubated in sterile DI water at 37 ^{0}C for 48 hrs to allow for complete degradation. PABAE degradation products were then freeze dried and dissolved in DMSO at a concentration of 100 mg/ml. These concentrated DMSO solutions were then used to prepare fresh dilute solutions of PABAE degradation products in cell media. Cells were treated with these PABAE solutions for their cytotoxicity and their effect on cellular oxidative stress levels. To prepare quercetin and curcumin solutions, antioxidants were dissolved in DMSO at a concentration of 10 mg/ml and diluted in cell media.

2',7'-dichlorodihydrofluorescein (DCF) fluorescence was used as marker of oxidative stress in the cells as described previously [334]. HUVECs were seeded onto a 96-well plate at a density of 35,000 cells/cm^2 and incubated at 37 ^{0}C. After 24 hrs, cell media was replaced with 100 μL of treatment solution (PABAE degradation products) and 100 μL of 10 μM DCF-DA solution. Fluorescence was measured after another 24 hrs using a bottom-reading GENios Pro fluorescence spectrophotometer (Tecan, Switzerland) at excitation and emission wavelengths of 485 nm and 535 nm respectively.

7.2.8 Cytotoxicity of PABAE Degradation Products

The MTT assay was used to measure cell viability after treating cells with PABAE degradation products. HUVECs were seeded onto a 96-well plate at a cell density of 35,000 cells/cm^2 and 24 hrs later, cell media was replaced with treatment solutions. 24 hrs post treatment, treatment solution was removed, cells washed twice in PBS and 200 µL of 0.5 mg/ml MTT solution in cell media was then added to each well. 96-well plate was then incubated at 37 ^{0}C for 12 hrs and cell media was gently removed from the wells. 100 µL of DMSO was added to each well to dissolve the formazan product. The absorbance intensity was recorded at 570 nm for formazan and at 690 for background using a Cary-50 Bio UV-Visible spectrophotometer equipped with a Cary 50 MPR microplate reader (Varian, Santa Clara, CA).

7.2.9 *In Vitro* Cell Protection Against Oxidative Stress Injury Induced by H2O2

HUVECs seeded at a cell density of 35,000 cells/cm^2 in a 96-well plate were treated with 100 µL of antioxidant or PABAE solution for 2 hrs prior to adding 100 µL of 1 mM H_2O_2 solution (in cell media). Cells were exposed to antioxidants at different concentrations and a final H_2O_2 concentration of 500 µM. 24 hrs later, cell viability was measured using MTT assay as described above.

7.3 Results

7.3.1 Synthesis and Characterization of Antioxidant Multiacrylates

Synthesis of antioxidant multiacrylates was verified using FT-IR and ^{1}H-NMR (**Figure 7-2 and Figure 7-3**). The peaks at 1740 and 1620 cm^{-1} in the FT-IR spectra of QMA and CMA (**Figure 7-2**) are characteristics of the resulting ester –C=O and –C=C-

bonds in the product. Conversion of antioxidant phenolic groups into ester was further confirmed using ^{1}H-NMR spectroscopy, where the peaks corresponding to the phenolic –OH in antioxidants (at 9.0 – 10.7 ppm for quercetin, at 9.6 ppm for curcumin) had reduced peak intensities in the NMR spectra of antioxidant multiacrylates. Also, peaks corresponding to –CH=CH_2 (in the range of 6.75 to 6 ppm) were present in the spectra of antioxidant multiacrylates. Average number of acrylate groups per molecule of antioxidant was quantified using ^{1}H-NMR spectroscopy. Analysis of ^{1}H-NMR spectra revealed presence of 4.28 and 2.66 acrylate groups per molecule of quercetin and curcumin respectively.

7.3.2 Synthesis of PABAE Hydrogels

For all the PABAE hydrogel synthesis reactions, acrylates were used in slight excess as compared to amines with the RTAA maintained at 1.2. It was observed that rate of the reaction increased with increase in antioxidant content in the reaction mixture. The system with 20% QMA and CMA polymerized faster than the corresponding 10% and 5% systems. In previous work, rate of polymerization for 0% PABAE was analyzed using FT-IR [326]. However, in case of antioxidant PABAE, rate of polymerization could not be analyzed using FT-IR because of the overlapping of characteristic peak of aromatic –C=C- in QMA and CMA with aliphatic C=C- peak.

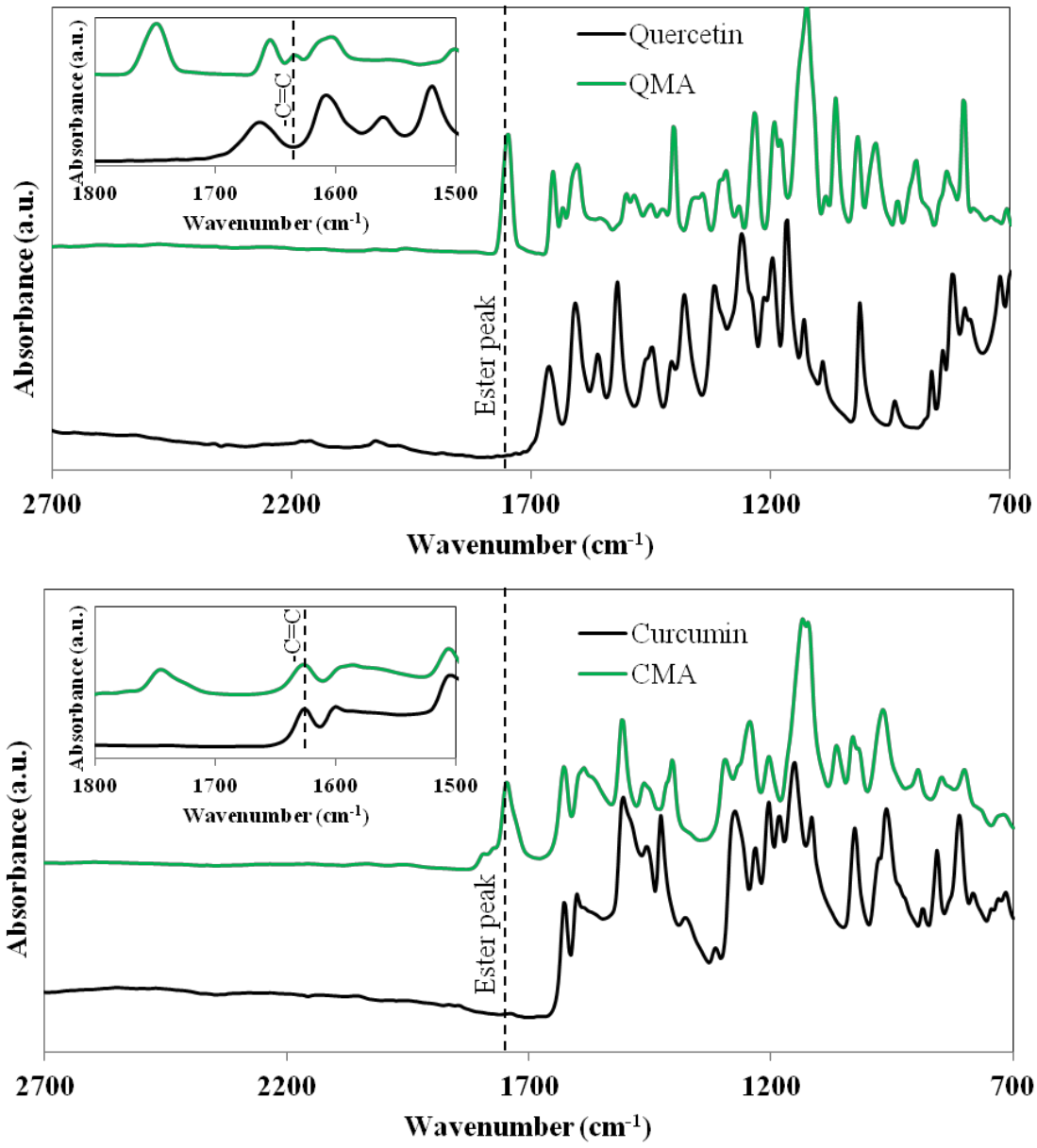

Figure 7-2. FTIR Characterization of Antioxidant Multiacrylates.

Quercetin and curcumin were functionalized with acrylate groups by reacting with acryoyl chloride. Presence of peak at ~ 1740 cm^{-1} in the spectra of QMA (top) and CMA (bottom), which is characteristic of ester carbonyl group, indicates successful acrylate functionalization of quercetin and curcumin.

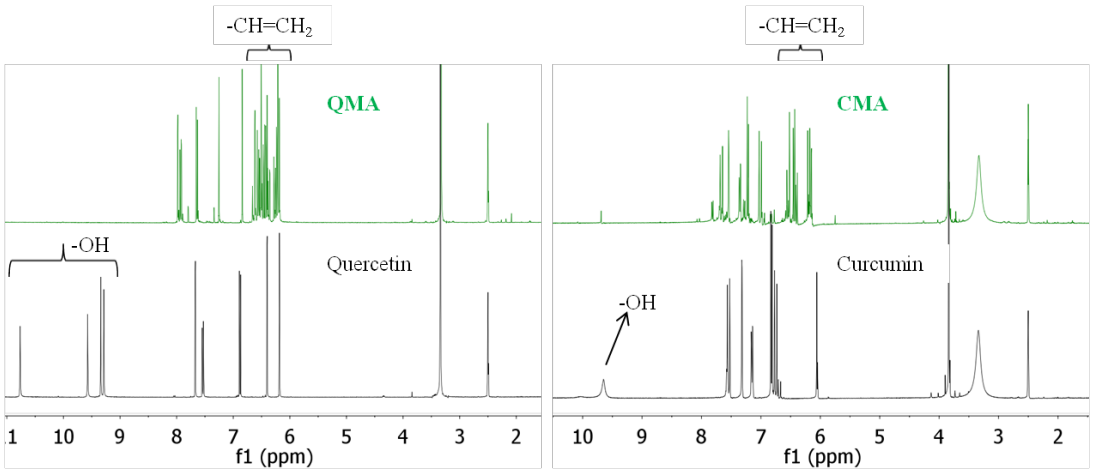

Figure 7-3. **^{1}H-NMR Characterization of Antioxidant Monomers.**

Reaction of antioxidant phenolic groups of with acryoyl chloride is confirmed by the absence of characteristic phenol peaks (9 – 11 ppm) in the QMA and CMA products. Analysis of QMA and CMA spectra reveal presence of 4.28 and 2.66 acrylate groups per molecule of quercetin and curcumin, respectively.

7.3.3 Degradation of PABAE Hydrogels

Degradation of all PABAE hydrogels was studied in PBS (pH = 7.4) at 37 ^{0}C. **Figure 7-4** shows degradation profiles for quercetin and curcumin PABAE hydrogels respectively. In both quercetin and curcumin PABAE systems, pH change associated with degradation was minimal where the pH of the suspension of the degradation products changed from 7.4 to 8 after complete degradation. Hydrogels that did not have antioxidants (0) degraded quickly, within 150 mins, as compared to the quercetin and curcumin PABAE hydrogels that degraded completely within 5-6 hrs. Except for 20% CMA hydrogels, there was not a significant dose dependent effect of polyphenolic content on the hydrogel degradation rate.

7.3.4 *In Vitro* Measurement of Antioxidant Activity of PABAE Degradation Products

Antioxidant activity of PABAE degradation products was further verified using another *in vitro* assay where the DCF fluorescence was again used as a marker of oxidation by free radicals. Total antioxidant activity of quercetin PABAE hydrogels was directly proportional to the initial QMA content in the hydrogel with ~60% recovery as compared to the theoretical activity (**Figure 7-5**). In case of curcumin PABAE hydrogels, recovery of antioxidant activity was lower as compared to quercetin PABAE. Degradation of 5% CMA resulted in 40% recovery of antioxidant activity where as degradation of 10% CMA and 20% CMA resulted in 20% recovery of antioxidant activity.

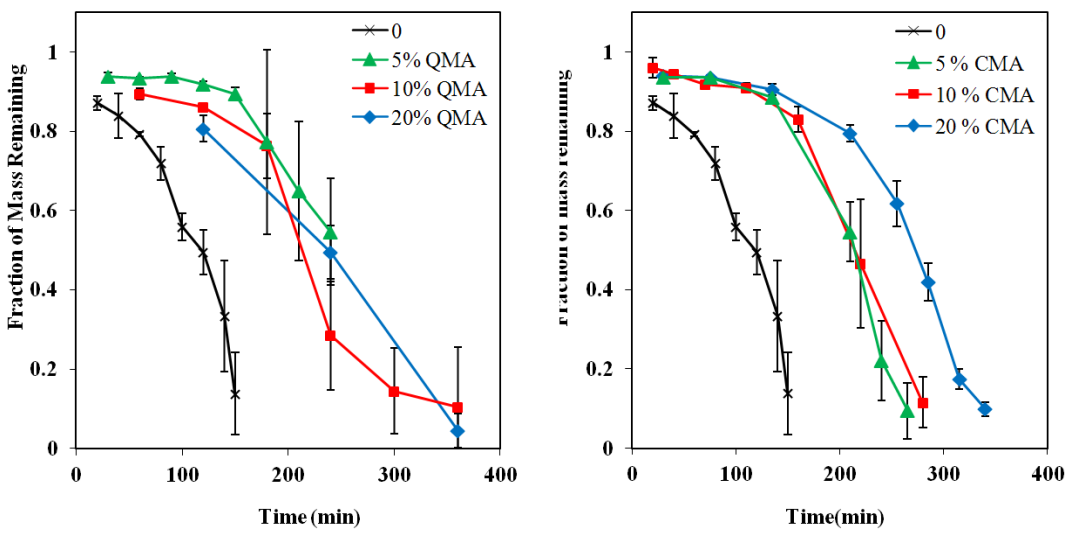

Figure 7-4. Degradation Profiles of Quercetin (left) and Curcumin (right) PABAE.

Quercetin (left) and curcumin (right) PABAE hydrogels degraded slower (within 250-350 mins) as compared to the fast degrading 0% PABAE hydrogel (in ~ 150 mins).

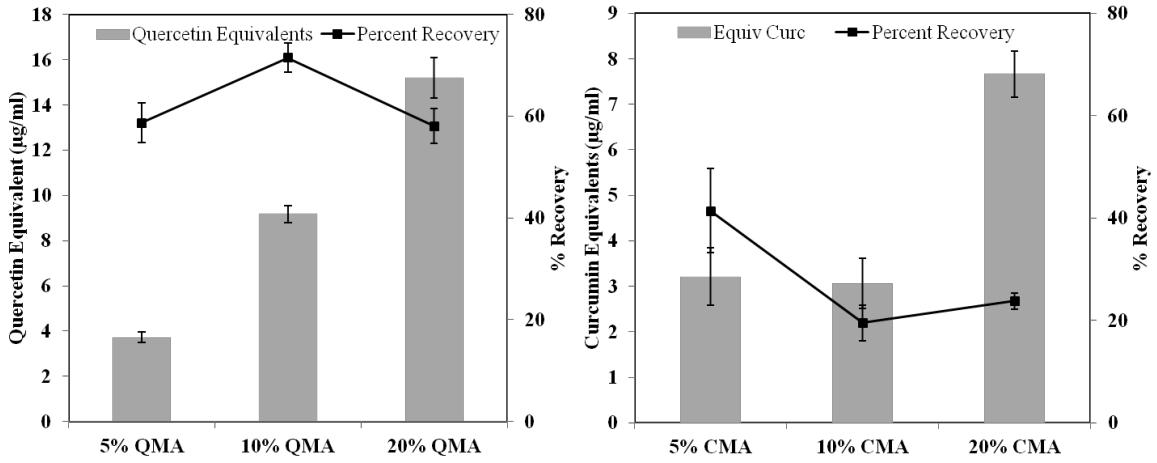

Figure 7-5. ***In Vitro*** **Measurement of Antioxidant Activity of PABAE Degradation Products Using a DCF-based Fluorescent Assay.**

7.3.5 Cytotoxicity of Degradation Products of PABAE Hydrogels

HUVECs were treated with degradation products of PABAE at different concentrations for 24 hrs and the cell viability was measured using a standard MTT assay (**Figure 7-6A and 7-6B**). Degradation products of 0% PABAE hydrogel had very little cytotoxicity up to a concentration of 1000 µg/ml. Like quercetin, degradation products of quercetin PABAE hydrogels did not have significant cytotoxicity except for high concentrations of 20% QMA where the cell viability dropped to 35% at a concentration of 1000 µg/ml. Curcumin PABAE hydrogels, like pure curcumin, were acutely toxic in proportion to their curcumin content.

7.3.6 Effect of PABAE Degradation Products on Oxidative Stress Levels in the Cells

HUVECs were treated with degradation products of PABAE hydrogels in the presence of DCF for 24 hrs and DCF fluorescence was then measured. In **Figure 7-7A and 7-7B**, DCF fluorescence in the cells is plotted compared to the untreated cells (% of Control). Both antioxidants querectin and curcumin have excitation and emission spectra similar to that of DCF and in order to avoid background fluorescence from antioxidants, the maximum concentration of PABAE degradation products that HUVECs were treated with was limited to 100 µg/ml. Degradation products of 0% PABAE did not affect DCF 146luorescence levels in HUVECs and did not exert antioxidant effect on the cells. However, quercetin and curcumin PABAE degradation products showed concentration dependant suppression in DCF fluorescence. At concentration of 100 µg/ml, querectin and curcumin PABAE hydrogels suppressed DCF fluorescence to a minimum of 35% and 55%, respectively.

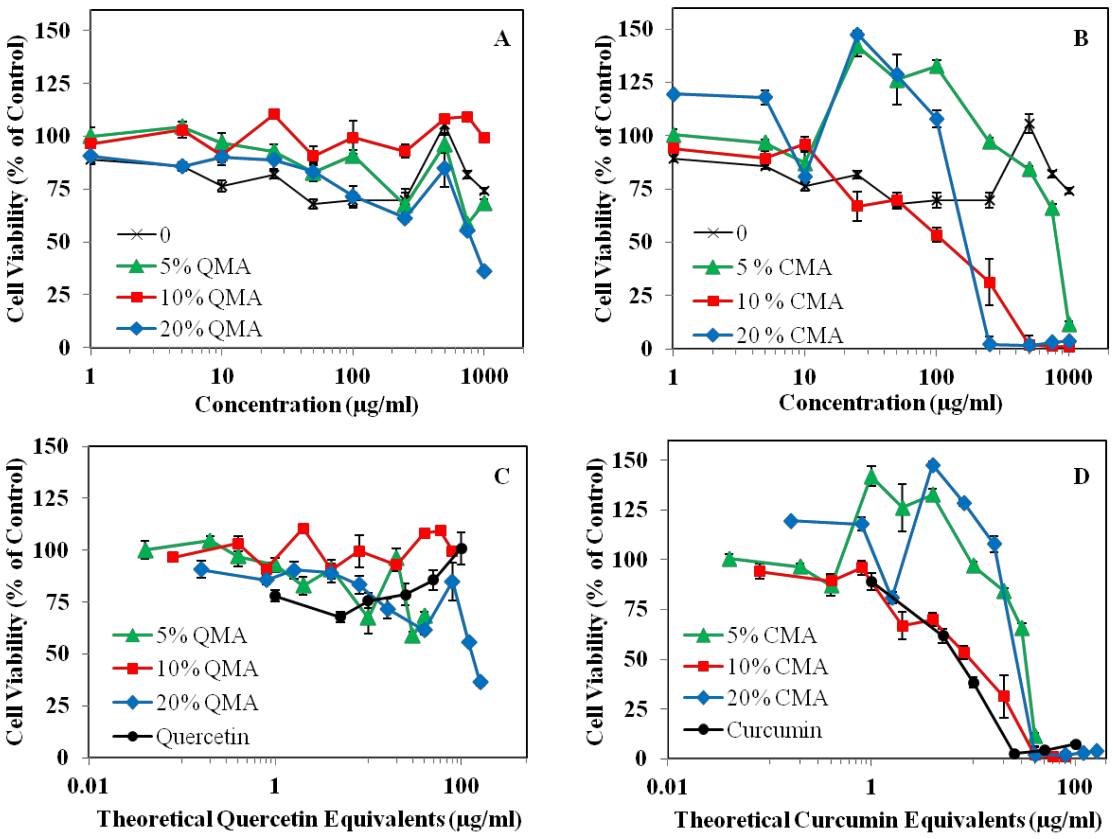

Figure 7-6. Cytotoxicity of PABAE Degradation Products.

(A and B) HUVECs were treated with PABAE degradation products for 24 hrs and post treatment, cell viability was measured using MTT assay. 0% PABAE hydrogels had did not have significant cytotoxicity.

(C and D) Data in A and B was re-plotted with respect to theoretical antioxidant content of PABAE degradation products and it shows that cytotoxicity of PABAE degradation products is a function of its antioxidant content. Curcumin PABAE degradation products had cytotoxicity similar to that of free curcumin.

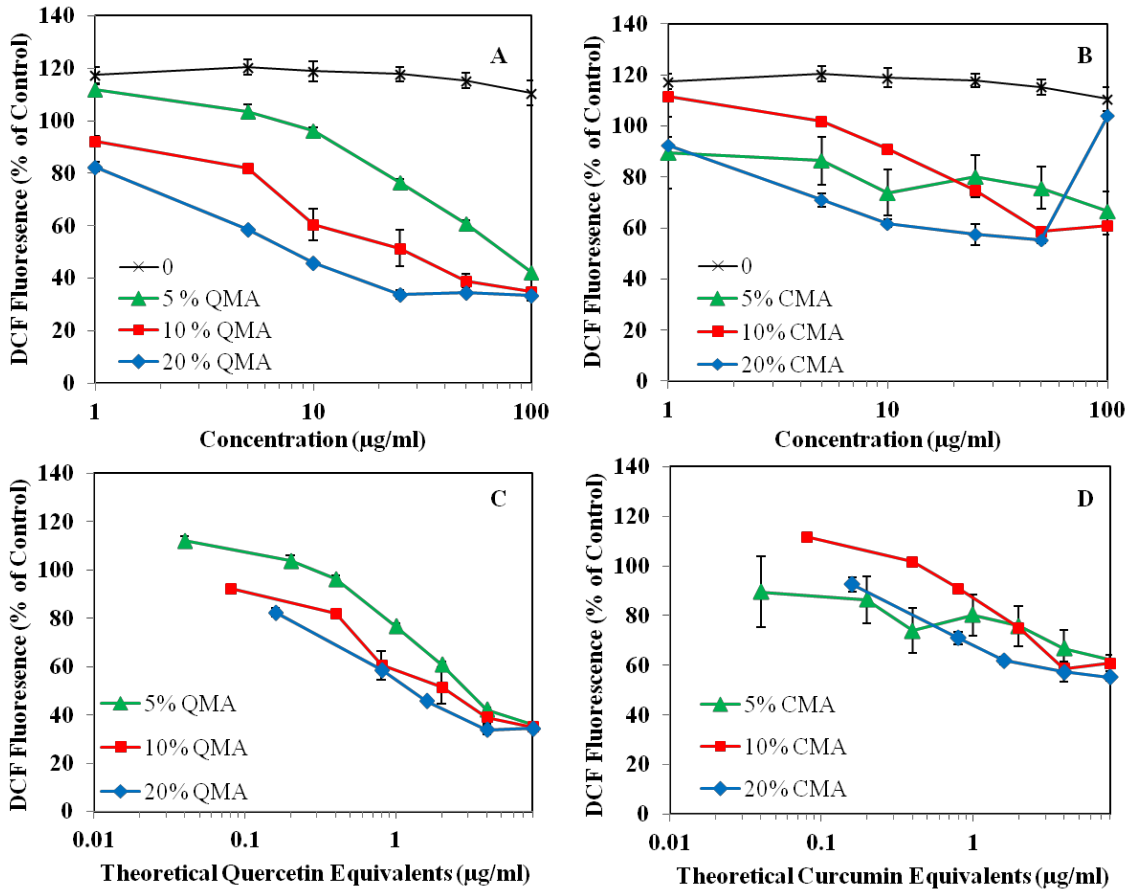

Figure 7-7. Effect of PABAE Degradation Products on Background Oxidative Stress in HUVECs.

(A and B) Treatment of HUVECs with quercetin and curcumin PABAE degradation products suppressed background oxidative stress levels in the cells in a concentration dependant manner.

(C and D) Data in A and B is re-plotted with respect to theoretical antioxidant content of PABAE degradation products.

7.3.7 H_2O_2 Induced Oxidative Stress Injury and Protection from PABAE Degradation Products

In this prophylactic study, HUVECs were treated with antioxidants or PABAE degradation products prior to adding H_2O_2 to induce the oxidative stress in cells. Cell viability, measured using MTT assay 24 hrs post treatment, was used as a measure of extent of injury to cells. As shown in **Figure 7-8**, treatment of HUVECs with H_2O_2 only resulted in a drop in cell viability to 70%. Pre-treatment of cells with quercetin and 10% QMA degradation product did not result in a drop in viability. However, pre-treatment with curcumin resulted in further decrease in cell viability to 57%. 10% CMA treatment provided modest protection with cell viability of 80%.

7.4 Discussion

In the present work, a modified poly(β-amino ester) chemistry [326] was used to successfully synthesize hydrolytically degradable cross-linked polymers for controlled release of polyphenolic antioxidants quercetin and curcumin. Some of the advantages of this poly(β-amino ester) chemistry are i.) it does not require free-radical polymerization, thereby allowing loading of antioxidant drugs that are susceptible to free-radical damage, ii.) the large libraries of commercial diacrylates [320, 321] could be used to tune polymer properties (e.g. degradation rate, mechanical strength, etc.) and iii.) it could be extended to other polyphenolic antioxidants.

Synthesized QMA and CMA were characterized using FT-IR and ^{1}H-NMR spectroscopy. Acrylate functionalization of phenol groups in the antioxidants was verified by both FT-IR and ^{1}H-NMR. QMA and CMA were synthesized with initial ratio of acryloyl chloride to quercetin at 4.5 and acryoyl chloride to curcumin ratio at 2.5.

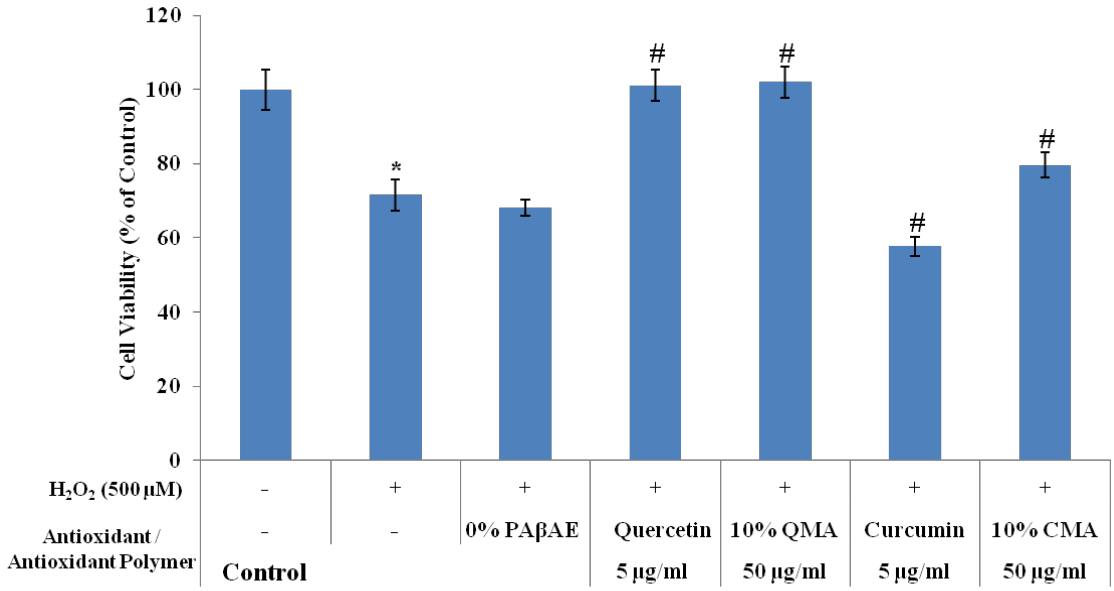

Figure 7-8. Cell Protection Against Oxidative Stress Injury by PABAE Degradation Products

HUVECs were treated with antioxidants or PABAE degradation products 2 hrs prior to inducing oxidative stress injury by addition of H_2O_2. Cell viability was measured after 24 hrs using MTT assay. (M $\pm$ SE). Groups were compared using Paired Student t-test. * indicates significant difference from control and # indicates significant difference from H_2O_2 only treatment, with $p<0.05$.

Synthesis of QMA resulted in 4.28 acrylate groups per molecule of quercetin, lower than the targeted number of 4.5 acrylate groups per molecule of quercetin. However, analysis of ^{1}H-NMR spectra of CMA revealed 2.66 acrylate groups per molecule of curcumin, which was higher than 2.5, the initial ratio of acryloyl chloride to curcumin during the synthesis of CMA. This could indicate presence of free acrylic acid impurity (byproduct of reaction of acryoyl chloride and water) remaining in the CMA product. Nonetheless, this slightly impure CMA was used for synthesis of PABAE hydrogels. Presence of unreacted phenol groups in the monomers (QMA and CMA) would have hindered hydrogel synthesis using the conventional free radical polymerization technique as a result of the radical scavenging ability of phenol groups. The Michael type addition chemistry used in this work to synthesize a crosslinked network overcomes this inability of free radical polymerization to incorporate phenolic compounds in polymer backbone.

We have previously reported synthesis and degradation characteristics of poly(β-amino ester) hydrogels that utilizes a Michael type addition reaction between multifunctional acrylates and tetrafunctional primarydiamines [326]. In this work, in addition to the commercial monomers PEG400DA and TTD, synthesized antioxidants multiacrylates were also used for PABAE hydrogel synthesis. As shown in Figure 4, 0% PABAE hydrogels degrade completely within 150 min. However, inclusion of as low as 5% of relatively hydrophobic antioxidant multiacrylates slowed the degradation rate of PABAE hydrogels where they completely degraded in 250-350 mins. One of the several advantages of this poly(β-amino ester) chemistry is that it can be easily tuned to synthesize slower degrading PABAE hydrogels by controlling the ratio of hydrophilic

monomers (PEG400DA and TTD) to relatively hydrophobic monomers (e.g. 1,3-butanediol diacrylate and hexamethylene diamine).

Quercetin is known to be a safe flavonol with relatively high IC_{50} values of 113 μM for human normal liver cells L-02 [335]. However, in contrast to the previously reported 18.4 μg/ml (61 μM) IC_{50} value of quercetin for HUVECs, we did not observe any significant quercetin toxicity to HUVECs up to a concentration of 100 μg/ml [336]. IC_{50} concentrations of curcumin PABAE hydrogels decreased with increase in CMA content where 5% CMA, 10% CMA and 20% CMA had IC_{50} concentrations of 62.1, 10.2 and 8.7 μg/ml. IC_{50} value of pure curcumin for HUVECs was found to be 6.8 μg/ml, which is similar to the previously reported value of 10.8 μg/ml [337]. When the data in Figure 6A and 6B is normalized with respect to antioxidant content in the PABAE hydrogels as shown in Figure 6C and 6D, the toxicity profiles of PABAE hydrogels are similar to that of pure antioxidants meaning that the toxicity of PABAE hydrogels is the result of their antioxidant content. This is particularly evident in case of curcumin PABAE hydrogels (Figure 6D) where all curcumin PABAE degradation products have an acute toxicity concentration of ~40 μg/ml curcumin equivalents.

Despite limitations with its specificity for the exact oxidative species [306-309, 334], DCF fluorescence is a commonly used marker to study oxidative stress in the cells and was applied to study effect of PABAE degradation products on oxidative stress levels in HUVECs. The model is based on the principle that DCF-DA (2',7'-dichlorodihydrofluorescein diacetate), a non-fluorescent ester form of the dye, is taken up by the cells and active esterases in the cells cleave it to a non-fluorescent product DCFH (2',7'-dichlorodihydrofluorescein). Free radicals in the cells can then react with DCFH to

result in a fluorescent product DCF (2',7'-dichlorofluorescein). When the data in Figure 7A and 7B is normalized with respect to the antioxidant content of PABAE hydrogels as plotted in Figure 7C and 7D, it is evident that suppression of DCF fluorescence by PABAE degradation products is a result of antioxidant content in PABAE.

H_2O_2 at submillimolar concentrations induce apoptosis in endothelial cells via redox dependant pathways [338]. It has been shown that several polyphenolic flavanoids including quercetin have antiapoptotic effect against H_2O_2 injury [339]. Treatment of HUVECs with 500 μM H_2O_2 for 24 hrs resulted in 30% cell death as measured by MTT assay. Previous studies have shown that treatment with 200 μM H_2O_2 can cause upto 70% cell death. Reduced cell death at higher H_2O_2 concentration observed in this study could be a result of 2% serum based cell media used to prepare H_2O_2 solutions, where catalase or other enzymes present in the serum can detoxify some of the H_2O_2. Nonetheless, treatment of HUVECs with 500 μM caused significant toxicity as compared to controls. Pre-treatment of HUVECs with 5 μg/ml quercetin and 50 μg/ml of 10% QMA degradation product (5 μg/ml theoretical quercetin equivalents) protected cells from H_2O_2 injury, which confirms with results from other studies [339]. As shown in Figure 7-6D, treatment of HUVECs with 5 μg/ml curcumin alone results in 40% cell death. Pre-treatment of HUVECs with curcumin, ads to the H_2O_2 injury. Protection provided by 10% CDA degradation products was very modest and improved cell viability by less than 10%.

7.5 Conclusions

The single-step polymerization method for synthesis of poly(β-amino ester) hydrogels [326] was successfully applied for incorporating polyphenolic antioxidants in

to the PABAE network by acrylate functionalization of polyphenols. Cytotoxicity of PABAE degradation products was a function of both, the type of antioxidant used and % antioxidant content in PABAE, where quercetin PABAE had very little to no cytotoxicity and curcumin PABAE had cytotoxicity similar to that of pure curcumin. Also, degradation products of PABAE hydrogels possessed antioxidant activity. Treatment of HUVECs with PABAE degradation products suppressed background oxidative stress in the cells. PABAE developed in this work can be used for various drug delivery and tissue engineering applications where controlled delivery of polyphenolic antioxidants is desired.

Chapter 8. Conclusions

In this work, three different antioxidant polymers were developed for controlled release of antioxidants to suppress oxidative stress. Initial studies involved synthesis and characterization of poly(trolox ester), which was formulated in to nanoparticles to determine its application as polymeric antioxidant carrier. *In vitro* degradation studies revealed that poly(trolox ester) is not hydrolytically degradable but undergoes enzymatic degradation to release degradation products that have antioxidant radical scavenging ability. Poly(trolox ester) nanoparticles do not have significant cytotoxicity and provided protection in an *in vitro* cell injury model where oxidative stress injury was induced by treating cells with metal nanoparticles. It was also observed that in absence of injury, poly(trolox ester) nanoparticles suppressed background oxidative stress in the cells. In order to explore this effect of poly(trolox ester), a detailed study was carried out to understand concentration dependant antioxidant and pro-oxidant effect of trolox and poly(trolox ester) nanoparticles. Poly(trolox ester) nanoparticles possessed a unique ability to suppress protein oxidation, a feature not seen in the free trolox form, emphasizing the advantage of delivery formulation upon regulating cellular responses. This study showed that poly(trolox ester) can be used to modulate cellular redox state, proving the concept of antioxidant polymers.

While the work on poly(trolox ester) is promising, it is limited by enzymatic degradation of polymer, not allowing significant control over its rate of degradation. Therefore, a hydrolytically degradable PABAE were synthesized. PABAE synthesis scheme is more robust and can be extended to all polyphenolic antioxidants while allowing control to tune the rate of polymer degradation. To demonstrate the flexibility of

PABAE synthesis scheme, quercetin and curcumin PABAE were synthesized and characterized. PABAE degradation products possessed antioxidant activity which was further confirmed by their ability to suppress oxidative stress in cells, both in absence and presence of injury agent.

Overall, this works shows the potential of antioxidant polymers to modulate cellular redox state by controlled release of antioxidants. This can have far reaching implications in field of biomaterials and in variety of biomedical, pharmaceutical and tissue engineering applications.

References

[1] V.R. Muzykantov, Delivery of antioxidant enzyme proteins to the lung, Antioxid Redox Signal, 3 (2001) 39-62.

[2] C. Suarna, B.J. Wu, K. Choy, T. Mori, K. Croft, O. Cynshi, R. Stocker, Protective effect of vitamin E supplements on experimental atherosclerosis is modest and depends on preexisting vitamin E deficiency, Free radical biology & medicine, 41 (2006) 722-730.

[3] R. Siekmeier, C. Steffen, W. Marz, Role of oxidants and antioxidants in atherosclerosis: results of in vitro and in vivo investigations, Journal of cardiovascular pharmacology and therapeutics, 12 (2007) 265-282.

[4] M.J. Thomson, V. Puntmann, J.C. Kaski, Atherosclerosis and oxidant stress: the end of the road for antioxidant vitamin treatment?, Cardiovascular drugs and therapy / sponsored by the International Society of Cardiovascular Pharmacotherapy, 21 (2007) 195-210.

[5] T.D. Dziubla, S. Muro, V.R. Muzykantov, M. Koval, Nanoscale antioxidant therapeutics, in: K.K. Singh (Ed.) Oxidative Stress, Disease and Cancer, Imperial College Press, London, 2006.

[6] C. Delles, W.H. Miller, A.F. Dominiczak, Targeting reactive oxygen species in hypertension, Antioxid Redox Signal, 10 (2008) 1061-1077.

[7] D.V. Ratnam, D.D. Ankola, V. Bhardwaj, D.K. Sahana, M.N. Kumar, Role of antioxidants in prophylaxis and therapy: A pharmaceutical perspective, Journal of Controlled Release, 113 (2006) 189-207.

[8] J.T. Hancock, The role of redox mechanisms in cell signalling, Mol Biotechnol, 43 (2009) 162-166.

[9] J.W. Heinecke, Oxidants and antioxidants in the pathogenesis of atherosclerosis: implications for the oxidized low density lipoprotein hypothesis, Atherosclerosis, 141 (1998) 1-15.

[10] M. Valko, D. Leibfritz, J. Moncol, M.T. Cronin, M. Mazur, J. Telser, Free radicals and antioxidants in normal physiological functions and human disease, Int J Biochem Cell Biol, 39 (2007) 44-84.

[11] S. Kinlay, P. Libby, P. Ganz, Endothelial function and coronary artery disease, Curr Opin Lipidol, 12 (2001) 383-389.

[12] Z.S. Nedeljkovic, N. Gokce, J. Loscalzo, Mechanisms of oxidative stress and vascular dysfunction, Postgrad Med J, 79 (2003) 195-199; quiz 198-200.

[13] G. Kojda, D. Harrison, Interactions between NO and reactive oxygen species: pathophysiological importance in atherosclerosis, hypertension, diabetes and heart failure, Cardiovascular Research, 43 (1999) 562-571.

[14] C. Delles, W.H. Miller, A.F. Dominiczak, Targeting Reactive Oxygen Species in Hypertension, Antioxid Redox Signal, (2008).

[15] J.C. Romero, J.F. Reckelhoff, State-of-the-Art lecture. Role of angiotensin and oxidative stress in essential hypertension, Hypertension, 34 (1999) 943-949.

[16] J. Pereda, L. Sabater, L. Aparisi, J. Escobar, J. Sandoval, J. Vina, G. Lopez-Rodas, J. Sastre, Interaction between cytokines and oxidative stress in acute pancreatitis, Curr Med Chem, 13 (2006) 2775-2787.

[17] M.P. Fink, Role of reactive oxygen and nitrogen species in acute respiratory distress syndrome, Curr Opin Crit Care, 8 (2002) 6-11.

[18] A.L. Lagan, D.D. Melley, T.W. Evans, G.J. Quinlan, Pathogenesis of the systemic inflammatory syndrome and acute lung injury: role of iron mobilization and decompartmentalization, Am J Physiol Lung Cell Mol Physiol, 294 (2008) L161-174.

[19] C.W. Chow, M.T. Herrera Abreu, T. Suzuki, G.P. Downey, Oxidative stress and acute lung injury, Am J Respir Cell Mol Biol, 29 (2003) 427-431.

[20] P. Kirkham, Oxidative stress and macrophage function: a failure to resolve the inflammatory response, Biochem Soc Trans, 35 (2007) 284-287.
[21] Z. Wei, K. Costa, A.B. Al-Mehdi, C. Dodia, V. Muzykantov, A.B. Fisher, Simulated ischemia in flow-adapted endothelial cells leads to generation of reactive oxygen species and cell signaling, Circ Res, 85 (1999) 682-689.
[22] R. Ferrari, O. Alfieri, S. Curello, C. Ceconi, A. Cargnoni, P. Marzollo, A. Pardini, E. Caradonna, O. Visioli, Occurrence of oxidative stress during reperfusion of the human heart, Circulation, 81 (1990) 201-211.
[23] S. Hirai, Systemic inflammatory response syndrome after cardiac surgery under cardiopulmonary bypass, Ann Thorac Cardiovasc Surg, 9 (2003) 365-370.
[24] A.C. Kulkarni, P. Kuppusamy, N. Parinandi, Oxygen, the lead actor in the pathophysiologic drama: enactment of the trinity of normoxia, hypoxia, and hyperoxia in disease and therapy, Antioxid Redox Signal, 9 (2007) 1717-1730.
[25] T.E. Zaher, E.J. Miller, D.M. Morrow, M. Javdan, L.L. Mantell, Hyperoxia-induced signal transduction pathways in pulmonary epithelial cells, Free radical biology & medicine, 42 (2007) 897-908.
[26] K.J. Barnham, C.L. Masters, A.I. Bush, Neurodegenerative diseases and oxidative stress, Nat Rev Drug Discov, 3 (2004) 205-214.
[27] Q. Shi, G.E. Gibson, Oxidative stress and transcriptional regulation in Alzheimer disease, Alzheimer Dis Assoc Disord, 21 (2007) 276-291.
[28] T. Finkel, N.J. Holbrook, Oxidants, oxidative stress and the biology of ageing, Nature, 408 (2000) 239-247.
[29] D. Pratico, Antioxidants and endothelium protection, Atherosclerosis, 181 (2005) 215-224.
[30] M. Gulumian, The role of oxidative stress in diseases caused by mineral dusts and fibres: current status and future of prophylaxis and treatment, Molecular and Cellular Biochemistry, 196 (1999) 69-77.
[31] A. Cataldi, Cell Responses to Oxidative Stressors, Curr Pharm Design, 16 (2010) 1387-1395.
[32] M.A. Ogasawara, H. Zhang, Redox regulation and its emerging roles in stem cells and stem-like cancer cells, Antioxid Redox Signal, 11 (2009) 1107-1122.
[33] R.K. Sharma, Q. Zhou, P.A. Netland, Effect of oxidative preconditioning on neural progenitor cells, Brain Res, 1243 (2008) 19-26.
[34] J. Smith, E. Ladi, M. Mayer-Proschel, M. Noble, Redox state is a central modulator of the balance between self-renewal and differentiation in a dividing glial precursor cell, Proc Natl Acad Sci U S A, 97 (2000) 10032-10037.
[35] B. Stanic, M. Katsuyama, F.J. Miller, Jr., An Oxidized Extracellular Oxidation-Reduction State Increases Nox1 Expression and Proliferation in Vascular Smooth Muscle Cells Via Epidermal Growth Factor Receptor Activation, Arterioscler Thromb Vasc Biol, 30 (2010) 2234-2241.
[36] R. Busse, I. Fleming, Regulation and functional consequences of endothelial nitric oxide formation, Ann Med, 27 (1995) 331-340.
[37] K. Jomova, M. Valko, Advances in metal-induced oxidative stress and human disease, Toxicology, (2011).
[38] A. Ishiyama, K. Atarashi, M. Minami, M. Takagi, K. Kimura, A. Goto, M. Omata, Role of free radicals in the pathogenesis of lipid-induced glomerulosclerosis in rats. (vol 55, pg 1348, 1999), Kidney Int, 56 (1999) 780-780.
[39] F. Jiang, Y. Zhang, G.J. Dusting, NADPH oxidase-mediated redox signaling: roles in cellular stress response, stress tolerance, and tissue repair, Pharmacol Rev, 63 (2011) 218-242.
[40] V.R. Muzykantov, Targeting of superoxide dismutase and catalase to vascular endothelium, Journal of Controlled Release, 71 (2001) 1-21.

[41] C.L. Rock, R.A. Jacob, P.E. Bowen, Update on the biological characteristics of the antioxidant micronutrients: vitamin C, vitamin E, and the carotenoids, J Am Diet Assoc, 96 (1996) 693-702; quiz 703-694.
[42] J. Stenesh, Biochemistry, Plenum, New York, 1998.
[43] L.V. Papp, J. Lu, A. Holmgren, K.K. Khanna, From selenium to selenoproteins: synthesis, identity, and their role in human health, Antioxid Redox Signal, 9 (2007) 775-806.
[44] J. Lu, A. Holmgren, Selenoproteins, Journal of Biological Chemistry, 284 (2009) 723-727.
[45] Y. Manevich, A.B. Fisher, Peroxiredoxin 6, a 1-Cys peroxiredoxin, functions in antioxidant defense and lung phospholipid metabolism, Free radical biology & medicine, 38 (2005) 1422-1432.
[46] S.G. Rhee, H.Z. Chae, K. Kim, Peroxiredoxins: a historical overview and speculative preview of novel mechanisms and emerging concepts in cell signaling, Free radical biology & medicine, 38 (2005) 1543-1552.
[47] M. Jastroch, A.S. Divakaruni, S. Mookerjee, J.R. Treberg, M.D. Brand, Mitochondrial proton and electron leaks, Essays Biochem, 47 (2010) 53-67.
[48] Z.G. Jin, Where is endothelial nitric oxide synthase more critical: Plasma membrane or Golgi?, Arterioscl Throm Vas, 26 (2006) 959-961.
[49] H.F.G. Heijnen, E. van Donselaar, J.W. Slot, D.M. Fries, B. Blachard-Fillion, R. Hodara, R. Lightfoot, M. Polydoro, D. Spielberg, L. Thomson, E.A. Regan, J. Crapo, H. Ischiropoulos, Subcellular localization of tyrosine-nitrated proteins is dictated by reactive oxygen species generating enzymes and by proximity to nitric oxide synthase, Free Radical Bio Med, 40 (2006) 1903-1913.
[50] T. Fukai, M. Ushio-Fukai, Superoxide Dismutases: Role in Redox Signaling, Vascular Function, and Diseases, Antioxid Redox Sign, 15 (2011) 1583-1606.
[51] J.M. Anderson, A.K. McNally, Biocompatibility of implants: lymphocyte/macrophage interactions, Semin Immunopathol, 33 (2011) 221-233.
[52] P. Martin, Wound healing--aiming for perfect skin regeneration, Science, 276 (1997) 75-81.
[53] C. Nathan, Neutrophils and immunity: challenges and opportunities, Nat Rev Immunol, 6 (2006) 173-182.
[54] G. Hubner, M. Brauchle, H. Smola, M. Madlener, R. Fassler, S. Werner, Differential regulation of pro-inflammatory cytokines during wound healing in normal and glucocorticoid-treated mice, Cytokine, 8 (1996) 548-556.
[55] G.C. Gurtner, S. Werner, Y. Barrandon, M.T. Longaker, Wound repair and regeneration, Nature, 453 (2008) 314-321.
[56] H.N. Lovvorn, D.T. Cheung, M.E. Nimni, N. Perelman, J.M. Estes, N.S. Adzick, Relative distribution and crosslinking of collagen distinguish fetal from adult sheep wound repair, J Pediatr Surg, 34 (1999) 218-223.
[57] N. Ojha, S. Roy, G. He, S. Biswas, M. Velayutham, S. Khanna, P. Kuppusamy, J.L. Zweier, C.K. Sen, Assessment of wound-site redox environment and the significance of Rac2 in cutaneous healing, Free Radical Bio Med, 44 (2008) 682-691.
[58] A. Gorlach, Redox regulation of the coagulation cascade, Antioxid Redox Sign, 7 (2005) 1398-1404.
[59] I.V. Klyubin, K.M. Kirpichnikova, I.A. Gamaley, Hydrogen peroxide-induced chemotaxis of mouse peritoneal neutrophils, Eur J Cell Biol, 70 (1996) 347-351.
[60] P. Niethammer, C. Grabher, A.T. Look, T.J. Mitchison, A tissue-scale gradient of hydrogen peroxide mediates rapid wound detection in zebrafish, Nature, 459 (2009) 996-999.
[61] H. Hattori, K.K. Subramanian, J. Sakai, Y.H. Jia, Y.T. Li, T.F. Porter, F. Loison, B. Sarraj, A. Kasorn, H. Jo, C. Blanchard, D. Zirkle, D. McDonald, S.Y. Pai, C.N. Serhan, H.R. Luo, Small-

molecule screen identifies reactive oxygen species as key regulators of neutrophil chemotaxis, Proceedings of the National Academy of Sciences of the United States of America, 107 (2010) 3546-3551.
[62] H. Nakamura, L.A. Herzenberg, J. Bai, S. Araya, N. Kondo, Y. Nishinaka, L.A. Herzenberg, J. Yodoi, Circulating thioredoxin suppresses lipopolysaccharide-induced neutrophil chemotaxis, Proceedings of the National Academy of Sciences of the United States of America, 98 (2001) 15143-15148.
[63] C.F. Nathan, Neutrophil activation on biological surfaces. Massive secretion of hydrogen peroxide in response to products of macrophages and lymphocytes, J Clin Invest, 80 (1987) 1550-1560.
[64] B.M. Babior, Phagocytes and oxidative stress, American Journal of Medicine, 109 (2000) 33-44.
[65] M. Baggiolini, F. Boulay, J.A. Badwey, J.T. Curnutte, Activation of Neutrophil Leukocytes - Chemoattractant Receptors and Respiratory Burst, Faseb J, 7 (1993) 1004-1010.
[66] T.L. Leto, M. Geiszt, Role of Nox family NADPH oxidases in host defense, Antioxid Redox Sign, 8 (2006) 1549-1561.
[67] C. Meischl, D. Roos, The molecular basis of chronic granulomatous disease, Springer Semin Immun, 19 (1998) 417-434.
[68] M.M. Shi, I.W. Chong, J.J. Godleski, J.D. Paulauskis, Regulation of macrophage inflammatory protein-2 gene expression by oxidative stress in rat alveolar macrophages, Immunology, 97 (1999) 309-315.
[69] M.M. Shi, J.J. Godleski, J.D. Paulauskis, Regulation of macrophage inflammatory protein-1 alpha mRNA by oxidative stress, Journal of Biological Chemistry, 271 (1996) 5878-5883.
[70] T. Marumo, V.B. SchiniKerth, B. Fisslthaler, R. Busse, Platelet-derived growth factor-stimulated superoxide anion production modulates activation of transcription factor NF-kappa B and expression of monocyte chemoattractant protein 1 in human aortic smooth muscle cells, Circulation, 96 (1997) 2361-2367.
[71] A. Soneja, M. Drews, T. Malinski, Role of nitric oxide, nitroxidative and oxidative stress in wound healing, Pharmacol Rep, 57 Suppl (2005) 108-119.
[72] K.E. Driscoll, TNFalpha and MIP-2: role in particle-induced inflammation and regulation by oxidative stress, Toxicol Lett, 112-113 (2000) 177-183.
[73] Y.H. Hong, H.B. Peng, V. LaFata, J.K. Liao, Hydrogen peroxide-mediated transcriptional induction of macrophage colony-stimulating factor by TGF-beta 1, J Immunol, 159 (1997) 2418-2423.
[74] V. Verhasselt, M. Goldman, F. Willems, Oxidative stress up-regulates IL-8 and TNF-alpha synthesis by human dendritic cells, Eur J Immunol, 28 (1998) 3886-3890.
[75] J.S. Lee, S.S. Kahlon, R. Culbreth, J.A.D. Cooper, Modulation of monocyte chemokine production and nuclear factor kappa B activity by oxidants, J Interf Cytok Res, 19 (1999) 761-767.
[76] J.J. Haddad, Redox regulation of pro-inflammatory cytokines and I kappa B-alpha/NF-kappa B nuclear translocation and activation (vol 296, pg 847, 2002), Biochem Bioph Res Co, 301 (2003) 625-625.
[77] I. Bejarano, M.P. Terron, S.D. Paredes, C. Barriga, A.B. Rodriguez, J.A. Pariente, Hydrogen peroxide increases the phagocytic function of human neutrophils by calcium mobilisation, Molecular and Cellular Biochemistry, 296 (2007) 77-84.
[78] J.S. Winn, J. Guille, J.M. Gebicki, R.O. Day, Hydrogen-Peroxide Modulation of the Respiratory Burst of Human Neutrophils, Biochem Pharmacol, 41 (1991) 31-36.

[79] A.A. Krjukov, G.N. Semenkova, S.N. Cherenkevich, V. Gerein, Activation of redox-systems of monocytes by hydrogen peroxide, Biofactors, 26 (2006) 283-292.
[80] J.K. Murphy, C.R. Hoyal, F.R. Livingston, H.J. Forman, Modulation of the alveolar macrophage respiratory burst by hydroperoxides, Free radical biology & medicine, 18 (1995) 37-45.
[81] T. Seres, R.G. Knickelbein, J.B. Warshaw, R.B. Johnston, The phagocytosis-associated respiratory burst in human monocytes is associated with increased uptake of glutathione, J Immunol, 165 (2000) 3333-3340.
[82] J.R. Klune, R. Dhupar, J. Cardinal, T.R. Billiar, A. Tsung, HMGB1: Endogenous danger signaling, Mol Med, 14 (2008) 476-484.
[83] M.E. Bianchi, A.A. Manfredi, High-mobility group box 1 (HMGB1) protein at the crossroads between innate and adaptive immunity, Immunol Rev, 220 (2007) 35-46.
[84] D. Tang, Y. Shi, R. Kang, T. Li, W. Xiao, H. Wang, X. Xiao, Hydrogen peroxide stimulates macrophages and monocytes to actively release HMGB1, J Leukoc Biol, 81 (2007) 741-747.
[85] A. Tsung, J.R. Klune, X. Zhang, G. Jeyabalan, Z. Cao, X. Peng, D.B. Stolz, D.A. Geller, M.R. Rosengart, T.R. Billiar, HMGB1 release induced by liver ischemia involves Toll-like receptor 4 dependent reactive oxygen species production and calcium-mediated signaling, Journal of Experimental Medicine, 204 (2007) 2913-2923.
[86] T.A. Springer, Traffic Signals for Lymphocyte Recirculation and Leukocyte Emigration - the Multistep Paradigm, Cell, 76 (1994) 301-314.
[87] M. Reyes-Reyes, N. Mora, G. Gonzalez, C. Rosales, beta 1 and beta 2 integrins activate different signalling pathways in monocytes, Biochem J, 363 (2002) 273-280.
[88] H.F. Lu, K. Youker, C. Ballantyne, M. Entman, C.W. Smith, Hydrogen peroxide induces LFA-1-dependent neutrophil adherence to cardiac myocytes, Am J Physiol-Heart C, 278 (2000) H835-H842.
[89] E. Blouin, L. Halbwachs-Mecarelli, P. Rieu, Redox regulation of beta 2-integrin CD11b/CD18 activation, Eur J Immunol, 29 (1999) 3419-3431.
[90] H.F. Lu, C. Ballantyne, C.W. Smith, LFA-1 (CD11a/CD18) triggers hydrogen peroxide production by canine neutrophils, J Leukocyte Biol, 68 (2000) 73-80.
[91] C. Nathan, S. Srimal, C. Farber, E. Sanchez, L. Kabbash, A. Asch, J. Gailit, S.D. Wright, Cytokine-Induced Respiratory Burst of Human-Neutrophils - Dependence on Extracellular-Matrix Proteins and Cd11/Cd18 Integrins, J Cell Biol, 109 (1989) 1341-1349.
[92] S.B. Shappell, C. Toman, D.C. Anderson, A.A. Taylor, M.L. Entman, C.W. Smith, Mac-1 (Cd11b Cd18) Mediates Adherence-Dependent Hydrogen-Peroxide Production by Human and Canine Neutrophils, J Immunol, 144 (1990) 2702-2711.
[93] K. Hashizume, Y. Hatanaka, I. Fukuda, T. Sano, Y. Yamaguchi, Y. Tani, G. Danno, K. Suzuki, H. Ashida, N-acetyl-L-cysteine suppresses constitutive expression of CD11a/LFA-1 alpha protein in myeloid lineage, Leukemia Res, 26 (2002) 939-944.
[94] A. Fraticelli, C.V. Serrano, B.S. Bochner, M.C. Capogrossi, J.L. Zweier, Hydrogen peroxide and superoxide modulate leukocyte adhesion molecule expression and leukocyte endothelial adhesion, Bba-Mol Cell Res, 1310 (1996) 251-259.
[95] H. Cai, Hydrogen peroxide regulation of endothelial function: Origins, mechanisms, and consequences, Cardiovascular Research, 68 (2005) 26-36.
[96] R. Carnemolla, V.V. Shuvaev, V.R. Muzykantov, Targeting Antioxidant and Antithrombotic Biotherapeutics to Endothelium, Semin Thromb Hemost, 36 (2010) 332-342.
[97] J.R. Bradley, D.R. Johnson, J.S. Pober, Endothelial Activation by Hydrogen-Peroxide - Selective Increases of Intercellular-Adhesion Molecule-1 and Major Histocompatibility Complex Class-I, Am J Pathol, 142 (1993) 1598-1609.

[98] A.K. Hubbard, R. Rothlein, Intercellular adhesion molecule-1 (ICAM-1) expression and cell signaling cascades, Free Radical Bio Med, 28 (2000) 1379-1386.
[99] K.A. Roebuck, A. Rahman, V. Lakshminarayanan, K. Janakidevi, A.B. Malik, H2o2 and Tumor-Necrosis-Factor-Alpha Activate Intercellular-Adhesion Molecule-1 (Icam-1) Gene-Transcription through Distinct Cis-Regulatory Elements within the Icam-1 Promoter, Journal of Biological Chemistry, 270 (1995) 18966-18974.
[100] M. Kawai, R. Nishikomori, E.Y. Jung, G.X. Tai, C. Yamanaka, M. Mayumi, T. Heike, Pyrrolidine Dithiocarbamate Inhibits Intercellular-Adhesion Molecule-1 Biosynthesis Induced by Cytokines in Human Fibroblasts, J Immunol, 154 (1995) 2333-2341.
[101] A. Saccani, S. Saccani, S. Orlando, M. Sironi, S. Bernasconi, P. Ghezzi, A. Mantovani, A. Sica, Redox regulation of chemokine receptor expression, Proc Natl Acad Sci U S A, 97 (2000) 2761-2766.
[102] G. Lehoux, C. Le Gouill, J. Stankova, M. Rola-Pleszczynski, Upregulation of expression of the chemokine receptor CCR5 by hydrogen peroxide in human monocytes, Mediators Inflamm, 12 (2003) 29-35.
[103] G. Wang, K. O, Homocysteine stimulates the expression of monocyte chemoattractant protein-1 receptor (CCR2) in human monocytes: possible involvement of oxygen free radicals, Biochem J, 357 (2001) 233-240.
[104] Raja, K. Sivamani, M.S. Garcia, R.R. Isseroff, Wound re-epithelialization: modulating keratinocyte migration in wound healing, Front Biosci, 12 (2007) 2249-2268.
[105] I. Haase, R. Evans, R. Pofahl, F.M. Watt, Regulation of keratinocyte shape, migration and wound epithelialization by IGF-1- and EGF-dependent signalling pathways, J Cell Sci, 116 (2003) 3227-3238.
[106] G. Vardatsikos, A. Sahu, A.K. Srivastava, The Insulin-Like Growth Factor Family: Molecular Mechanisms, Redox Regulation, and Clinical Implications, Antioxid Redox Sign, 11 (2009) 1165-1190.
[107] Y. Higashi, T. Peng, J. Du, S. Sukhanov, Y.X. Li, H. Itabe, S. Parthasarathy, P. Delafontaine, A redox-sensitive pathway mediates oxidized LDL-induced downregulation of insulin-like growth factor-1 receptor, J Lipid Res, 46 (2005) 1266-1277.
[108] S. Hober, J.L. Ljung, M. Uhlen, B. Nilsson, Insulin-like growth factors I and II are unable to form and maintain their native disulfides under in vivo redox conditions, Febs Lett, 443 (1999) 271-276.
[109] E. Nishio, Y. Watanabe, The involvement of reactive oxygen species and arachidonic acid in alpha 1-adrenoceptor-induced smooth muscle cell proliferation and migration, Br J Pharmacol, 121 (1997) 665-670.
[110] P. Ranjan, V. Anathy, P.M. Burch, K. Weirather, J.D. Lambeth, N.H. Heintz, Redox-dependent expression of cyclin D1 and cell proliferation by Nox1 in mouse lung epithelial cells, Antioxid Redox Signal, 8 (2006) 1447-1459.
[111] B. Stanic, M. Katsuyama, F.J. Miller, Jr., An oxidized extracellular oxidation-reduction state increases Nox1 expression and proliferation in vascular smooth muscle cells via epidermal growth factor receptor activation, Arterioscler Thromb Vasc Biol, 30 (2010) 2234-2241.
[112] S. Rajagopalan, X.P. Meng, S. Ramasamy, D.G. Harrison, Z.S. Galis, Reactive oxygen species produced by macrophage-derived foam cells regulate the activity of vascular matrix metalloproteinases in vitro. Implications for atherosclerotic plaque stability, J Clin Invest, 98 (1996) 2572-2579.
[113] L. Grange, M.V. Nguyen, B. Lardy, M. Derouazi, Y. Campion, C. Trocme, M.H. Paclet, P. Gaudin, F. Morel, NAD(P)H oxidase activity of Nox4 in chondrocytes is both inducible and involved in collagenase expression, Antioxid Redox Signal, 8 (2006) 1485-1496.

[114] S.O. Yoon, S.J. Park, S.Y. Yoon, C.H. Yun, A.S. Chung, Sustained production of H(2)O(2) activates pro-matrix metalloproteinase-2 through receptor tyrosine kinases/phosphatidylinositol 3-kinase/NF-kappa B pathway, Journal of Biological Chemistry, 277 (2002) 30271-30282.
[115] R.A.F. Clark, The Molecular and Cellular Biology of Wound Repair, 2nd ed., Plenum Press, New York, 1996.
[116] S. Roy, S. Khanna, K. Nallu, T.K. Hunt, C.K. Sen, Dermal wound healing is subject to redox control, Mol Ther, 13 (2006) 211-220.
[117] J.L. Arbiser, J. Petros, R. Klafter, B. Govindajaran, E.R. McLaughlin, L.F. Brown, C. Cohen, M. Moses, S. Kilroy, R.S. Arnold, J.D. Lambeth, Reactive oxygen generated by Nox1 triggers the angiogenic switch, Proc Natl Acad Sci U S A, 99 (2002) 715-720.
[118] X.Z. West, N.L. Malinin, A.A. Merkulova, M. Tischenko, B.A. Kerr, E.C. Borden, E.A. Podrez, R.G. Salomon, T.V. Byzova, Oxidative stress induces angiogenesis by activating TLR2 with novel endogenous ligands, Nature, 467 (2010) 972-976.
[119] H. Kamencic, R.W. Griebel, A.W. Lyon, P.G. Paterson, B.H.J. Juurlink, Promoting glutathione synthesis after spinal cord trauma decreases secondary damage and promotes retention of function, Faseb J, 15 (2001) 243-250.
[120] A. Shukla, A.M. Rasik, G.K. Patnaik, Depletion of reduced glutathione, ascorbic acid, vitamin E and antioxidant defence enzymes in a healing cutaneous wound, Free Radical Res, 26 (1997) 93-101.
[121] A.M. Rasik, A. Shukla, Antioxidant status in delayed healing type of wounds, Int J Exp Pathol, 81 (2000) 257-263.
[122] B.P. Mudge, C. Harris, R.R. Gilmont, B.S. Adamson, R.S. Rees, Role of glutathione redox dysfunction in diabetic wounds, Wound Repair Regen, 10 (2002) 52-58.
[123] A. Gupta, R.L. Singh, R. Raghubir, Antioxidant status during cutaneous wound healing in immunocompromised rats, Molecular and Cellular Biochemistry, 241 (2002) 1-7.
[124] B. Adamson, D. Schwarz, P. Klugston, R. Gilmont, L. Perry, J. Fisher, W. Lindblad, R. Rees, Delayed repair: The role of glutathione in a rat incisional wound model, J Surg Res, 62 (1996) 159-164.
[125] R.S. Rees, D.J. Smith, B. Adamson, M. Im, D. Hinshaw, Oxidant Stress - the Role of the Glutathione Redox Cycle in Skin Preconditioning, J Surg Res, 58 (1995) 395-400.
[126] E.J. Levy, M.E. Anderson, A. Meister, Transport of Glutathione Diethyl Ester into Human-Cells, Proceedings of the National Academy of Sciences of the United States of America, 90 (1993) 9171-9175.
[127] M. Musalmah, M.Y. Nizrana, A.H. Fairuz, A.H. NoorAini, A.L. Azian, M.T. Gapor, W.Z.W. Ngah, Comparative effects of palm vitamin E and alpha-tocopherol on healing and wound tissue antioxidant enzyme levels in diabetic rats, Lipids, 40 (2005) 575-580.
[128] W.M. Ringsdorf, Jr., E. Cheraskin, Vitamin C and human wound healing, Oral Surg Oral Med Oral Pathol, 53 (1982) 231-236.
[129] C.C. Lima, A.P.C. Pereira, J.R.F. Silva, L.S. Oliveira, M.C.C. Resck, C.O. Grechi, M.T.C.P. Bernardes, F.M.P. Olimpio, A.M.M. Santos, E.K. Incerpi, J.A.D. Garcia, Ascorbic acid for the healing of skin wounds in rats, Braz J Biol, 69 (2009) 1195-1201.
[130] D. Chan, S.R. Lamande, W.G. Cole, J.F. Bateman, Regulation of procollagen synthesis and processing during ascorbate-induced extracellular matrix accumulation in vitro, Biochem J, 269 (1990) 175-181.
[131] T.L. Duarte, M.S. Cooke, G.D. Jones, Gene expression profiling reveals new protective roles for vitamin C in human skin cells, Free radical biology & medicine, 46 (2009) 78-87.
[132] R.L. Thangapazham, A. Sharma, R.K. Maheshwari, Beneficial role of curcumin in skin diseases, Adv Exp Med Biol, 595 (2007) 343-357.

[133] R. Madhyastha, H. Madhyastha, Y. Nakajima, S. Omura, M. Maruyama, Curcumin Facilitates Fibrinolysis and Cellular Migration during Wound Healing by Modulating Urokinase Plasminogen Activator Expression, Pathophysiol Haemost Thromb, (2010).
[134] S.K. Biswas, D. McClure, L.A. Jimenez, I.L. Megson, I. Rahman, Curcumin induces glutathione biosynthesis and inhibits NF-kappa B activation and interleukin-8 release in alveolar epithelial cells: Mechanism of free radical scavenging activity, Antioxid Redox Sign, 7 (2005) 32-41.
[135] M.G. Traber, Podda, M., Weber, C., Yan, L.J., Packer L., Diet Derived and Topically Applied Tocotrienols Accumulate in Skin and Protect the Tissue Against UV-Induced Oxidative Stress, Asia Pac. J. Clin. Nutr., 6 (1997) 63-67.
[136] E. Serbinova, V. Kagan, D. Han, L. Packer, Free-Radical Recycling and Intramembrane Mobility in the Antioxidant Properties of Alpha-Tocopherol and Alpha-Tocotrienol, Free Radical Bio Med, 10 (1991) 263-275.
[137] Y. Suzuki, M. Tsuchiya, S.R. Wassall, Y.M. Choo, G. Govil, V.E. Kagan, L. Packer, Structural and Dynamic Membrane-Properties of Alpha-Tocopherol and Alpha-Tocotrienol - Implication to the Molecular Mechanism of Their Antioxidant Potency, Biochemistry-Us, 32 (1993) 10692-10699.
[138] D. Altavilla, M. Galeano, A. Bitto, L. Minutoli, G. Squadrito, P. Seminara, F.S. Venuti, V. Torre, M. Calo, M. Colonna, P. Lo Cascio, G. Giugliano, N. Scuderi, C. Mioni, S. Leone, F. Squadrito, Lipid peroxidation inhibition by raxofelast improves angiogenesis and wound healing in experimental burn wounds, Shock, 24 (2005) 85-91.
[139] D. Altavilla, A. Saitta, D. Cucinotta, M. Galeano, B. Deodato, M. Colonna, V. Torre, G. Russo, A. Sardella, G. Urna, G.M. Campo, V. Cavallari, G. Squadrito, F. Squadrito, Inhibition of lipid peroxidation restores impaired vascular endothelial growth factor expression and stimulates wound healing and angiogenesis in the genetically diabetic mouse, Diabetes, 50 (2001) 667-674.
[140] A.J. Ruby, G. Kuttan, K.D. Babu, K.N. Rajasekharan, R. Kuttan, Antitumor and Antioxidant Activity of Natural Curcuminoids, Cancer Lett, 94 (1995) 79-83.
[141] A.B. Kunnumakkara, P. Anand, B.B. Aggarwal, Curcumin inhibits proliferation, invasion, angiogenesis and metastasis of different cancers through interaction with multiple cell signaling proteins, Cancer Lett, 269 (2008) 199-225.
[142] R.K. Maheshwari, A.K. Singh, J. Gaddipati, R.C. Srimal, Multiple biological activities of curcumin: a short review, Life Sci, 78 (2006) 2081-2087.
[143] M. Panchatcharam, S. Miriyala, V.S. Gayathri, L. Suguna, Curcumin improves wound healing by modulating collagen and decreasing reactive oxygen species, Molecular and Cellular Biochemistry, 290 (2006) 87-96.
[144] G.S. Sidhu, A.K. Singh, D. Thaloor, K.K. Banaudha, G.K. Patnaik, R.C. Srimal, R.K. Maheshwari, Enhancement of wound healing by curcumin in animals, Wound Repair Regen, 6 (1998) 167-177.
[145] G.S. Sidhu, H. Mani, J.P. Gaddipati, A.K. Singh, P. Seth, K.K. Banaudha, G.K. Patnaik, R.K. Maheshwari, Curcumin enhances wound healing in streptozotocin induced diabetic rats and genetically diabetic mice, Wound Repair Regen, 7 (1999) 362-374.
[146] B.J. Faler, R.A. Macsata, D. Plummer, L. Mishra, A.N. Sidawy, Transforming growth factor-beta and wound healing, Perspect Vasc Surg Endovasc Ther, 18 (2006) 55-62.
[147] J. Gailit, M.P. Welch, R.A. Clark, TGF-beta 1 stimulates expression of keratinocyte integrins during re-epithelialization of cutaneous wounds, Journal of Investigative Dermatology, 103 (1994) 221-227.

[148] P.F. Choong, A.P. Nadesapillai, Urokinase plasminogen activator system: a multifunctional role in tumor progression and metastasis, Clin Orthop Relat Res, (2003) S46-58.
[149] G.C. Jagetia, G.K. Rajanikant, M.S. Baliga, K.V. Rao, P. Kumar, Augmentation of wound healing by ascorbic acid treatment in mice exposed to gamma-radiation, Int J Radiat Biol, 80 (2004) 347-354.
[150] B. Peterkofsky, Ascorbate requirement for hydroxylation and secretion of procollagen: relationship to inhibition of collagen synthesis in scurvy, Am J Clin Nutr, 54 (1991) 1135S-1140S.
[151] K. Gomathi, D. Gopinath, M. Rafiuddin Ahmed, R. Jayakumar, Quercetin incorporated collagen matrices for dermal wound healing processes in rat, Biomaterials, 24 (2003) 2767-2772.
[152] O. Senel, O. Cetinkale, G. Ozbay, F. Ahcioglu, R. Bulan, Oxygen free radicals impair wound healing in ischemic rat skin, Ann Plast Surg, 39 (1997) 516-523.
[153] M. Abdelmalek, J. Spencer, Retinoids and wound healing, Dermatol Surg, 32 (2006) 1219-1230.
[154] S. Chigurupati, M.R. Mughal, S.L. Chan, T.V. Arumugam, A. Baharani, S.C. Tang, Q.S. Yu, H.W. Holloway, R. Wheeler, S. Poosala, N.H. Greig, M.P. Mattson, A synthetic uric acid analog accelerates cutaneous wound healing in mice, PLoS One, 5 (2010) e10044.
[155] Y. Iuchi, D. Roy, F. Okada, N. Kibe, S. Tsunoda, S. Suzuki, M. Takahashi, H. Yokoyama, J. Yoshitake, S. Kondo, J. Fujii, Spontaneous skin damage and delayed wound healing in SOD1-deficient mice, Molecular and Cellular Biochemistry, 341 (2010) 181-194.
[156] H. Steiling, B. Munz, S. Werner, M. Brauchle, Different types of ROS-scavenging enzymes are expressed during cutaneous wound repair, Exp Cell Res, 247 (1999) 484-494.
[157] H. Bayir, V.E. Kagan, R.S. Clark, K. Janesko-Feldman, R. Rafikov, Z. Huang, X. Zhang, V. Vagni, T.R. Billiar, P.M. Kochanek, Neuronal NOS-mediated nitration and inactivation of manganese superoxide dismutase in brain after experimental and human brain injury, Journal of Neurochemistry, 101 (2007) 168-181.
[158] E. Pigeolet, P. Corbisier, A. Houbion, D. Lambert, C. Michiels, M. Raes, M.D. Zachary, J. Remacle, Glutathione peroxidase, superoxide dismutase, and catalase inactivation by peroxides and oxygen derived free radicals, Mech Ageing Dev, 51 (1990) 283-297.
[159] A. Alacam, O. Tulunoglu, T. Oygur, S. Bilici, Effects of topical Catalase application on dental pulp tissue: a histopathological evaluation, J Dent, 28 (2000) 333-339.
[160] D.J. Ceradini, D. Yao, R.H. Grogan, M.J. Callaghan, D. Edelstein, M. Brownlee, G.C. Gurtner, Decreasing intracellular superoxide corrects defective ischemia-induced new vessel formation in diabetic mice, Journal of Biological Chemistry, 283 (2008) 10930-10938.
[161] J.D. Luo, Y.Y. Wang, W.L. Fu, J. Wu, A.F. Chen, Gene therapy of endothelial nitric oxide synthase and manganese superoxide dismutase restores delayed wound healing in type 1 diabetic mice, Circulation, 110 (2004) 2484-2493.
[162] A. Kumin, C. Huber, T. Rulicke, E. Wolf, S. Werner, Peroxiredoxin 6 is a potent cytoprotective enzyme in the epidermis, Am J Pathol, 169 (2006) 1194-1205.
[163] M. Schafer, S. Werner, Oxidative stress in normal and impaired wound repair, Pharmacol Res, 58 (2008) 165-171.
[164] E.J. Marrotte, D.D. Chen, J.S. Hakim, A.F. Chen, Manganese superoxide dismutase expression in endothelial progenitor cells accelerates wound healing in diabetic mice, J Clin Invest, 120 (2010) 4207-4219.
[165] C.K. Sen, S. Khanna, B.M. Babior, T.K. Hunt, E.C. Ellison, S. Roy, Oxidant-induced vascular endothelial growth factor expression in human keratinocytes and cutaneous wound healing, Journal of Biological Chemistry, 277 (2002) 33284-33290.
[166] J. Grzenkowicz-Wydra, J. Cisowski, J. Nakonieczna, A. Zarebski, N. Udilova, H. Nohl, A. Jozkowicz, A. Podhajska, J. Dulak, Gene transfer of CuZn superoxide dismutase enhances the

synthesis of vascular endothelial growth factor, Molecular and Cellular Biochemistry, 264 (2004) 169-181.
[167] M. Ushio-Fukai, R.W. Alexander, Reactive oxygen species as mediators of angiogenesis signaling - Role of NAD(P)H oxidase, Molecular and Cellular Biochemistry, 264 (2004) 85-97.
[168] A. Kumin, M. Schaefer, N. Epp, P. Bugnon, C. Born-Berclaz, A. Oxenius, A. Klippel, W. Bloch, S. Werner, Peroxiredoxin 6 is required for blood vessel integrity in wounded skin, J Cell Biol, 179 (2007) 747-760.
[169] U. auf dem Keller, A. Kumin, S. Braun, S. Werner, Reactive oxygen species and their detoxification in healing skin wounds, J Invest Derm Symp P, 11 (2006) 106-111.
[170] B. Munz, S. Frank, G. Hubner, E. Olsen, S. Werner, A novel type of glutathione peroxidase: expression and regulation during wound repair, Biochem J, 326 (Pt 2) (1997) 579-585.
[171] X. Wang, S.A. Phelan, K. Forsman-Semb, E.F. Taylor, C. Petros, A. Brown, C.P. Lerner, B. Paigen, Mice with targeted mutation of peroxiredoxin 6 develop normally but are susceptible to oxidative stress, Journal of Biological Chemistry, 278 (2003) 25179-25190.
[172] C. Wicke, B. Halliday, D. Allen, N.S. Roche, H. Scheuenstuhl, M.M. Spencer, A.B. Roberts, T.K. Hunt, Effects of steroids and retinoids on wound healing, Arch Surg-Chicago, 135 (2000) 1265-1270.
[173] E. Hood, E. Simone, P. Wattamwar, T. Dziubla, V. Muzykantov, Nanocarriers for vascular delivery of antioxidants, Nanomedicine (Lond), 6 (2011) 1257-1272.
[174] D. Gopinath, M.R. Ahmed, K. Gomathi, K. Chitra, P.K. Sehgal, R. Jayakumar, Dermal wound healing processes with curcumin incorporated collagen films, Biomaterials, 25 (2004) 1911-1917.
[175] J.G. Merrell, S.W. McLaughlin, L. Tie, C.T. Laurencin, A.F. Chen, L.S. Nair, Curcumin-loaded poly(epsilon-caprolactone) nanofibres: Diabetic wound dressing with anti-oxidant and anti-inflammatory properties, Clin Exp Pharmacol P, 36 (2009) 1149-1156.
[176] O. Suwantong, P. Opanasopit, U. Ruktanonchal, P. Supaphol, Electrospun cellulose acetate fiber mats containing curcumin and release characteristic of the herbal substance, Polymer, 48 (2007) 7546-7557.
[177] A. Chiumiento, S. Lamponi, R. Barbucci, A. Dominguez, Y. Perez, R. Villalonga, Immobilizing Cu,Zn-superoxide dismutase in hydrogels of carboxymethylcellulose improves its stability and wound healing properties, Biochemistry-Moscow+, 71 (2006) 1324-1328.
[178] W.Y.J. Kao, K.R. Kleinbeck, L.D. Faucher, Biomaterials modulate interleukin-8 and other inflammatory proteins during reepithelialization in cutaneous partial-thickness wounds in pigs, Wound Repair Regen, 18 (2010) 486-498.
[179] W.W. Jiang, S.H. Su, R.C. Eberhart, L.P. Tang, Phagocyte responses to degradable polymers, J Biomed Mater Res A, 82A (2007) 492-497.
[180] W. Geurtsen, F. Lehmann, W. Spahl, G. Leyhausen, Cytotoxicity of 35 dental resin composite monomers/additives in permanent 3T3 and three human primary fibroblast cultures, J Biomed Mater Res, 41 (1998) 474-480.
[181] M. Lefeuvre, W. Amjaad, M. Goldberg, L. Stanislawski, TEGDMA induces mitochondrial damage and oxidative stress in human gingival fibroblasts, Biomaterials, 26 (2005) 5130-5137.
[182] M.C. Serrano, R. Pagani, J. Pena, M.T. Portoles, Transitory oxidative stress in L929 fibroblasts cultured on poly(epsilon-caprolactone) films, Biomaterials, 26 (2005) 5827-5834.
[183] C. Fleming, A. Maldjian, D. Da Costa, A.K. Rullay, D.M. Haddleton, J.S. John, P. Penny, R.C. Noble, N.R. Cameron, B.G. Davis, A carbohydrate-antioxidant hybrid polymer reduces oxidative damage in spermatozoa and enhances fertility, Nat Chem Biol, 1 (2005) 270-274.

[184] U.G. Spizzirri, F. Iemma, F. Puoci, G. Cirillo, M. Curcio, O.I. Parisi, N. Picci, Synthesis of Antioxidant Polymers by Grafting of Gallic Acid and Catechin on Gelatin, Biomacromolecules, 10 (2009) 1923-1930.
[185] Y.Z. Wang, A. Singh, P. Xu, M.A. Pindrus, D.J. Blasioli, D.L. Kaplan, Expansion and osteogenic differentiation of bone marrow-derived mesenchymal stem cells on a vitamin C functionalized polymer, Biomaterials, 27 (2006) 3265-3273.
[186] S.R. Williams, B.S. Lepene, C.D. Thatcher, T.E. Long, Synthesis and Characterization of Poly(ethylene glycol)-Glutathione Conjugate Self-Assembled Nanoparticles for Antioxidant Delivery, Biomacromolecules, 10 (2009) 155-161.
[187] K. Udipi, R.L. Ornberg, K.B. Thurmond, S.L. Settle, D. Forster, D. Riley, Modification of inflammatory response to implanted biomedical materials in vivo by surface bound superoxide dismutase mimics, J Biomed Mater Res, 51 (2000) 549-560.
[188] N. Tsukimura, M. Yamada, H. Aita, N. Hori, F. Yoshino, M.C.I. Lee, K. Kimoto, A. Jewett, T. Ogawa, N-acetyl cysteine (NAC)-mediated detoxification and functionalization of poly(methyl methacrylate) bone cement, Biomaterials, 30 (2009) 3378-3389.
[189] B.D. Ratner, Biomaterials science : an introduction to materials in medicine, 2nd ed., Elsevier Academic Press, Amsterdam ; Boston, 2004.
[190] D.F. Williams, Definitions in biomaterials, Elsevier, Amsterdam, 1987.
[191] D.F. Williams, On the mechanisms of biocompatibility, Biomaterials, 29 (2008) 2941-2953.
[192] L.A. Matheson, J.P. Santerre, R.S. Labow, Changes in macrophage function and morphology due to biomedical polyurethane surfaces undergoing biodegradation, J Cell Physiol, 199 (2004) 8-19.
[193] M.S. Shive, J.M. Anderson, Biodegradation and biocompatibility of PLA and PLGA microspheres, Adv Drug Deliv Rev, 28 (1997) 5-24.
[194] R. Langer, K. Fu, D.W. Pack, A.M. Klibanov, Visual evidence of acidic environment within degrading poly(lactic-co-glycolic acid) (PLGA) microspheres, Pharmaceut Res, 17 (2000) 100-106.
[195] J.H. Jeng, M.C. Chang, L.I. Chen, C.P. Chan, J.J. Lee, T.M. Wang, T.T. Yang, P.S. Lin, H.J. Lin, H.H. Chang, The role of reactive oxygen species and hemeoxygenase-1 expression in the cytotoxicity, cell cycle alteration and apoptosis of dental pulp cells induced by BisGMA, Biomaterials, 31 (2010) 8164-8171.
[196] J.H. Jeng, H.H. Chang, M.K. Guo, F.H. Kasten, M.C. Chang, G.F. Huang, Y.L. Wang, R.S. Wang, Stimulation of glutathione depletion, ROS production and cell cycle arrest of dental pulp cells and gingival epithelial cells by HEMA, Biomaterials, 26 (2005) 745-753.
[197] J.H. Jeng, M.C. Chang, L.D. Lin, C.P. Chan, H.H. Chang, L.I. Chen, H.J. Lin, H.W. Yeh, W.Y. Tseng, P.S. Lin, C.C. Lin, The effect of BisGMA on cyclooxygenase-2 expression, PGE(2) production and cytotoxicity via reactive oxygen species- and MEK/ERK-dependent and -independent pathways, Biomaterials, 30 (2009) 4070-4077.
[198] W.E. Liu, M.L. Ma, K.M. Bratlie, T.T. Dang, R. Langer, D.G. Anderson, Real-time in vivo detection of biomaterial-induced reactive oxygen species, Biomaterials, 32 (2011) 1796-1801.
[199] S.S. Kaplan, R.E. Basford, E. Mora, M.H. Jeong, R.L. Simmons, Biomaterial-Induced Alterations of Neutrophil Superoxide Production, J Biomed Mater Res, 26 (1992) 1039-1051.
[200] V.R. Muzykantov, Targeting of superoxide dismutase and catalase to vascular endothelium, J Control Release, 71 (2001) 1-21.
[201] S. Rangaswamy, M.S. Penn, G.M. Saidel, G.M. Chisolm, Exogenous oxidized low-density lipoprotein injures and alters the barrier function of endothelium in rats in vivo, Circ Res, 80 (1997) 37-44.
[202] C.A. Papaharalambus, K.K. Griendling, Basic mechanisms of oxidative stress and reactive oxygen species in cardiovascular injury, Trends Cardiovasc Med, 17 (2007) 48-54.

[203] W.A. Skinner, Parkhurs.Rm, Oxidation Products of Vitamin E and Its Model 6-Hydroxy-2,2,5,7,8-Pentamethylchroman .8. Oxidation with Benzoyl Peroxide, Journal of Organic Chemistry, 31 (1966) 1248-&.
[204] D. Villano, M.S. Fernandez-Pachon, M.L. Moya, A.M. Troncoso, M.C. Garcia-Parrilla, Radical scavenging ability of polyphenolic compounds towards DPPH free radical, Talanta, 71 (2007) 230-235.
[205] S. Muro, X. Cui, C. Gajewski, J.C. Murciano, V.R. Muzykantov, M. Koval, Slow intracellular trafficking of catalase nanoparticles targeted to ICAM-1 protects endothelial cells from oxidative stress, Am J Physiol Cell Physiol, 285 (2003) C1339-1347.
[206] T.D. Dziubla, A. Karim, V.R. Muzykantov, Polymer nanocarriers protecting active enzyme cargo against proteolysis, Journal of Controlled Release, 102 (2005) 427-439.
[207] L.M. Hoesel, M.A. Flierl, A.D. Niederbichler, D. Rittirsch, S.D. Mcclintock, J.S. Reuben, M.J. Pianko, W. Stone, H.S. Yang, M. Smith, J.V. Sarma, P.A. Ward, Ability of antioxidant liposomes to prevent acute and progressive pulmonary injury, Antioxid Redox Sign, 10 (2008) 973-981.
[208] J. Sinha, N. Das, M.K. Basu, Liposomal antioxidants in combating ischemia-reperfusion injury in rat brain, Biomedicine & Pharmacotherapy, 55 (2001) 264-271.
[209] T. Yao, S.D. Esposti, L. Huang, R. Arnon, A. Spangenberger, M.A. Zern, Inhibition of Carbon Tetrachloride-Induced Liver-Injury by Liposomes Containing Vitamin-E, American Journal of Physiology, 267 (1994) G476-G484.
[210] J. Kristl, K. Teskac, C. Caddeo, Z. Abramovic, M. Sentjurc, Improvements of cellular stress response on resveratrol in liposomes, European Journal of Pharmaceutics and Biopharmaceutics, 73 (2009) 253-259.
[211] T.H. Marczylo, R.D. Verschoyle, D.N. Cooke, P. Morazzoni, W.P. Steward, A.J. Gescher, Comparison of systemic availability of curcumin with that of curcumin formulated with phosphatidylcholine, Cancer Chemotherapy and Pharmacology, 60 (2007) 171-177.
[212] B.W. Qi, Y.L. Zhao, X. Wei, W.J. Xiao, H. Zheng, Z.Z. Chen, X.M. Duan, X. Zhao, Y.Q. Wei, L.J. Chen, A further investigation concerning correlation between anti-fibrotic effect of liposomal quercetin and inflammatory cytokines in pulmonary fibrosis, European Journal of Pharmacology, 642 (2010) 134-139.
[213] H. Aoki, M. Fujita, C.Q. Sun, K. Fuji, K. Miyajima, High-efficiency entrapment of superoxide dismutase into cationic liposomes containing synthetic aminoglycolipid, Chemical & Pharmaceutical Bulletin, 45 (1997) 1327-1331.
[214] F. Zhou, B.T. Rouse, L. Huang, An Improved Method of Loading Ph-Sensitive Liposomes with Soluble-Proteins for Class-I Restricted Antigen Presentation, Journal of Immunological Methods, 145 (1991) 143-152.
[215] R.G. Rengel, K. Barisic, Z. Pavelic, T.Z. Grubisic, I. Cepelak, J. Filipovic-Grcic, High efficiency entrapment of superoxide dismutase into mucoadhesive chitosan-coated liposomes, European Journal of Pharmaceutical Sciences, 15 (2002) 441-448.
[216] R.G. Rengel, J. Filipovic-Grcic, I. Cepelak, T. Zanic-Grubisic, K. Barisic, The effect of liposomes with superoxide dismutase on A2182 cells, European Journal of Pharmaceutics and Biopharmaceutics, 60 (2005) 47-51.
[217] M.P. Lupo, Antioxidants and vitamins in cosmetics, Clinics in Dermatology, 19 (2001) 467-473.
[218] Y. Barenholz, Liposome application: problems and prospects, Current Opinion in Colloid & Interface Science, 6 (2001) 66-77.
[219] T. Boulikas, Clinical overview on Lipoplatin (TM): a successful liposomal formulation of cisplatin, Expert Opinion on Investigational Drugs, 18 (2009) 1197-1218.

[220] M. Spina, E. Chimienti, F. Martellotta, E. Vaccher, M. Berretta, E. Zanet, A. Lleshi, V. Canzonieri, P. Bulian, U. Tirelli, Phase 2 Study of Intrathecal, Long-Acting Liposomal Cytarabine in the Prophylaxis of Lymphomatous Meningitis in Human Immunodeficiency Virus-Related Non-Hodgkin Lymphoma, Cancer, 116 (2010) 1495-1501.
[221] M. Rawat, D. Singh, S. Saraf, S. Saraf, Lipid carriers: A versatile delivery vehicle for proteins and peptides, Yakugaku Zasshi-Journal of the Pharmaceutical Society of Japan, 128 (2008) 269-280.
[222] M.M. Gaspar, O.C. Boerman, P. Laverman, M.L. Corvo, G. Storm, M.E.M. Cruz, Enzymosomes with surface-exposed superoxide dismutase: In vivo behaviour and therapeutic activity in a model of adjuvant arthritis, Journal of Controlled Release, 117 (2007) 186-195.
[223] R.H. Muller, M. Radtke, S.A. Wissing, Solid lipid nanoparticles (SLN) and nanostructured lipid carriers (NLC) in cosmetic and dermatological preparations, Adv Drug Deliv Rev, 54 Suppl 1 (2002) S131-155.
[224] E.K. Noriega-Pelaez, N. Mendoza-Munoz, A. Ganem-Quintanar, D. Quintanar-Guerrero, Optimization of the emulsification and solvent displacement method for the preparation of solid lipid nanoparticles, Drug Dev Ind Pharm, 37 (2011) 6.
[225] S. Trombino, R. Cassano, R. Muzzalupo, A. Pingitore, E. Cione, N. Picci, Stearyl ferulate-based solid lipid nanoparticles for the encapsulation and stabilization of beta-carotene and alpha-tocopherol, Colloids and Surfaces B-Biointerfaces, 72 (2009) 181-187.
[226] J.P. Jee, S.J. Lim, J.S. Park, C.K. Kim, Stabilization of all-trans retinol by loading lipophilic antioxidants in solid lipid nanoparticles, Eur J Pharm Biopharm, 63 (2006) 134-139.
[227] H. Li, X. Zhao, Y. Ma, G. Zhai, L. Li, H. Lou, Enhancement of gastrointestinal absorption of quercetin by solid lipid nanoparticles, Journal of Controlled Release, 133 (2009) 238-244.
[228] Z. Liu, X. Zhang, H. Wu, J. Li, L. Shu, R. Liu, L. Li, N. Li, Preparation and evaluation of solid lipid nanoparticles of baicalin for ocular drug delivery system in vitro and in vivo, Drug Dev Ind Pharm, 37 (2011) 7.
[229] K. Teskac, J. Kristl, The evidence for solid lipid nanoparticles mediated cell uptake of resveratrol, Int J Pharm, 390 61-69.
[230] W. Tiyaboonchai, W. Tungpradit, P. Plianbangchang, Formulation and characterization of curcuminoids loaded solid lipid nanoparticles, Int J Pharm, 337 (2007) 299-306.
[231] T.D. Dziubla, V.V. Shuvaev, N.K. Hong, B.J. Hawkins, M. Madesh, H. Takano, E. Simone, M.T. Nakada, A. Fisher, S.M. Albelda, V.R. Muzykantov, Endothelial targeting of semi-permeable polymer nanocarriers for enzyme therapies, Biomaterials, 29 (2008) 215-227.
[232] S. Freiberg, X. Zhu, Polymer microspheres for controlled drug release, International Journal of Pharmaceutics, 282 (2004) 1-18.
[233] F. Mohamed, C.F. van der Walle, Engineering biodegradable polyester particles with specific drug targeting and drug release properties, Journal of Pharmaceutical Sciences, 97 (2008) 71-87.
[234] K. Avgoustakis, A. Beletsi, Z. Panagi, P. Klepetsanis, A.G. Karydas, D.S. Ithakissios, PLGA-mPEG nanoparticles of cisplatin: in vitro nanoparticle degradation, in vitro drug release and in Vivo drug residence in blood properties, Journal of Controlled Release, 79 (2002) 123-135.
[235] G. Gaucher, M.H. Dufresne, V.P. Sant, N. Kang, D. Maysinger, J.C. Leroux, Block copolymer micelles: preparation, characterization and application in drug delivery, Journal of Controlled Release, 109 (2005) 169-188.
[236] J. Matsumoto, Y. Nakada, K. Sakurai, T. Nakamura, Y. Takahashi, Preparation of nanoparticles consisted of poly(L-lactide)-poly(ethylene glycol)-poly(L-lactide) and their evaluation in vitro, International Journal of Pharmaceutics, 185 (1999) 93-101.

[237] E.A. Simone, T.D. Dziubla, F. Colon-Gonzalez, D.E. Discher, V.R. Muzykantov, Effect of polymer amphiphilicity on loading of a therapeutic enzyme onto protective fulamentous and spherical polymer nanocarrlers, Biomacromolecules, 8 (2007) 3914-3921.
[238] B.M. Discher, Y.Y. Won, D.S. Ege, J.C.M. Lee, F.S. Bates, D.E. Discher, D.A. Hammer, Polymersomes: Tough vesicles made from diblock copolymers, Science, 284 (1999) 1143-1146.
[239] D.E. Discher, A. Eisenberg, Polymer vesicles, Science, 297 (2002) 967-973.
[240] D.A. Christian, S. Cai, D.M. Bowen, Y. Kim, J.D. Pajerowski, D.E. Discher, Polymersome carriers: From self-assembly to siRNA and protein therapeutics, European Journal of Pharmaceutics and Biopharmaceutics, 71 (2009) 463-474.
[241] P.J. Photos, L. Bacakova, B. Discher, F.S. Bates, D.E. Discher, Polymer vesicles in vivo: correlations with PEG molecular weight, Journal of Controlled Release, 90 (2003) 323-334.
[242] F. Ahmed, R.I. Pakunlu, A. Brannan, F. Bates, T. Minko, D.E. Discher, Biodegradable polymersomes loaded with both paclitaxel and doxorubicin permeate and shrink tumors, inducing apoptosis in proportion to accumulated drug, Journal of Controlled Release, 116 (2006) 150-158.
[243] S.L. Li, B. Byrne, J. Welsh, A.F. Palmer, Self-assembled poly(butadiene)-b-poly(ethylene oxide) polymersomes as paclitaxel carriers, Biotechnology Progress, 23 (2007) 278-285.
[244] F. Ahmed, D.E. Discher, Self-porating polymersomes of PEG-PLA and PEG-PCL: hydrolysis-triggered controlled release vesicles, Journal of Controlled Release, 96 (2004) 37-53.
[245] E. Simone, B.S. Ding, V. Muzykantov, Targeted delivery of therapeutics to endothelium, Cell and Tissue Research, 335 (2009) 283-300.
[246] M. Yan, J.J. Du, Z. Gu, M. Liang, Y.F. Hu, W.J. Zhang, S. Priceman, L.L. Wu, Z.H. Zhou, Z. Liu, T. Segura, Y. Tang, Y.F. Lu, A novel intracellular protein delivery platform based on single-protein nanocapsules, Nature Nanotechnology, 5 (2010) 48-53.
[247] D. Kim, E. Kim, J. Kim, K.M. Park, K. Baek, M. Jung, Y.H. Ko, W. Sung, H.S. Kim, J.H. Suh, C.G. Park, O.S. Na, D.K. Lee, K.E. Lee, S.S. Han, K. Kim, Direct synthesis of polymer nanocapsules with a noncovalently tailorable surface, Angewandte Chemie-International Edition, 46 (2007) 3471-3474.
[248] E. Kim, D. Kim, H. Jung, J. Lee, S. Paul, N. Selvapalam, Y. Yang, N. Lim, C.G. Park, K. Kim, Facile, Template-Free Synthesis of Stimuli-Responsive Polymer Nanocapsules for Targeted Drug Delivery, Angewandte Chemie-International Edition, 49 (2010) 4405-4408.
[249] S.K. Sandur, H. Ichikawa, M.K. Pandey, A.B. Kunnumakkara, B. Sung, G. Sethi, B.B. Aggarwal, Role of pro-oxidants and antioxidants in the anti-inflammatory and apoptotic effects of curcumin (diferuloylmethane), Free radical biology & medicine, 43 (2007) 568-580.
[250] C.A. de la Lastra, I. Villegas, Resveratrol as an antioxidant and pro-oxidant agent: mechanisms and clinical implications, Biochem Soc Trans, 35 (2007) 1156-1160.
[251] P.P. Wattamwar, Hardas, S.S., Butterfield, D.A., Anderson, K.W., Dziubla, T.D., Tuning of the Pro-oxidant and Antioxidant Activity of Trolox Through the Controlled Release from Biodegradable Poly(trolox ester) Polymers, J Biomed Mater Res A, 99A (2011) 8.
[252] V. Kumar, R.K. Prud'Homme, Thermodynamic Limits on Drug Loading in Nanoparticle Cores, Journal of Pharmaceutical Sciences, 97 (2008) 4904-4914.
[253] M.M. De Villiers, P. Aramwit, G.S. Kwon, Nanotechnology in drug delivery, Springer ; AAPS Press, New York, NY and Arlington, VA, 2009.
[254] R. Gref, Y. Minamitake, M.T. Peracchia, V. Trubetskoy, V. Torchilin, R. Langer, Biodegradable long-circulating polymeric nanospheres, Science, 263 (1994) 1600-1603.
[255] G. Leonarduzzi, G. Testa, B. Sottero, P. Gamba, G. Poli, Design and development of nanovehicle-based delivery systems for preventive or therapeutic supplementation with flavonoids, Curr Med Chem, 17 (2010) 74-95.

[256] P.P. Wattamwar, Y.Q. Mo, R. Wan, R. Palli, Q.W. Zhang, T.D. Dziubla, Antioxidant Activity of Degradable Polymer Poly(trolox ester) to Suppress Oxidative Stress Injury in the Cells, Advanced Functional Materials, 20 (2010) 147-154.
[257] S.C. Yang, M. Bhide, I.N. Crispe, R.H. Pierce, N. Murthy, Polyketal copolymers: a new acid-sensitive delivery vehicle for treating acute inflammatory diseases, Bioconjug Chem, 19 (2008) 1164-1169.
[258] C. Fleming, A. Maldjian, D. Da Costa, A.K. Rullay, D.M. Haddleton, J. St John, P. Penny, R.C. Noble, N.R. Cameron, B.G. Davis, A carbohydrate-antioxidant hybrid polymer reduces oxidative damage in spermatozoa and enhances fertility, Nat Chem Biol, 1 (2005) 270-274.
[259] S.R. Williams, et al., Synthesis and Characterization of Poly(ethylene glycol)#Glutathione Conjugate Self-Assembled Nanoparticles for Antioxidant Delivery, Biomacromolecules, 10 (2009) 155-161.
[260] L. Erdmann, K.E. Uhrich, Synthesis and degradation characteristics of salicylic acid-derived poly(anhydride-esters), Biomaterials, 21 (2000) 1941-1946.
[261] E. Cadenas, G. Merenyi, J. Lind, Pulse radiolysis study of the reactivity of Trolox C phenoxyl radical with superoxide anion, Febs Lett, 253 (1989) 235-238.
[262] M.J. Davies, L.G. Forni, R.L. Willson, Vitamin E analogue Trolox C. E.s.r. and pulse-radiolysis studies of free-radical reactions, Biochem J, 255 (1988) 513-522.
[263] K.I. Priyadarsini, S. Kapoor, D.B. Naik, One- and two-electron oxidation reactions of trolox by peroxynitrite, Chem Res Toxicol, 14 (2001) 567-571.
[264] H. Wiener, C. Gilon, An Improved Method for the Catalytic Preparation of Tert-Butyl Esters of Carboxylic and Fatty-Acids, Journal of Molecular Catalysis, 37 (1986) 45-52.
[265] J.S. Moore, S.I. Stupp, Room-Temperature Polyesterification, Macromolecules, 23 (1990) 65-70.
[266] G. Aldini, K.J. Yeum, R.M. Russell, N.I. Krinsky, A method to measure the oxidizability of both the aqueous and lipid compartments of plasma, Free Radical Bio Med, 31 (2001) 1043-1050.
[267] Q. Zhang, I. Matsuzaki, S. Chatterjee, A.B. Fisher, Activation of endothelial NADPH oxidase during normoxic lung ischemia is KATP channel dependent, Am J Physiol Lung Cell Mol Physiol, 289 (2005) L954-961.
[268] H. Arai, A. Nagao, J. Terao, T. Suzuki, K. Takama, Effect of d-alpha-tocopherol analogues on lipoxygenase-dependent peroxidation of phospholipid-bile salt micelles, Lipids, 30 (1995) 135-140.
[269] Y. Pocker, M.W. Beug, Kinetic studies of bovine carbonic anhydrase catalyzed hydrolyses of para-substituted phenyl esters, Biochemistry-Us, 11 (1972) 698-707.
[270] R.P. Henry, S.J. Dodgson, R.E. Forster, B.T. Storey, Rat lung carbonic anhydrase: activity, localization, and isozymes, J Appl Physiol, 60 (1986) 638-645.
[271] W.S. Sly, P.Y. Hu, Human carbonic anhydrases and carbonic anhydrase deficiencies, Annu Rev Biochem, 64 (1995) 375-401.
[272] L.A. Matheson, J.P. Santerre, R.S. Labow, Changes in macrophage function and morphology due to biomedical polyurethane surfaces undergoing biodegradation, Journal of Cellular Physiology, 199 (2004) 8-19.
[273] W. Geurtsen, F. Lehmann, W. Spahl, G. Leyhausen, Cytotoxicity of 35 dental resin composite monomers/additives in permanent 3T3 and three human primary fibroblast cultures, J Biomed Mater Res, 41 (1998) 474-480.
[274] W.W. Jiang, S.H. Su, R.C. Eberhart, L. Tang, Phagocyte responses to degradable polymers, J Biomed Mater Res A, 82 (2007) 492-497.

[275] Y. Wang, A. Singh, P. Xu, M.A. Pindrus, D.J. Blasioli, D.L. Kaplan, Expansion and osteogenic differentiation of bone marrow-derived mesenchymal stem cells on a vitamin C functionalized polymer, Biomaterials, 27 (2006) 3265-3273.
[276] E.R. Stadtman, Protein oxidation and aging, Free Radic Res, 40 (2006) 1250-1258.
[277] H. Esterbauer, P. Ramos, Chemistry and pathophysiology of oxidation of LDL, Reviews of Physiology Biochemistry and Pharmacology, Vol 127, 127 (1996) 31-64.
[278] D.A. Butterfield, M.L.B. Lange, R. Sultana, Involvements of the lipid peroxidation product, HNE, in the pathogenesis and progression of Alzheimer's disease, Bba-Mol Cell Biol L, 1801 (2010) 924-929.
[279] J.L. Betters, D.S. Criswell, R.A. Shanely, D. Van Gammeren, D. Falk, K.C. Deruisseau, M. Deering, T. Yimlamai, S.K. Powers, Trolox attenuates mechanical ventilation-induced diaphragmatic dysfunction and proteolysis, Am J Respir Crit Care Med, 170 (2004) 1179-1184.
[280] E. Soheili Majd, M. Goldberg, L. Stanislawski, In vitro effects of ascorbate and Trolox on the biocompatibility of dental restorative materials, Biomaterials, 24 (2003) 3-9.
[281] O. Wongmekiat, K. Thamprasert, D. Lumlertgul, Renoprotective effect of trolox against ischaemia-reperfusion injury in rats, Clin Exp Pharmacol Physiol, 34 (2007) 753-759.
[282] K.M. Ko, P.K. Yick, M.K. Poon, S.P. Ip, Prooxidant and antioxidant effects of Trolox on ferric ion-induced oxidation of erythrocyte membrane lipids, Mol Cell Biochem, 141 (1994) 65-70.
[283] B. Poljsak, P. Raspor, The antioxidant and pro-oxidant activity of vitamin C and trolox in vitro: a comparative study, J Appl Toxicol, 28 (2008) 183-188.
[284] S. Tafazoli, J.S. Wright, P.J. O'Brien, Prooxidant and antioxidant activity of vitamin E analogues and troglitazone, Chem Res Toxicol, 18 (2005) 1567-1574.
[285] G.R. Buettner, The Pecking Order of Free-Radicals and Antioxidants - Lipid-Peroxidation, Alpha-Tocopherol, and Ascorbate, Archives of Biochemistry and Biophysics, 300 (1993) 535-543.
[286] R. Albertini, P.M. Abuja, Prooxidant and Antioxidant Properties of Trolox C, Analogue of Vitamin E, in Oxidation of Low-Density Lipoprotein, Free Radic Res, 30 (1998) 181-188.
[287] V.W. Bowry, R. Stocker, Tocopherol-Mediated Peroxidation - the Prooxidant Effect of Vitamin-E on the Radical-Initiated Oxidation of Human Low-Density-Lipoprotein, Journal of the American Chemical Society, 115 (1993) 6029-6044.
[288] M.J. Thomas, B.H.J. Bielski, Oxidation and Reaction of Trolox-C, a Tocopherol Analog, in Aqueous-Solution - a Pulse-Radiolysis Study, Journal of the American Chemical Society, 111 (1989) 3315-3319.
[289] V.W. Bowry, Stocker,R., Tocopherol-mediated peroxidation. The prooxidant effect of Vitamin E on the radical-initiated oxidation of human low-density lipoprotein, J. Am. Chem. Soc., 115 (1993) 6029-6044.
[290] C. Suarna, D.C. Craig, K.J. Cross, P.T. Southwellkeely, Oxidations of Vitamin-E (Alpha-Tocopherol) and Its Model-Compound 2,2,5,7,8-Pentamethyl-6-Hydroxychroman - a New Dimer, Journal of Organic Chemistry, 53 (1988) 1281-1284.
[291] D.A. Butterfield, Stadtman, E.R., Protein oxidation processes in aging brain, 1997.
[292] R. Sultana, A. Ravagna, H. Mohmmad-Abdul, V. Calabrese, D.A. Butterfield, Ferulic acid ethyl ester protects neurons against amyloid beta- peptide(1-42)-induced oxidative stress and neurotoxicity: relationship to antioxidant activity, J Neurochem, 92 (2005) 749-758.
[293] T. Xia, M. Kovochich, M. Liong, L. Madler, B. Gilbert, H.B. Shi, J.I. Yeh, J.I. Zink, A.E. Nel, Comparison of the Mechanism of Toxicity of Zinc Oxide and Cerium Oxide Nanoparticles Based on Dissolution and Oxidative Stress Properties, Acs Nano, 2 (2008) 2121-2134.
[294] R. Wan, Y.Q. Mo, X. Zhang, S.F. Chien, D.J. Tollerud, Q.W. Zhang, Matrix metalloproteinase-2 and-9 are induced differently by metal nanoparticles in human monocytes:

The role of oxidative stress and protein tyrosine kinase activation, Toxicol Appl Pharm, 233 (2008) 276-285.
[295] M.T. Zhu, W.Y. Feng, B. Wang, T.C. Wang, Y.Q. Gu, M. Wang, Y. Wang, H. Ouyang, Y.L. Zhao, Z.F. Chai, Comparative study of pulmonary responses to nano- and submicron-sized ferric oxide in rats, Toxicology, 247 (2008) 102-111.
[296] A.S. Azmi, S.H. Bhat, S.M. Hadi, Resveratrol-Cu(II) induced DNA breakage in human peripheral lymphocytes: implications for anticancer properties, Febs Lett, 579 (2005) 3131-3135.
[297] A. Banerjee, A. Kunwar, B. Mishra, K.I. Priyadarsini, Concentration dependent antioxidant/pro-oxidant activity of curcumin studies from AAPH induced hemolysis of RBCs, Chem Biol Interact, 174 (2008) 134-139.
[298] V.Z. Lankin, A.K. Tikhaze, G.G. Konovalova, A.I. Kozachenko, [Concentration inversion of the antioxidant and pro-oxidant effects of beta-carotene in tissues in vivo], Biull Eksp Biol Med, 128 (1999) 314-316.
[299] K.J. Lampe, R.M. Namba, T.R. Silverman, K.B. Bjugstad, M.J. Mahoney, Impact of Lactic Acid on Cell Proliferation and Free Radical-Induced Cell Death in Monolayer Cultures of Neural Precursor Cells, Biotechnology and Bioengineering, 103 (2009) 1214-1223.
[300] G.C. Brown, V. Borutaite, Regulation of apoptosis by the redox state of cytochrome c, Biochim Biophys Acta, 1777 (2008) 877-881.
[301] S.M. Hadi, M.F. Ullah, A.S. Azmi, A. Ahmad, U. Shamim, H. Zubair, H.Y. Khan, Resveratrol mobilizes endogenous copper in human peripheral lymphocytes leading to oxidative DNA breakage: a putative mechanism for chemoprevention of cancer, Pharm Res, 27 979-988.
[302] P. Kaur, L. Evje, M. Aschner, T. Syversen, The in vitro effects of Trolox on methylmercury-induced neurotoxicity, Toxicology, 276 73-78.
[303] C.S. Malcolm, K.R. Benwell, H. Lamb, D. Bebbington, R.H. Porter, Characterization of iodoacetate-mediated neurotoxicity in vitro using primary cultures of rat cerebellar granule cells, Free radical biology & medicine, 28 (2000) 102-107.
[304] J.C. Mayo, D.X. Tan, R.M. Sainz, M. Natarajan, S. Lopez-Burillo, R.J. Reiter, Protection against oxidative protein damage induced by metal-catalyzed reaction or alkylperoxyl radicals: comparative effects of melatonin and other antioxidants, Biochim Biophys Acta, 1620 (2003) 139-150.
[305] O. Friaa, D. Brault, Kinetics of the reaction between the antioxidant Trolox and the free radical DPPH in semi-aqueous solution, Org Biomol Chem, 4 (2006) 2417-2423.
[306] C.P. LeBel, H. Ischiropoulos, S.C. Bondy, Evaluation of the probe 2',7'-dichlorofluorescin as an indicator of reactive oxygen species formation and oxidative stress, Chem Res Toxicol, 5 (1992) 227-231.
[307] C. Rota, Y.C. Fann, R.P. Mason, Phenoxyl free radical formation during the oxidation of the fluorescent dye 2',7'-dichlorofluorescein by horseradish peroxidase. Possible consequences for oxidative stress measurements, J Biol Chem, 274 (1999) 28161-28168.
[308] J.A. Royall, H. Ischiropoulos, Evaluation of 2',7'-dichlorofluorescin and dihydrorhodamine 123 as fluorescent probes for intracellular H2O2 in cultured endothelial cells, Arch Biochem Biophys, 302 (1993) 348-355.
[309] M. Wrona, K.B. Patel, P. Wardman, The roles of thiol-derived radicals in the use of 2',7'-dichlorodihydrofluorescein as a probe for oxidative stress, Free radical biology & medicine, 44 (2008) 56-62.
[310] D. Shenoy, S. Little, R. Langer, M. Amiji, Poly(Ethylene Oxide)-Modified Poly(β-Amino Ester) Nanoparticles as a pH-Sensitive System for Tumor-Targeted Delivery of Hydrophobic Drugs: Part 2. <i>In Vivo</i> Distribution and Tumor Localization Studies, Pharmaceut Res, 22 (2005) 2107-2114.

[311] Y. Shen, H. Tang, Y. Zhan, E.A. Van Kirk, W.J. Murdoch, Degradable Poly(β-amino ester) nanoparticles for cancer cytoplasmic drug delivery, Nanomedicine : nanotechnology, biology, and medicine, 5 (2009) 192-201.
[312] H. Devalapally, D. Shenoy, S. Little, R. Langer, M. Amiji, Poly(ethylene oxide)-modified poly(beta-amino ester) nanoparticles as a pH-sensitive system for tumor-targeted delivery of hydrophobic drugs: part 3. Therapeutic efficacy and safety studies in ovarian cancer xenograft model, Cancer Chemotherapy and Pharmacology, 59 (2007) 477-484.
[313] D. Jere, C.-X. Xu, R. Arote, C.-H. Yun, M.-H. Cho, C.-S. Cho, Poly([beta]-amino ester) as a carrier for si/shRNA delivery in lung cancer cells, Biomaterials, 29 (2008) 2535-2547.
[314] D.M. Brey, I. Erickson, J.A. Burdick, Influence of macromer molecular weight and chemistry on poly(β-amino ester) network properties and initial cell interactions, J Biomed Mater Res A, 85A (2008) 731-741.
[315] J.L. Ifkovits, J.A. Burdick, Review: Photopolymerizable and Degradable Biomaterials for Tissue Engineering Applications, Tissue Engineering, 13 (2007) 2369-2385.
[316] D. Berry, D.M. Lynn, R. Sasisekharan, R. Langer, Poly(²-amino ester)s Promote Cellular Uptake of Heparin and Cancer Cell Death, Chemistry & biology, 11 (2004) 487-498.
[317] L. Brito, S. Little, R. Langer, M. Amiji, Poly(β-amino ester) and Cationic Phospholipid-Based Lipopolyplexes for Gene Delivery and Transfection in Human Aortic Endothelial and Smooth Muscle Cells, Biomacromolecules, 9 (2008) 1179-1187.
[318] A. Akinc, D.M. Lynn, D.G. Anderson, R. Langer, Parallel Synthesis and Biophysical Characterization of a Degradable Polymer Library for Gene Delivery, Journal of the American Chemical Society, 125 (2003) 5316-5323.
[319] J.-S. Lee, J.J. Green, K.T. Love, J. Sunshine, R. Langer, D.G. Anderson, Gold, Poly(β-amino ester) Nanoparticles for Small Interfering RNA Delivery, Nano Letters, 9 (2009) 2402-2406.
[320] D.G. Anderson, D.M. Lynn, R. Langer, Semi-automated synthesis and screening of a large library of degradable cationic polymers for gene delivery, Angewandte Chemie-International Edition, 42 (2003) 3153-3158.
[321] D.G. Anderson, C.A. Tweedie, N. Hossain, S.M. Navarro, D.M. Brey, K.J. Van Vliet, R. Langer, J.A. Burdick, A combinatorial library of photocrosslinkable and degradable materials, Adv Mater, 18 (2006) 2614-+.
[322] A.M. Hawkins, T.A. Milbrandt, D.A. Puleo, J.Z. Hilt, Synthesis and analysis of degradation, mechanical and toxicity properties of poly([beta]-amino ester) degradable hydrogels, Acta Biomaterialia, 7 (2011) 1956-1964.
[323] C.G. Williams, A.N. Malik, T.K. Kim, P.N. Manson, J.H. Elisseeff, Variable cytocompatibility of six cell lines with photoinitiators used for polymerizing hydrogels and cell encapsulation, Biomaterials, 26 (2005) 1211-1218.
[324] R.A. Scott, N.A. Peppas, Highly crosslinked, PEG-containing copolymers for sustained solute delivery (vol 20, pg 1371, 1999), Biomaterials, 21 (2000) 863-863.
[325] N.A. Peppas, J.H. Ward, Preparation of controlled release systems by free-radical UV polymerizations in the presence of a drug, Journal of Controlled Release, 71 (2001) 183-192.
[326] D. Biswal, P.P. Wattamwar, T.D. Dziubla, J.Z. Hilt, A single-step polymerization method for poly(β-amino ester) biodegradable hydrogels, Polymer, 52 (2011) 5985-5992.
[327] R.A. Frimpong, S. Fraser, J. Zach Hilt, Synthesis and temperature response analysis of magnetic-hydrogel nanocomposites, J Biomed Mater Res A, 80A (2007) 1-6.
[328] J. Brandrup, E.H. Immergut, E.A. Grulke, Polymer handbook. 4th ed, John Wiley, New York, 1999.

[329] D.W.V. Krevelen, Properties of polymers: their correlation with chemical structure, their numerical estimation and prediction from additive group contributions, Elsevier. xxii, Amsterdam, New York, 1990.

, A. Güner, Solubility profiles of poly(ethylene glycol)/solvent systems. II. comparison of thermodynamic parameters from viscosity measurements, Journal of Applied Polymer Science, 117 (2010) 1100-1119.

[331] D. Biswal, P.P. Wattamwar, T.D. Dziubla, J.Z. Hilt, Characterization of poly(β–amino ester) degradation in alcohols (to be Submitted).

[332] D.M. Brey, J.L. Ifkovits, R.I. Mozia, J.S. Katz, J.A. Burdick, Controlling poly([beta]-amino ester) network properties through macromer branching, Acta Biomaterialia, 4 (2008) 207-217.

[333] C.J. Boudreaux, W.C. Bunyard, C.L. McCormick, Controlled activity polymers .8. Copolymers of acrylic acid and isomeric N-akylacrylamide with pendent beta-naphthol esters moieties: Synthesis and characterization, Journal of Controlled Release, 40 (1996) 223-233.

[334] P.P. Wattamwar, S. Hardas, D.A. Butterfield, K.W. Anderson, T.D. Dziubla, Tuning of the Pro-oxidant and Antioxidant Activity of Trolox Through the Controlled Release from Biodegradable Poly(trolox ester) Polymers, J Biomed Mater Res A, (In Press).

[335] N. Li, J.H. Liu, J. Zhang, B.Y. Yu, Comparative evaluation of cytotoxicity and antioxidative activity of 20 flavonoids, J Agr Food Chem, 56 (2008) 3876-3883.

[336] M. Matsuo, N. Sasaki, K. Saga, T. Kaneko, Cytotoxicity of flavonoids toward cultured normal human cells, Biol Pharm Bull, 28 (2005) 253-259.

[337] H.B. Woo, W.S. Shin, S. Lee, C.M. Ahn, Synthesis of novel curcumin mimics with asymmetrical units and their anti-angiogenic activity, Bioorg Med Chem Lett, 15 (2005) 3782-3786.

[338] Y.J. Choi, Y.J. Jeong, Y.J. Lee, H.M. Kwon, Y.H. Kang, (-)Epigallocatechin gallate and quercetin enhance survival signaling in response to oxidant-induced human endothelial apoptosis, J Nutr, 135 (2005) 707-713.

[339] Y.J. Choi, J.S. Kang, J.H.Y. Park, Y.J. Lee, J.S. Choi, Y.H. Kang, Polyphenolic flavonoids differ in their antiapoptotic efficacy in hydrogen peroxide-treated human vascular endothelial cells, J Nutr, 133 (2003) 985-991.

VITA

Paritosh Prashant Wattamwar was born on 4th August, 1985 in Nanded, Maharashtra, India. He completed Bachelors in Chemical Engineering with First Class with Distinction from the Institute of Chemical Technology (formerly known as UDCT), Mumbai, India, in May 2006. He joined Department of Chemical and Materials Engineering at the University of Kentucky in August 2006 to pursue a Doctorate of Philosophy in Chemical Engineering.

HONORS AND AWARDS

- 1st place in graduate student poster session at Department of Chemical and Materials Engineering, University of Kentucky, Fall 2009 and Fall 2010
- Recipient of Research Challenge Trust Fund Fellowship, University of Kentucky, 2007- 2009
- 4th place in poster session at Cardiovascular Research Day, Gill Heart Institute of the University of Kentucky, 2008
- Recipient of "Gujarat Ambuja Cement Best Home Paper Award" for Best Undergraduate Project Design, Institute of Chemical Technology, 2006

PUBLICATIONS

P.P. Wattamwar, D. Biswal, A. Lyvers, D. Cochran, J.Z. Hilt and T.D. Dziubla, "Synthesis and Characterization of Poly(antioxidant β-amino esters) for Controlled Release of Polyphenolic Antioxidants", Acta Biomaterialia (to be s*ubmitted*)

D. Biswal, P.P. Wattamwar, T.D. Dziubla and J.Z. Hilt, "Poly(β-amino ester) Hydrogel Synthesis by Single Step Polymerization Method", Polymer, 2011, 52, 5985-5992

P.P. Wattamwar and T.D. Dziubla, "Modulation of Wound Healing Response Through Oxidation Active Materials", To appear in : "Engineering Biomaterials For Regenerative Medicine: Novel Technologies for Clinical Applications", S. Bhatia (Editor), Springer (*Submitted*)

E. Hood, E. Simone, P.P. Wattamwar, T.D. Dziubla and V.R. Muzykantov, "Polymeric Carriers for Antioxidant Enzymes and Small Molecules", Review article, Nanomedicine, 2011, 6(7), 1257-1272

P.P. Wattamwar, S.S. Hardas, D. Allan Butterfield, K.W. Anderson and T.D. Dziubla, "Tuning of the Pro-oxidant and Antioxidant Activity of Trolox Through the Controlled Release from Biodegradable Poly(trolox ester) Polymers", Journal of Biomedical Materials Research Part A, 2011, 99A, 184-191.

P.P. Wattamwar, Y. Mo, R. Wan, R. Palli, Q. Zhang and T.D. Dziubla, "Antioxidant Activity of Degradable Polymer Poly(trolox) to Suppress Oxidative Stress Injury in the Cells", Advanced Functional Materials, 2010, 20, 147-154.

PATENT APPLICATIONS

T.D. Dziubla, J. Z. Hilt, D. Biswal, D.B. Cochran and P. P. Wattamwar, "Compounds and Methods for Reducing Oxidative Stress", US Patent Application, November 5, 2010

CONFERENCE PRESENTATIONS

Paritosh has presented papers and posters at several national, regional and local meetings including AIChE Annual Meetings (Salt Lake City, 2007; Philadelphia, 2008; Nashville, 2009; Salt Lake City, 2010) and SFB Annual Meetings (Seattle, 2010; Orlando, 2011)